Development of a Wireless MEMS Multifunction Sensor System and Field Demonstration of Embedded Sensors for Monitoring Concrete Pavements

Volume I - Field Demonstration of Embedded Sensors for Monitoring Concrete Pavements

August 2016

National Concrete Pavement Technology Center






IOWA STATE UNIVERSITY
Institute for Transportation

Sponsored by
Iowa Highway Research Board
(IHRB Project TR-637)
Iowa Department of Transportation
(InTrans Project 12-417)

About ProSPER

The overall goal of the Program for Sustainable Pavement Engineering and Research (ProSPER) is to advance research, education, and technology transfer in the area of sustainable highway and airport pavement infrastructure systems.

About the National CP Tech Center

The mission of the National Concrete Pavement Technology (CP Tech) Center is to unite key transportation stakeholders around the central goal of advancing concrete pavement technology through research, tech transfer, and technology implementation.

About InTrans

The mission of the Institute for Transportation (InTrans) at Iowa State University is to develop and implement innovative methods, materials, and technologies for improving transportation efficiency, safety, reliability, and sustainability while improving the learning environment of students, faculty, and staff in transportation-related fields.

Disclaimer Notice

The contents of this report reflect the views of the authors, who are responsible for the facts and the accuracy of the information presented herein. The opinions, findings and conclusions expressed in this publication are those of the authors and not necessarily those of the sponsors.

The sponsors assume no liability for the contents or use of the information contained in this document. This report does not constitute a standard, specification, or regulation.

The sponsors do not endorse products or manufacturers. Trademarks or manufacturers' names appear in this report only because they are considered essential to the objective of the document.

Non-Discrimination Statement

Iowa State University does not discriminate on the basis of race, color, age, ethnicity, religion, national origin, pregnancy, sexual orientation, gender identity, genetic information, sex, marital status, disability, or status as a U.S. veteran. Inquiries regarding non-discrimination policies may be directed to Office of Equal Opportunity, Title IX/ADA Coordinator, and Affirmative Action Officer, 3350 Beardshear Hall, Ames, Iowa 50011, 515-294-7612, email eooffice@iastate.edu.

Iowa Department of Transportation Statements

Federal and state laws prohibit employment and/or public accommodation discrimination on the basis of age, color, creed, disability, gender identity, national origin, pregnancy, race, religion, sex, sexual orientation or veteran's status. If you believe you have been discriminated against, please contact the Iowa Civil Rights Commission at 800-457-4416 or Iowa Department of Transportation's affirmative action officer. If you need accommodations because of a disability to access the Iowa Department of Transportation's services, contact the agency's affirmative action officer at 800-262-0003.

The preparation of this report was financed in part through funds provided by the Iowa Department of Transportation through its "Second Revised Agreement for the Management of Research Conducted by Iowa State University for the Iowa Department of Transportation" and its amendments.

The opinions, findings, and conclusions expressed in this publication are those of the authors and not necessarily those of the Iowa Department of Transportation.

Technical Report Documentation Page

1. Report No.	2. Government Accession No.	3. Recipient's Catalog No.
IHRB Project TR-637		

4. Title and Subtitle	5. Report Date
Development of a Wireless MEMS Multifunction Sensor System and Field Demonstration of Embedded Sensors for Monitoring Concrete Pavements: Volume I - Field Demonstration of Embedded Sensors for Monitoring Concrete Pavements	August 2016
	6. Performing Organization Code

7. Author(s)	8. Performing Organization Report No.
Halil Ceylan (orcid.org/0000-0003-1133-0366), Liang Dong (orcid.org/0000-0002-0967-4955), Shuo Yang (orcid.org/0000-0002-2653-5199), Yueyi Jiao (orcid.org/0000-0002-8264-5771), Seval Yavas (orcid.org/0000-0002-4173-2633), Sunghwan Kim (orcid.org/0000-0002-1239-2350), Kasthurirangan Gopalakrishnan (orcid.org/0000-0001-8346-5580), and Peter Taylor (orcid.org/0000-0002-4030-1727)	InTrans Project 12-417

9. Performing Organization Name and Address	10. Work Unit No. (TRAIS)
Institute for Transportation Iowa State University 2711 South Loop Drive, Suite 4700 Ames, IA 50010-8664	**11. Contract or Grant No.**

12. Sponsoring Organization Name and Address	13. Type of Report and Period Covered
Iowa Highway Research Board and Iowa Department of Transportation 800 Lincoln Way Ames, IA 50010	Final Report Volume I
	14. Sponsoring Agency Code IHRB Project TR-637

15. Supplementary Notes

Visit www.intrans.iastate.edu for color pdfs of this and other research reports.

16. Abstract

Pavements tend to deteriorate with time under repeated traffic and/or environmental loading. By detecting pavement distresses and damage early enough, it is possible for transportation agencies to develop more effective pavement maintenance and rehabilitation programs and thereby achieve significant cost and time savings. The structural health monitoring (SHM) concept can be considered as a systematic method for assessing the structural state of pavement infrastructure systems and documenting their condition. Over the past several years, this process has traditionally been accomplished through the use of wired sensors embedded in bridge and highway pavement. However, the use of wired sensors has limitations for long-term SHM and presents other associated cost and safety concerns. Recently, micro-electromechanical sensors and systems (MEMS) and nano-electromechanical systems (NEMS) have emerged as advanced/smart-sensing technologies with potential for cost-effective and long-term SHM.

This two-pronged study evaluated the performance of commercial off-the-shelf (COTS) MEMS sensors embedded in concrete pavement (Final Report Volume I) and developed a wireless MEMS multifunctional sensor system for health monitoring of concrete pavement (Final Report Volume II).

In this part of the study (Volume I), the COTS MEMS sensors and the wireless sensors were deployed in a newly constructed concrete highway pavement. During the monitoring period, the temperature, moisture, and strain profiles were obtained and analyzed. The monitored data captured the effects of daily and seasonal weather changes on concrete pavement, especially the early-age curling and warping behavior of concrete pavement. These sensors, however, presented issues for long-term operation. So, to improve performance, a ZigBee protocol-based wireless communication system was implemented for the MEMS sensors.

By synthesizing knowledge and experience gained from a literature review, field demonstrations, and implementation of wireless systems, issues associated with sensor selection, sensor installation, sensor packaging (to prevent damage from road construction), and monitoring for concrete pavement SHM are summarized. The requirements for achieving Smart Pavement SHM are then explored to develop a conceptual design of smart health monitoring of both highway and airport pavement systems for next-generation pavement SHM. A preliminary cost evaluation was also performed for traditional as well as MEMS sensors and other potential smart technologies for pavement SHM.

17. Key Words	18. Distribution Statement
concrete pavements—field demonstration—pavement health monitoring—wireless MEMS	No restrictions.

19. Security Classification (of this report)	20. Security Classification (of this page)	21. No. of Pages	22. Price
Unclassified.	Unclassified.	134	NA

Form DOT F 1700.7 (8-72) **Reproduction of completed page authorized**

DEVELOPMENT OF A WIRELESS MEMS MULTIFUNCTION SENSOR SYSTEM AND FIELD DEMONSTRATION OF EMBEDDED SENSORS FOR MONITORING CONCRETE PAVEMENTS: VOLUME I - FIELD DEMONSTRATION OF EMBEDDED SENSORS FOR MONITORING CONCRETE PAVEMENTS

Final Report
August 2016

Principal Investigator
Halil Ceylan, Professor, Civil, Construction, and Environmental Engineering (CCEE)
Director, Program for Sustainable Pavement Engineering and Research (PROSPER)
Institute for Transportation, Iowa State University

Co-Principal Investigators
Liang Dong, Associate Professor, Electrical and Computer Engineering
Kasthurirangan Gopalakrishnan, Research Associate Professor, CCEE
Sunghwan Kim, Research Scientist, CCEE
Iowa State University

Peter Taylor, Director
National Concrete Pavement Technology Center, Iowa State University

Research Assistants
Shuo Yang, Yueyi Jiao, and Seval Yavas

Authors
Halil Ceylan, Liang Dong, Shuo Yang, Yueyi Jiao, Seval Yavas, Sunghwan Kim, Kasthurirangan Gopalakrishnan, and Peter Taylor

Sponsored by
the Iowa Highway Research Board and
the Iowa Department of Transportation (IHRB Project TR-637)

Preparation of this report was financed in part
through funds provided by the Iowa Department of Transportation
through its Research Management Agreement with the
Institute for Transportation (InTrans Project 12-417)

A report from
Institute for Transportation
Iowa State University
2711 South Loop Drive, Suite 4700
Ames, IA 50010-8664
Phone: 515-294-8103 / Fax: 515-294-0467
www.intrans.iastate.edu

TABLE OF CONTENTS

LIST OF FIGURES

LIST OF TABLES

ACKNOWLEDGMENTS

The authors would like to thank the Iowa Highway Research Board (IHRB) and the Iowa Department of Transportation (DOT) for sponsoring this research. The project technical advisory committee (TAC) members from the Iowa DOT and the Federal Highway Administration (FHWA), including Ahmad Abu-Hawash, Chris Brakke, Mark Dunn, Vanessa Goetz, Todd Hanson, Lisa McDaniel, Kevin D. Merryman, and Robert (Bob) Younie, are gratefully acknowledged for their guidance, support, and direction throughout the research.

WAKE, Inc., Sensirion, Inc. USA, and Maxim Integrated Products are gratefully acknowledged for supplying their sensors and systems for research evaluation. Thanks to Richard Yesh of WAKE, Inc. for his prompt assistance.

Special thanks are extended to Daji Qiao and Keyan Shen of the Department of Electrical and Computer Engineering (ECpE) at Iowa State University (ISU) for their insightful discussions and assistance with this project. The research team would also like to thank Bob Steffes with the National Concrete Pavement Technology (CP Tech) Center and many graduate and undergraduate students in the Departments of Civil, Construction, and Environmental Engineering (CCEE) and ECpE at Iowa State University for their assistance with the laboratory and field tests.

EXECUTIVE SUMMARY

Like any other man-made structural system, pavement systems can fail due to repeated traffic loading, environmental loading, or a combination of both. Environmental loads such as temperature (which produces curling stress) and moisture (which produces warping stress) can cause volumetric distortion during the early life of portland cement concrete (PCC) pavement. Such environmental and mechanical loads combined with PCC aging greatly influence long-term pavement performance and the development of pavement distresses.

According to the American Society of Civil Engineers (ASCE) 2013 Report Card, the national pavement system is assessed a "D" grade, reflecting poor pavement condition. The Federal Highway Administration (FHWA) estimates that approximately $170 billion is needed to effectively improve network-level pavement condition and performance. Therefore, the ability to track the condition of newly constructed and in-service pavements and develop effective pavement preservation practices are high-priority needs for highway agencies.

Structural health monitoring (SHM) is considered to be a systematic approach that could be employed to monitor and preserve rapidly deteriorating pavement assets. Traditional SHM approaches utilizing wired sensors have been used to track pavement response under environmental and traffic loads, including temperature, moisture, strain, stress, deflection, etc. However, over the past 20 years fewer pavement instrumentation projects have been initiated, and almost all of them experienced negative issues such as high array density, wire damage, high installation costs and lengthy installation times, low survivability of wired sensors for long-term operation, etc. Recent achievements in micro-electromechanical sensors and systems (MEMS) or nano-electromechanical systems (NEMS) technology make it possible to manufacture sensors using microfabrication techniques. This kind of advanced/smart-sensing technology, including wireless sensors, shows vast potential for improving the traditional SHM approach. However, MEMS-based and wireless-based smart-sensing technologies have up to now been rarely used for monitoring pavement response in the field, and the requirements for using these kinds of smart sensing technologies have not yet been thoroughly examined.

The primary objectives of this two-pronged research study are (1) to deploy some of the promising commercial off-the-shelf (COTS) MEMS sensors developed for monitoring concrete pavements in a live field project and (2) to develop a wireless MEMS multifunction sensor (WMS) system capable of real-time remote monitoring of strain, moisture content, and temperature in pavement concrete. Accordingly, two final report volumes have been prepared targeting each of the objectives:

- The Volume I final report (this current report) focuses on the deployment and field evaluation of COTS MEMS sensors.
- The Volume II final report describes the development of a WMS system for concrete pavement health monitoring.

This report (Volume I) synthesizes knowledge and experience gained from a literature review, field demonstrations, and implementation of wireless systems into an examination of COTS

MEMS sensors. The issues associated with sensor selection, sensor installation, sensor packaging (to prevent damage from road construction), and monitoring for concrete pavement SHM are summarized to identify the requirements for achieving Smart Pavement SHM. Based on the study findings, a conceptual design of smart health monitoring for both highway and airport pavement for the next-generation pavement SHM is developed and discussed. A preliminary cost evaluation was also performed for traditional as well as MEMS sensors and other potential smart technologies for pavement SHM.

INTRODUCTION

Background and Motivation

The development of novel "smart" structures by embedding sensing capabilities directly into construction materials during the manufacturing and deployment process has attracted significant attention in the context of autonomous structural health monitoring (SHM). Advancements in micro-electromechanical sensors and systems (MEMS) technology and wireless sensor networks provide opportunities for long-term, continuous, real-time structural health monitoring of pavements and bridges at low cost within the context of sustainable infrastructure systems.

MEMS represent an innovative solution in infrastructure condition monitoring that can be used to wirelessly detect and monitor the initiation and growth of structural and material durability related damage and distresses in concrete structures. A number of advantages have been reported regarding the use of MEMS-based monitoring systems over other condition monitoring and assessment methods. First developed in the 1970s and then commercialized in the 1990s, MEMS make it possible for systems of all kinds to be smaller, faster, more energy efficient, and less expensive. In a typical MEMS configuration, integrated circuits (ICs) provide the "thinking" part of the system, while MEMS complement this intelligence with active perception and control functions (AllAboutMEMS 2002).

MEMS devices can be classified into three broad categories (Maluf 2000): sensors, actuators, and passive structures. Transducers that convert mechanical, thermal, or other forms of energy into electrical energy are considered to be sensors, whereas actuators do the exact opposite. Devices in which no transducing occurs are passive structures. Some intrinsic properties of the component, such as piezoresistivity, piezoelectricity, or thermoelectricity, determine the actuation or sensing ability of MEMS (Attoh-Okine and Mensah 2003).

The Iowa Highway Research Board (IHRB) project by Ceylan et al. (2011), "A Feasibility Study on Embedded Micro-Electromechanical Sensors (MEMS) and Systems for Monitoring Highway Structures," provided a comprehensive synthesis of the latest information available on off-the-shelf MEMS devices as well as research prototypes for bridge, pavement, and traffic applications (Ceylan et al. 2011).

Under the IHRB MEMS project, a commercially available wireless concrete monitoring system based on radio frequency identification (RFID) technology and off-the-shelf temperature and humidity sensors were also tested under controlled laboratory and field conditions. The test results validated the ability of the RFID wireless concrete monitoring system to accurately measure the temperature both in the laboratory and in the field under severe weather conditions. In consultation with the project Technical Advisory Committee (TAC), the most relevant MEMS-based transportation infrastructure research applications that could be explored in the future phases of the research project were highlighted and summarized. The most prominent of these included the following:

- Overweight/heavy vehicle pre-alert and detection system
- Ice detection and warning system
- Traffic flow detection and wrong-way vehicle control and warning system
- Critical STOP sign tracking/monitoring system

Research Objectives

Multi-sensor systems are promising in that they have the potential to monitor structural health, supporting efficient operation and maintenance of civil infrastructure through simultaneous measurement of multiple properties. The primary objectives of this research were twofold:

- Deploy some of the promising off-the-shelf MEMS sensors developed for monitoring concrete pavements in a live field project

- Develop a wireless MEMS multifunction sensor (WMS) system capable of real-time remote monitoring of strain, moisture content, and temperature in pavement concrete

Report Content: Volume I

Volume I of the final report presents detailed information on the research efforts to fulfill first objective: Deploy some of the promising off-the-shelf MEMS tags and sensors developed for monitoring concrete pavements in a live field project. This report includes the following chapters:

- **Chapter 1: Introduction.** A description of the background and objectives of this study
- **Chapter 2: Literature Review.** A comprehensive literature review of SHM, including recent successes in applying MEMS and wireless system technology to SHM
- **Chapter 3: Field Instrumentation and Evaluation of Commercial Off-the-Shelf MEMS Sensors and Wireless Sensors.** Discussions on the instrumentation and performance of off-the-shelf MEMS sensors for monitoring US Highway 30 pavement section
- **Chapter 4: Integration of Wireless Communication System with MEMS Sensors.** Discussion of the implementation and performance of a wireless system for off-the-shelf MEMS sensors
- **Chapter 5: Requirements for Structural Health Monitoring System Using Smart Sensing Technologies.** Discussion of the issues and costs associated with SHM and the requirements and conceptual design of Smart Pavement SHM
- **Chapter 6: Summary and Recommendations.** A summary of the important findings and recommendations from this study

LITERATURE REVIEW

Structure Health Monitoring

History of SHM in Civil Infrastructure

Structural health monitoring is the process of implementing a structural damage detection strategy and evaluating structural state to determine load and response mechanisms (Farrar and Worden 2007, Brownjohn 2007). In recent years, it has become a rapidly growing priority for transportation agencies to identify and monitor structural deterioration. An ideal SHM application can monitor the integrity of in-service structures on a continuous real-time basis, and data processing and analysis can subsequently be used to assess the symptoms of operational anomalies that may cause service or safety issues (Wong 2004).

Early development of health monitoring techniques focusing on vibration-based damage identification methods can be traced to the 1970s in the oil industry and the aerospace community in conjunction with offshore platforms and space shuttles, respectively. The modal properties and related quantities of civil infrastructures, such as bridges and buildings, using vibration-based damage identification methods have been investigated since the 1980s. However, difficulties in using vibration-based damage identification methods for large-scale structures during that time sometimes occurred, often due to variable environmental and operational conditions; this frequently resulted in an expensive and time-consuming process of damage assessment (Phares et al. 2005, Qi et al. 2005, Farrar and Worden 2007).

SHM can be widely used as an approach to in-service structural integrity assessment in bridges, buildings, towers, dams, offshore installations, pavements, etc. Traditional SHM systems for such civil infrastructure have utilized wired sensors strategically deployed within the structures to monitor and record external conditions and the associated structural responses. Among these structures, bridges and buildings have represented the most common SHM applications in civil infrastructure. SHM in bridges has been used to characterize their dynamic behavior under unpredictable mechanical and environmental loads that may result in unanticipated behavior (Modares and Waksmanski 2012). The most common techniques include eddy current sensing, ultrasonic sensing, acoustic-based sensing, strain monitoring, corrosion monitoring, etc. SHM in building structures has been deployed to monitor structural performance under natural disaster conditions such as earthquakes, storms, and harsh winds (Brownjohn 2007). Furthermore, it is a common practice for SHM implemented in concrete structures to also monitor concrete temperature and moisture. The data generated can be used to determine frame removal time during construction through monitoring of concrete maturity and the curing process.

Unlike in bridges and building structures, the application of SHM in pavement systems has been used to document structural responses from a combination of vehicle and environmental loads. Monitoring sensors embedded in the pavement structure have been investigated since the 1960s to improve pavement design methods (Potter et al. 1969, Rollings and Pittman 1992). However, the survivability of embedded sensors in a pavement structure is not always high because they can easily be damaged by the asphalt/concrete medium and harsh climate conditions.

Global and Local Health Monitoring

According to Plankis and Heyliger (2013), there are four levels of damage identification. From the first level to the fourth level, these are, in sequence, determination of damage presence, identification of damage location, evaluation of damage, and prediction of the structure's remaining service life. To address the first three levels, health monitoring methods can be divided into global and local health monitoring. Global health monitoring is the concept of using technology to detect changes in properties such as stiffness, mass, and other dynamic global properties caused by significant structural damage. For global health monitoring, there is no need to know the location or potential location of damage. The important modal properties for global health monitoring are resonant frequencies, mode shape vectors, mode shape curvatures, a dynamic flexibility matrix, updates to the modal parameters, and acoustic properties (Plankis and Heyliger 2013). Local health monitoring refers to tracking the progress of damage and evaluating the level of damage at known or predicted damage locations. In summary, global techniques are used for damage detection that may affect the integrity of a whole structure, while local techniques focus on small defects (Haque et al. 2012). Technically, traditional wired sensor–based SHM represents a type of local health monitoring technology.

Smart Structural Health Monitoring

Lynch (2002) defines the term "smart structure" as "sensing and/or actuation technologies embedded within the system to provide insight to the structure's response and an opportunity to limit responses." Spencer et al. (2004) states that a sensor must have features such as an onboard central processing unit (CPU), small size, wireless capability, and the promise of low cost to be considered a smart sensor. Similarly, Nagayama and Spencer (2007) state that a sensor can be considered "smart" if it includes an onboard microprocessor, a wireless communication system, and sensing capability. It also should be battery powered and have a low cost. However, Phares et al. (2005) give a more detailed definition of the term "smart." The term "smart" technology is a "system [that] systematically reports on the condition of the structure by automatically making engineering-based judgments, recording a history of past patterns and intensities, and providing early warning for excessive conditions or for impending failure without requiring human intervention. These features make the system capable of providing and facilitating self-diagnostic, real-time continuous sensing, advanced remote sensing, self-organizing, self-identification, or self-adaptation (decision making and alarm triggering) functions."

In short, smart SHM should enable structures to be capable of real-time continuous sensing of both external and internal condition changes and responding to these changes to improve performance without human intervention. To apply this concept to pavement, a Smart Pavement SHM should be capable of long-term use and should be cost-effective. However, a truly "smart" system or structure meeting all these requirements has never existed, if this definition is rigorously followed. It is clear, however, that a practical smart SHM could be achieved by employing a "smart sensor" system having the features of small size, wireless functionality, low cost, and an onboard CPU.

Traditional SHM Approach to Pavement Infrastructure Systems

Highway Pavement

In the US, traditional SHM approaches for highway pavement infrastructure systems have utilized full-scale test tracks instrumented with a large number of sensors such as strain gages, pressure cells, displacement gauges, subgrade moisture sensors, etc. The motivation underlying constructing and operating a full-scale pavement test track is to understand pavement response and behavior under realistic but controlled conditions (Hugo and Epps Martin 2004).

Figure 1, from Hugo and Epps Martin (2004), summarizes the common sensors used in various test tracks.

RIOH–ALF			RIOH–ALF		
WesTrack			HVS–A	RIOH–ALF	
HVS–A			TxMLS	WesTrack	
TxMLS			RRT–Rom	HVS–A	
PRF–La			MnROAD	TxMLS	
MnROAD			LCPC–Fr	RRT–Rom	
LINTRACK			K–ATL	NCAT	
LCPC–Fr	RIOH–ALF		In–APLF	MnROAD	
K–ATL	HVS–A		HVS–SA	LCPC–Fr	
ISETH	TxMLS		HVS–Nordic	K–ATL	
In–APLF	PRF–La		NAPTF	HVS–SA	MnROAD
HVS–SA	MnROAD		HVS–CRREL	NAPTF	LINTRACK
HVS–Nordic	LCPC–Fr	RIOH–ALF	CEDEX	DRTM	FHWA–PTF
FHWA–PTF	K–ATL	HVS–A	CAPTIF–NZ	HVS–CRREL	DRTM
NAPTF	HVS–Nordic	TxMLS	CAL/APT	CEDEX	CAPTIF–NZ
DRTM	NAPTF	PRF–La	ARRB–ALF	CAL/APT	CAL/APT
HVS–CRREL	DRTM	MnROAD	Oh–APLF	ARRB–ALF	Oh–APLF
CEDEX	HVS–CRREL				
CAL/APT	CEDEX				
ARRB–ALF	CAPTIF–NZ				
Oh–APLF	ARRB–ALF				
Strain gages	Pressure cells	Load cells	Displacement gauges	Subgrade moisture sensors	Other*

*Other instruments cited by respondents:

Temperature sensors—Oh–APLF; CAL/APT
Temperature gauge—DRTM
Emu & Bison strain coils—CAPTIF–NZ
LVDT—FHWA–PTF
Several attempts for measurement of asphalt sublayers: LINTRACK–NL
MnROAD—see website (mnroad.dot.state.mn.us/researc/Mnresearc.asp) and beyond the surface handout.

From Hugo and Epps Martin 2004 (Source: Significant findings from full-scale/APT, Question 5.2)

Figure 1. Sensors used in traditional pavement health monitoring

Detailed descriptions of full-scale test tracks, including MnROAD, the Virginia Smart Road, and the National Center for Asphalt Technology (NCAT) Test Track, are summarized in Table 1.

Table 1. Test track instrumentation

Projects	Monitoring System	Year
MnROAD	Over 9,500 sensors, including linear variable differential transformers (LVDTs), strain gages, dynamic soil pressure cells, moisture gauges, thermocouples, and resistivity probes, were installed.	1991
Virginia Smart Road	Over 400 sensors, including moisture, temperature, strain, vibration, and weigh-in-motion sensors, were installed	1997
NCAT Test Track at Auburn University	Copper-based strain gages, temperature sensors, soil pressures, and soil moisture sensors were installed.	2000

MnROAD

In 1991, the MnROAD test track (see Figure 2) was constructed to enable civil engineers to conduct research on making roads longer lived, safer, and cheaper.

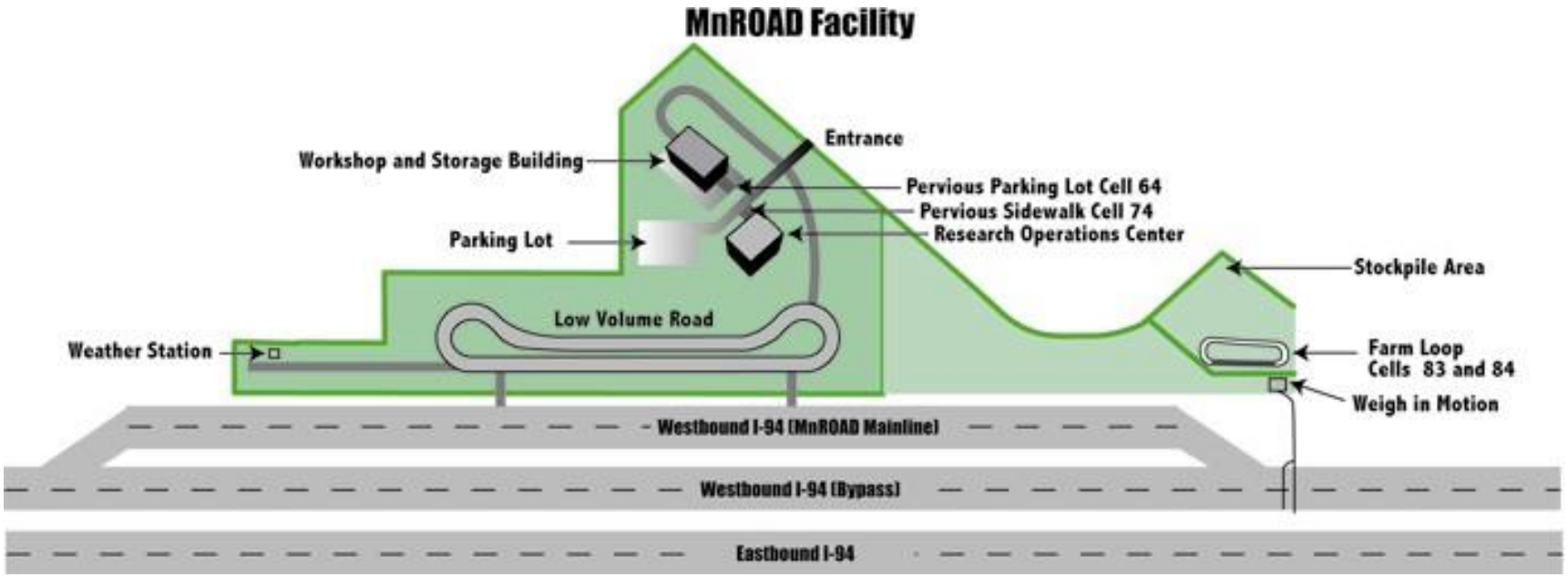

MnDOT 2016

Figure 2. MnROAD test track facility

The project funding, approximately $25,000,000, was used to build a 2.5-mile low-volume road and a 3.5-mile main line on I-94. Since the 1990s, more than 9,500 sensors have been installed in the test track to document the effects produced by test vehicles. These sensors were linked by fiber optic or copper wires to a data acquisition system (DAS) connected to the MnROAD main building. The data collected from MnROAD have been used to improve pavement performance and lifespan, with cost savings related to maintenance, repairs, user delays, and congestion (MnROAD 2014). Table 2 lists a summary of the estimated overall cost savings from the MnROAD Phase 1 research (1994 to 2006).

Table 2. MnROAD cost savings

Phase I (MN) Implemented Research	Annual Savings
Spring Load Restriction Policy	$14 Million
Winter Load Increase Policy	$7 Million
Low Temperature Cracking Reduction	$5.7 Million
ME Flexible Design Method	$4 Million
ME Rigid Design Method	$1.2 Million
Sealing Pavement/Shoulder Joints	$1.2 Million
Total	**$ 33.1 Million**

Source: MnROAD 2014

It is claimed that a total of $33 million has been saved for Minnesota and a potential $749 million has been saved for the nation overall.

At the MnROAD test track, the DAS is distributed as data acquisition nodes near the test cells. Each data acquisition node consists of a series of cabinets containing sensors, data collection devices, and AC power sources as well as communication systems. The insulated cabinets are heated during the winter and cooled during the summer by installed fans. In order to cost-effectively install so many sensors, the construction manager of MnROAD paid considerable attention to sensor life span and the sensor installation plan. However, there were still many sensor failures reported, requiring the replacement of many sensors after road construction. In replacing the sensors, it was found that the in situ sensor positions differed a great deal from the instrumentation plan, so MnROAD personnel had to install sensors into new holes using full-depth coring. After installation, they assumed that the data from the new sensors were accurate (Tompkins and Khazanovich 2007).

Virginia Smart Road

The Virginia Smart Road (see Figure 3) was a 5.7-mile-long limited-access highway constructed at the end of the 1990s.

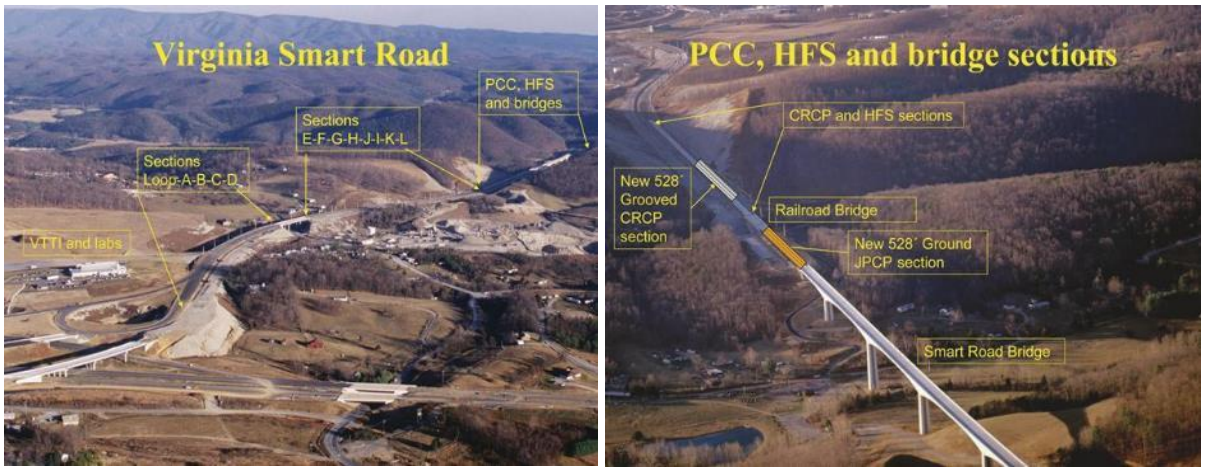

Edgar de Leon Izeppi, Virginia Transportation Institute

Figure 3. Virginia Smart Road

This road links I-81 and Blacksburg, Virginia, and has all-weather test towers, variable-lighting sections, and experimental sections, as well as a control room for data analysis. The Virginia Smart Road contains more than 400 installed sensors, including thermocouples, strain gages, pressure cells, time-domain reflectometry probes, resistivity probes, etc. However, approximately 70% of the sensors failed after two years (Al-Qadi et al. 2004).

Auburn University NCAT Test Track

The NCAT Test Track, shown in Figure 4, was designed and built in 2000 to evaluate and improve current pavement design.

National Center for Asphalt Technology

Figure 4. NCAT Test Track

This 1.7-mile long test track contains more than 46 experimental sections. The test period of the NCAT Test Track can be divided into a first and a second round of tests. The first round of tests was initiated in 2000 and finished in 2002. The second round started in 2003 after several sections were replaced. While many sensors, including strain gages, temperature sensors, soil pressure sensors, and soil moisture sensors, were embedded in the subgrade and asphalt pavement, almost 35% of them failed before 2003 (Timm et al. 2004).

Airfield Pavement

Pavement deterioration caused by aircraft loading and temperature and moisture variation can be a major concern for airport safety. Compared to highway pavement, airfield pavement typically deals with higher load magnitudes and higher tire pressures but fewer load repetitions from airplanes. Additionally, although both airfield and highway pavements are prone to deterioration from traffic and environmental loads, airfield pavement usually predominately exhibits environmental load–related rather than traffic load–related stresses (FAA 2011).

In summer 2011, the Ankeny Regional Airport in Ankeny, Iowa, reported a serious portland cement concrete (PCC) pavement distress blowup in its runway, which was caused by extremely hot weather and an associated heat wave. In this particular case, a Raytheon Premier One jet hit the blowup spot during takeoff and damaged its landing gear, as shown in Figure 5.

Snyder & Associates, Inc. (left) and Polk County Aviation Authority (right)

Figure 5. Pavement blowup and damaged aircraft on Ankeny Regional Airport runway

Blowup in an airport runway is, of course, very dangerous for aircraft operation. It is therefore important to install sensors in airfield pavement to enable SHM systems to monitor pavement properties and provide warning of pavement overheating before actual pavement distress occurs so that the appropriate maintenance process can be launched. Table 3 lists traditional SHM applications in the US for airport pavement systems (Mullen 2011).

Table 3. Airfield pavement instrumentation

Projects	Monitoring System	Year
Denver International Airport (DIA)	Over 460 sensors, including strain gages, thermocouples, and time-domain reflectometers (TDRs), were installed.	1990
Federal Aviation Administration (FAA) National Airport Pavement Test Facility (NAPTF)	Over 1,000 sensors, including temperature sensors, moisture sensors, and strain gages, were installed.	1997

Runway Instrumentation at Denver International Airport

In the 1990s, the Denver International Airport began construction of a runway with comprehensive instrumentation of strain gages, thermocouples, and TDRs. A total of 460 sensors were embedded in 16 slabs of the runway to monitor the pavement response generated by aircraft wheel and environmental loading. Among the installed sensors were dynamic sensors that could measure strain, vertical displacement, airplane speed, and acceleration whenever a passing airplane triggered them. A DAS was placed in situ for data collection and downloading to the database managed by the FAA technical center (Lee et al. 1997, Dong and Hayhoe 2000, Rufino et al. 2004).

Federal Aviation Administration National Airport Pavement Test Facility

In 1997, the FAA began to build a full-scale pavement test facility dedicated to pavement research, as shown in Figure 6. NAPTF was built to provide traffic data for improving pavement thickness design procedures, investigating pavement response and failure mechanisms related to airplane landing, and examining the California bearing ratio (CBR) method for asphalt pavement design.

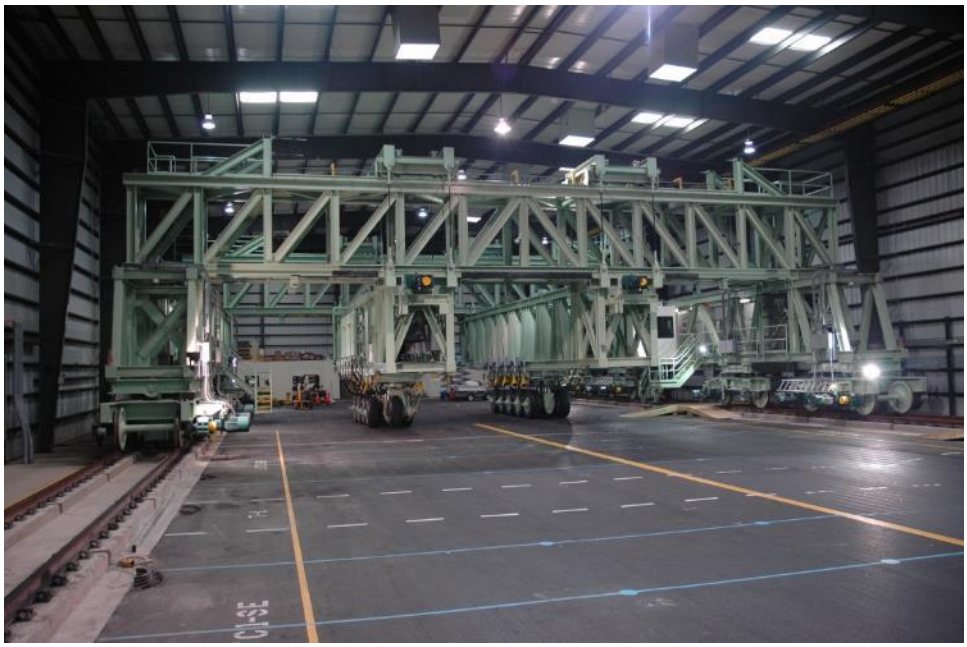

Federal Aviation Administration

Figure 6. National Airport Pavement Test Facility

Sensors embedded in the NAPTF can be divided into two groups: static sensors and dynamic sensors. Static sensors are used to monitor temperature, moisture, and crack status every hour, while dynamic sensors are used to measure strain and deflection under vehicle or aircraft loads. However, many sensors were damaged, and the pavements containing the sensors were scheduled for replacement on an 18-month cycle (Hayhoe 2004).

Limitations of Current SHM Practices for Pavement System

Current SHM practice for pavement systems has been mainly to use wired sensing technologies, resulting in the low survivability of sensors with respect to both pavement construction and long-term operation. It is difficult to provide either continuously long-term monitoring for pavement structural behavior changes or real-time warning for in-service pavement failure. Furthermore, wired sensors always require high installation costs and lengthy installation times. If many sensors are used, the cost of the DAS may also increase due to a limit in the number of data logger connection ports. Current SHM practice also may not be to directly integrate actual pavement management information systems to establish maintenance and rehabilitation strategies for in-service pavement systems. Other limitations, such as the difficulty of installing an SHM system and the lack of optimized collection and storage mechanisms for field data, may also hamper the implementation of pavement SHM (FHWA 2012).

Hence, implementation of smart sensors should be investigated as a means for overcoming current limitations. MEMS and wireless sensor systems are reviewed in the following section to evaluate their potential for smart sensor development.

MEMS

Overview

The emergence of MEMS and their recent achievements represent an alternative solution to achieving long-term, continuous, real-time, and cost-effective SHM for pavement systems. MEMS refers to miniaturized systems consisting of microsensors and actuators fabricated by using microfabrication techniques; their critical physical dimensions could range from just one micron up to one millimeter (MEMSnet 2014). This allows the use of integrated circuits and onboard CPUs to make the system intelligent. As a result, microsensors and actuators with active perception and microcircuit control can effectively sense their environments and be able to react to changes in those environments (Varadan and Varadan 2000, AllAboutMEMS 2002, Phares et al. 2005).

The early motivation of small-size sensing devices can be traced back to the first point-contact transistor developed in the 1940s by Shockley et al. at Bell Laboratories; these devices were about one-half of an inch high (SCME 2013). Since the 1970s, the manufacturing processes of electronic devices have undergone remarkable progress associated with the use of silicon as the dominant material. MEMS devices were first developed and widely commercialized in the 1990s. Nowadays, MEMS technologies are used in many applications (AllAboutMEMS 2002, Lee 2004, SCME 2013).

MEMS-based sensors are generally comprised of miniaturized mechanical sensing elements fabricated on silicon chips. Contemporary microfabrication techniques enable a variety of complex electromechanical systems to be integrated into such miniaturized sensing elements (MEMSnet 2014). The most distinguishing features of a typical MEMS sensor are incredibly small size and an onboard microprocessor, or CPU. Such a sensor has a much lower price than other sensors due to the materials used and integrated interconnection. The microprocessor supports digital processing, analog-digital conversion, and basic computation. Compared to MEMS sensors, traditional sensors have both relatively larger sizes and higher prices. Additionally, traditional sensors must always be equipped with a data management system, so the instrumentation of traditional sensors may require a large array density in the structure if many sensors are used, which itself may result in pavement distress (e.g., cracking). MEMS sensors, in contrast, could potentially be used to improve the current SHM of pavement system performance with relatively little concern for inherent compromising properties.

Commercial Off-the-Shelf MEMS Sensors for Civil Infrastructure SHM

The potential applications of MEMS-based sensor networks for transportation infrastructure applications are summarized in Table 4, which highlights the latest information on the availability of the listed MEMS .

Table 4. Potential commercial MEMS-based sensors or sensor networks for transportation infrastructure applications

MEMS Sensors and Systems	Applications	Commercial Vendor
Q350 series RFID tag	Wireless temperature monitoring	Identec Solutions
GT-301 NFC temperature sensor tag		GENTAG, Inc.
SAW RFID chips		RF SAW, Inc.
PaveTag RFID		Minds, Inc.
EmbedSense wireless sensor		MicroStrain, Inc.
Temperaure iButtons	Wired temperature monitoring	Maxim Integrated Products, Inc.
Digital temperature and humidity sensor SHT7x series	Wired temperature and humidity monitoring	Sensirion, Inc.
Humidity iButtons	Wired humidity monitoring	Maxim Integrated Products, Inc.
Triple-axis accelerometer board	Wireless bridge and highway safety monitoring	Freescale Semiconductor
3-Axis Magnetic sensor		Honeywell
Sensor networks by Crossbow Technologies	Wireless monitoring of load condition and/or measuring of strain and stress information of pavements and bridges	Crossbow Technologies
Sensor networks by Sensicast		Sensicast Systems, Inc.
Sensys Networks, Inc. wireless vehicle detection system	Traffic flow monitoring and identification under different vehicular loadings	Sensys Networks, Inc.

Source: Liu et al. 2007

Among these, the WAKE, Inc. wireless HardTrack Concrete Monitoring System (which uses Identec Solutions' RFID-based temperature sensor) and the Sensirion, Inc. digital humidity sensor were selected for the IHRB MEMS feasibility study. As a reference MEMS sensor, the Thermochron iButtons by Maxim Integrated Products, Inc. were also used.

WAKE, Inc. HardTrack Concrete Monitoring System

The HardTrack Concrete Monitoring System (see Figure 7) from WAKE, Inc. uses RFID technology to gather temperature data from in situ concrete in a very efficient and cost-effective manner.

Figure 7. RFID-based wireless concrete monitoring system: RFID tags with/without a temperature probe (top left), installation of wireless RFID tag in the base course (top middle), installation of wireless RFID tag buried in concrete (top right), HardTrack portable with detected wireless RFID tags on the screen (bottom left), data acquisition in the field (bottom right)

The HardTrack concrete monitoring system consists of an RFID tag and a portable transceiver. The RFID tag has the capability to capture the ambient temperature of the concrete it is buried in and to communicate the information to the portable transceiver. Once data are collected, they can be imported into the portable transceiver wirelessly for maturity calculation and the data can be saved to a computer for posterity.

It should be noted that the RFID tags equipped with temperature sensors by Identec Solutions have been successfully utilized in a number of recent infrastructure applications. A recent study extrapolated that the cost savings (through reduced wait time) per pour would be approximately $2,000 if the RFID system were used in combination with one-third of the test cylinders typically used in the project examined (O'Connor 2006). Identec Solutions RFID temperature tracking tags were also used in the construction of the Freedom Tower at the former World Trade Center site in New York to determine optimum concrete strength and to document curing rates (Identec Solutions 2008, Daly et al. 2010). Additional technical details regarding the RFID temperature tag are discussed in the following sections. Furthermore, Identec Solutions is currently in the process of developing RFID-based humidity tracking tags, which are expected to have great potential for concrete infrastructure monitoring.

Sensirion Digital Humidity Sensor

Sensirion has developed a pin-type relative temperature and humidity sensor (SHT 7x series) combined with analog and digital signal processing circuitry on a tiny silicon chip by means of MEMS technology. Figure 8 presents the SHT75 digital temperature and humidity sensor.

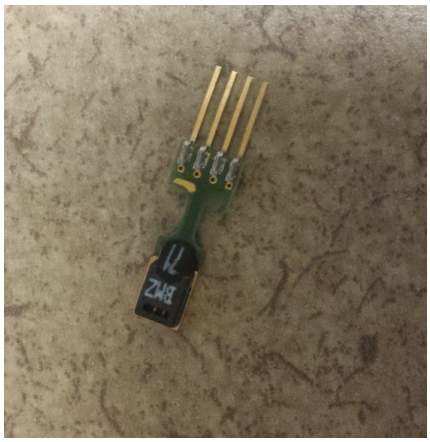

Figure 8. SHT75 Sensirion digital temperature and humidity sensor

Sensirion series temperature and humidity sensors are fully calibrated and packaged in a pin-type configuration, which allows them to be easily integrated with other systems (e.g., a wireless transmission system). Furthermore, this type of sensor has other advantages, such as digital output, low power consumption, and excellent long-term stability, which makes it popular for research investigating moisture content inside concrete (Wells 2005, Ye et al. 2006, Choi and Won 2008, Lian 2010, Quinn and Kelly 2010, Barroca et al. 2013, Wang 2013). Additional details regarding this kind of sensor are provided in the following sections.

Research Related to MEMS Sensor Development for Civil Infrastructure SHM

Current research related to SHM primarily focuses on the development of MEMS sensors and wireless sensor systems. Norris et al. (2008) developed a MEMS sensor capable of measuring temperature and moisture inside concrete using the microcantilever principle. The cantilever beam used in this sensor can measure stresses related to concrete moisture. Beam curvature is produced, and the deflection can be measured as resistance by an embedded nano-strain gage (resistor) so that the stress can be calculated. Then, based on the established relationship between stress and water concentration, the moisture content can be determined. Temperature is measured using an on-chip temperature sensor.

The MEMS sensor was fabricated using a combination of standard and customized semiconductor processing steps. Standard complementary metal oxide semiconductor (CMOS) procedures, i.e., photolithography and chemical wet etching, were used to form the silicon platform. After patterning and activating the moisture-sensing element, the cantilever beam was

released through plasma etching. The sensor die was then surrounded by a polymeric coating and the entire chip embedded in a stainless steel jacket to protect it from the enclosing concrete.

Other MEMS sensors developed for concrete monitoring include “Smart Aggregate” by Sackin et al. (2000), “Smart Pebbles” by Watters et al. (2003), “Smart Dust” by Pei et al. (2007, 2009), and “Self-sustaining damage detection sensor” by Kuang (2014). Table 5 lists MEMS sensors developed through previous research efforts; however, not all of them can be used for concrete pavement.

Table 5. Research related to MEMS temperature, moisture, and strain sensors

Type	Applications	Reference
Temperature	Early age concrete property monitoring	Saafi and Romine (2005)
	Monitoring pavement condition using "Smart Dust"	Pei et al. (2007)
	Cascaded "triple-bent-beam" MEMS sensor for contactless temperature measurements in non-accessible environments	Andò et al. (2011)
	Wireless temperature microsensors integrated into bearings	Scott et al. (2011)
	Highly reliable MEMS temperature sensors for 275°C applications	Scott et al. (2012)
	Multisensor MEMS for temperature, relative humidity, and high-g shock monitoring	Smith (2012)
	MEMS-based Pt film temperature sensor	Han et al. (2014)
	Rapid temperature measurement of meteorological detection system based on MEMS	Lu et al. (2014)
	Differential-pressure-based fiber optic MEMS temperature sensor using Fabry-Perot interferometry	Liu et al. (2015)
Moisture	Early-age concrete property monitoring	Saafi and Romine (2005)
	Monitoring pavement condition using "Smart Dust"	Pei et al. (2007)
	A wireless, passive embedded sensor for real-time monitoring of water content in civil engineering materials	Ong et al. (2008)
	Multisensor MEMS for temperature, relative humidity, and high-g shock monitoring	Smith (2012)
	A highly sensitive humidity sensor with a novel hole array structure using a polyimide sensing layer	Choi et al. (2014)
	A CMOS humidity sensor for passive RFID sensing applications	Deng et al. (2014)
	Digital hygrometer for trace moisture measurement	Islam et al. (2014)
	MEMS-based humidity sensor based on thiol-coated gold nanoparticles	Lin et al. (2014)
	Low-draft humidity sensor by intermittent heating	Ooe et al. (2015)
Strain	Early-age concrete property monitoring	Saafi and Romine (2005)
	A carbon nanotube strain sensor for SHM	Kang et al. (2006)
	Microwave weigh-in-motion (WIM) sensor	Liu et al. (2007)
	Smart pavement monitoring system	Lajnef et al. (2011)
	High-performance piezoresistive MEMS strain sensor with low thermal sensitivity	Mohammed et al. (2011)
	Novel MEMS strain sensor	Saboonchi and Ozevin (2012)
	Surface-bonded MEMS strain sensors	Moradi and Sivoththaman (2013)
	Novel interdigitated capacitive strain sensor integrated with wireless system for SHM	Cao et al. (2015)

Although there has been considerable research focusing on MEMS sensors, the majority of studies are still at the proof-of-concept level. For MEMS sensors used in pavement SHM, one must consider short-term effects such as the high-temperature, high-moisture, and high-alkali environment in fresh concrete, as well as the effect of fine particles from concrete compounds. Long-term effects such as freezing-thawing cycles in actual pavement must also be considered.

Wireless Sensor Network (WSN)

Traditional wired sensors generally require high installation costs and lengthy installation times, as well as avoidance of wire damage problems. For example, Cho et al. (2008) reported that a contractor spent over $5,000 on each wired sensing channel in an SHM system in a high-rise building. Furthermore, the Hong Kong government spent more than $8 million to install a total of 350 wired sensing channels in the Tsing Ma Suspension Bridge (Farrar 2001). In view of such examples, economic motivation facilitates the adoption of wireless sensors to replace traditional wired sensors. In general, a wireless sensor network can utilize radio frequency (RF), acoustics, infrared transmission, and lasers as transmission media. In terms of SHM, RF has mainly been used, and it follows specific topologies and protocols associated with signal transmission.

Wireless Network Topologies

A WSN can be represented as a cluster in an SHM system, so the whole system can be structured using three common topologies for civil infrastructures: star, peer-to-peer, and multi-tier, as shown in Figure 9 (Lynch and Loh 2006).

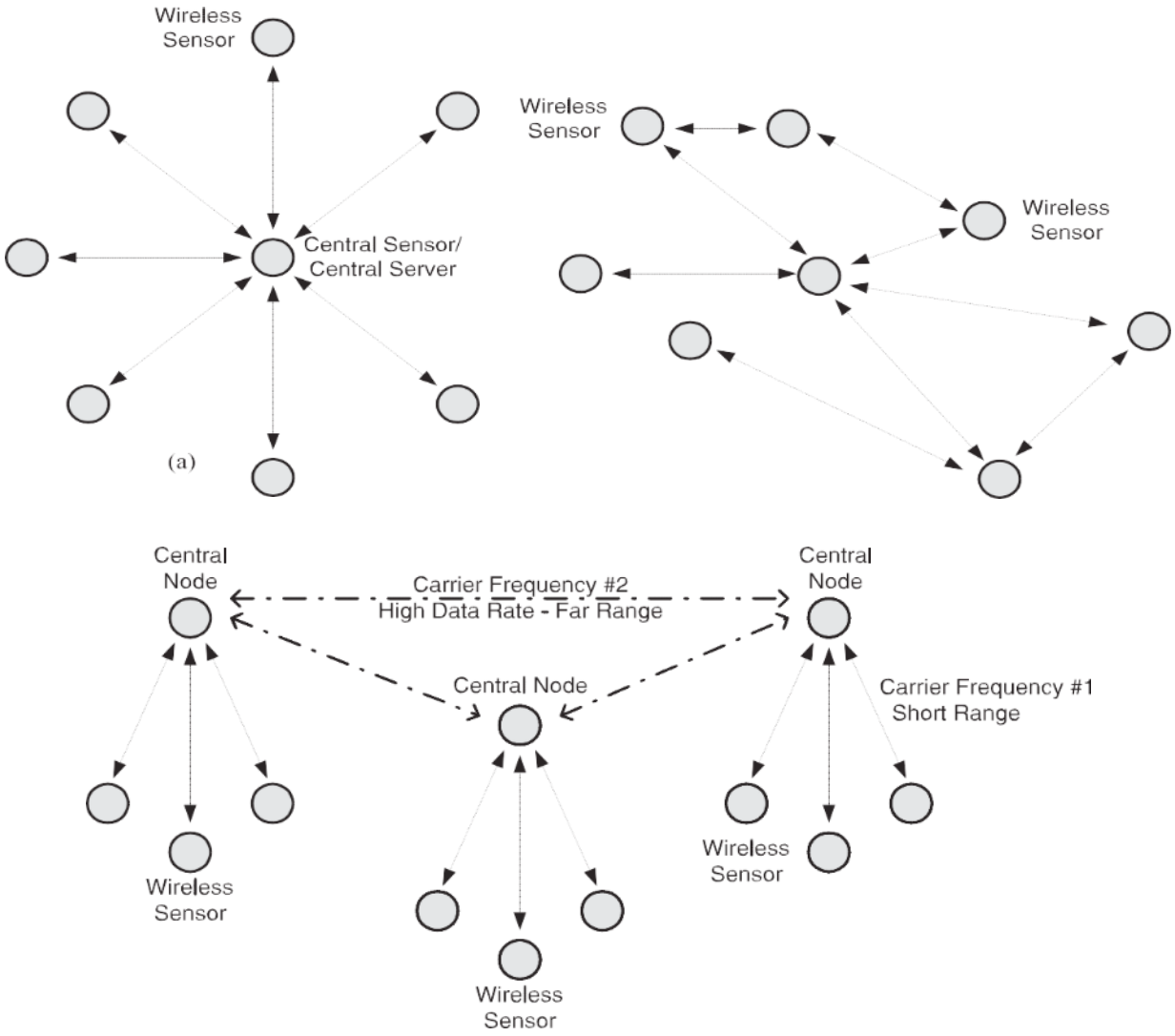

Lynch and Loh ©2006 SAGE Publications

Figure 9. Wireless network topologies: star (top left), peer-to-peer (top right), and multi-tier (bottom)

A star topology is designed to allow each node (wireless sensor) to communicate only with a designated central server. The connection between each node and the central server is usually via coaxial or fiber optical cable; the central server should be capable of data storage and high-rate transmission. A peer-to-peer topology is designed such that each node can communicate with any other without a central server in the system. This topology leaves sensors free to join or disconnect from the network. In other words, it can provide resiliency if an existing sensor fails or a new sensor is added. A multi-tier network is a topology in which there is more than one central server in the wireless system. In this topology, central servers can communicate with one another, and each of them can communicate with several designated wireless sensors as well (Lynch 2002, Lewis 2004, Lynch and Loh 2006, Aygun and Gungor 2011).

Wireless Network Protocols

Wireless network protocols are defined to standardize rules, conventions, and data structure for networked communication using various wireless devices (Lloret 2009). Such protocols govern how data are packaged, sent, and received in the entire wireless system. In general, wireless protocols are mainly based on two Institute of Electrical and Electronics Engineers (IEEE) communication standards: IEEE 802.11 and IEEE 802.15.4. These two standards for wireless systems have generally been associated with low power consumption, high throughput, and reasonable communication range. However, compared to an IEEE 802.11 device, an IEEE 802.15.4-based wireless system typically has longer battery life and greater range. ZigBee is a typical IEEE 802.15.4-based protocol; it will be further discussed in Chapter 4 (Al-Khatib et al. 2009, Aygun and Gungor 2011).

Passive and Active Sensors: Case of RFID System

RFID is a wireless identification technology using radio waves to identify an object (tag), acquire data, and write data to the tag (Ruan et al. 2011). Typically, an RFID system is composed of an RFID tag and an RFID reader. In general, RFID can be divided into passive and active sensor systems. Passive RFID needs no battery. Instead, its power comes from a wireless signal received and converted by an antenna. Conversely, active RFID requires a battery to provide its energy for functioning; active RFID is usually more expensive (Bouhouche et al. 2014). Inclusion of the battery leads the sensor to have a larger size and a limited lifetime. Active RFID also uses a larger capacity memory module than passive RFID. Additionally, active RIFD usually employs read/write devices, while passive RIFD uses read tags only. Passive RFID generally has a shorter read range (< 5 m), and a higher powered reader is therefore required (Roberts 2006). Moreover, RFID performance could be adversely affected by electromagnetically "noisy" environments (Lynch and Loh 2006, Roberts 2006). However, even though the terms "passive" or "active" are mainly used for RFID tags, sensor systems may generally be defined as passive or active depending on whether or not they are self-powered.

Wireless Sensor System Application in SHM of Pavement

As promising sensing paradigms providing Smart Pavement SHM, wireless sensors and sensor networks have been extensively investigated during the 21st century in both the academic and commercial fields; these technologies represent improvements in installation processes, data aggregation, signal analysis, sensor clustering, event localization, time synchronization, measurement progress, discrete monitoring, and event-based monitoring, as well as cost savings (Krüger et al. 2005). They also reduce the threat of wire damage in concrete.

Wireless sensor technologies were initially developed and deployed only for military and heavy industrial purposes (Silicon Laboratories, Inc. 2014a). Early applications of wireless sensor–based SHM in civil infrastructure began with bridges and buildings. Maser et al. (1996) built a two-level wireless telemetry system to measure strain and dynamic load changing in a highway bridge. The first level of this system contained small transducers powered by self-contained batteries that were used to detect the rotation, acceleration, and strain of the bridge structure. The

measured data were first transmitted through a wireless transceiver to an on-site data repository and then transmitted via cellular link to a second-level wireless system at the agency office (Maser et al. 1996). For pavement applications, Bennett et al. (1999) in the UK carried out a study assessing the performance of wireless sensors developed for monitoring strain and temperature in asphalt pavements; this might be the earliest wireless sensor–based pavement monitoring system. In the study, two strain gages and two thermometers were placed in an instrumented cylindrical core embedded in the pavement. Data collected from sensors were transmitted to a roadside laptop via an RF wireless link located approximately 4 m from the core. A success rate test conducted before opening to traffic proved that the wireless system had good reliability. However, after traffic opening, a decrease in transmission reliability was observed.

In the latter part of the 1990s, many researchers began working on wireless sensor platforms for civil infrastructure in which mobile computing and wireless transmission components converged with the sensing transducers (Lynch and Loh 2006). Table 6 provides a summary of the development of wireless sensor platforms and their corresponding technical parameters in both the commercial and academic fields from 1998 to 2009, based on the work by Lynch and Loh (2006), Cho et al. (2008), and Aygun and Gungor (2011).

Table 6. Summary table of development of wireless sensor platforms from 1998 to 2009

Developer and Year	Processor	Radio	Frequency	Availability
Straser and Kiremidjian (1998)	Motorola 68HC11	Proxim/ProxLink	900 MHz	Research
Bennett and Hayes-Gill (1999)	Hitachi H8/329	Radiometrix	418 MHz	Research
Lynch (2002)	Atmel AVR8515	Proxim RangeLan2	2.4 GHz	Research
Mitchell et al. (2002)	Cygnal 8051	Ericsson Bluetooth	2.4 GHz	Research
Kottapalli et al. (2003)	Microchip PIC16F73	BlueChip RBF915	900 MHz	Research
Lynch et al. (2003)	AV90S8515	Proxim RangeLan2	2.4 GHz	Research
Aoki et al. (2003)	Renesas H8/4069F	RealtekRTL-8019AS	–	Research
Basheer et al. (2003)	ARM7TDMI	Philips Blueberry	2.4 GHz	Research
Casciati et al. (2004)	–	Aurel XTR-915	914.5 MHz	Research
Wang et al. (2004)	Analog ADuC832	Linx Technologies	916 MHZ	Research
Mastroleon et al. (2004)	Microchip PIC-micro	BlueChip RFB915B	900 MHz	Research
Ou et al. (2004)	Atmega 8L	Chipcon CC1000	433 MHz	Research
Sazonov et al. (2004)	MSP 430F1611	Chipcon CC2420	2.4 GHz	Research
Farrar et al. (2005)	Intel Pentium	MotorolaneuRFon	2.4 GHz	Research
Pei et al. (2005)	Motorola 68HC11	Max-stream Xstream	2.4 GHz	Research
Musiani et al. (2007)	ATMega128L	ChipconCC1100	1 MHz	Research
Wang et al. (2007)	ATMega128	9XCite	900 MHz	Research
Bocca et al. (2009)	MSP430	ChipconCC2420	2.4 GHz	Research
Zhou et al. (2009)	MSP430	ChipconCC2500	2.4 GHz	Research
Zhu et al. (2009)	Atmega128	XStream	2.4 GHz	Research
Rockwell, Agre et al. (1999)	Intel Stron	Conexant RDSS9M	916 MHz	Commercial
US Berkeley- Crossbow (2003)	Atmega128L	Chipcon CC1000	916 MHz	Commercial
Intel-iMote2 (2003)	ARM7TDMI	Wireless BT Zeevo	2.4 GHz	Commercial
Microstrain, Galbreath et al. (2003)	PIC16F877	RF Monolithics	916 MHz	Commercial

Sources: Lynch and Loh 2006, Cho et al. 2008, and Aygun and Gungor 2011

Among the studies shown in the table, the focus was mainly on developing new wireless sensing units, and detailed descriptions of the underlying processes were summarized by Lynch and Loh (2006). Through standardization and establishment of the IEEE 802.15.4 standard in 2007, researchers began adapting IEEE 802.15.4 standards-based devices to traditional sensors to make them "wireless" (Salman et al. 2010). Because of these standards, it was unnecessary to develop all layers of the open systems interconnection (OSI) reference model for new systems from scratch, and these standards-based, independently developed wireless systems could easily communicate with one another as well (Nagayama and Spencer 2007).

As a common wireless technology, RFID has been used a great deal in wireless sensor systems as well. Lajnef et al. (2013) conducted a study to develop a passive RFID strain sensing system for asphalt pavement health monitoring and fatigue damage detection. The wireless sensor

system developed in this study was a passive RF system containing a low-power-consumption wireless integrated circuit sensor interfaced with a piezoelectric transducer. This piezoelectric ceramic transducer was designed with an array of ultra-low power floating gate (FG) computational circuits and could generate enough power to supply an FG analog processor for the sensor under stress. Each sensor node distributed in the pavement could store the data and then periodically transmit it to a vehicle-mounted RF reader.

A wireless sensor network can also be built by connecting traditional sensors to a commercial wireless transmission node. Xue et al. (2014) designed a sensing network with various commercial sensors for pavement health monitoring. In that report, which documented a 2011 study on Virginia State Route 114, the sensors included horizontal and vertical strain gages, load cells, thermocouples, and moisture sensors embedded at the bottom of a reconstruction pavement section. All embedded sensors were connected to V-Link wireless voltage nodes near the pavement through wires of different diameters connected to a wireless data logger to collect sensor data and transmit it to a base station via RF. In this system, V-Link nodes had to be first interfaced with the sensors using wires. Once data were collected, numerical simulation was conducted using the monitored strain response data through finite element analysis (FEA)–based software to compare it with the measured field data. Backcalculation of pavement dynamic modulus was also demonstrated in this study using data collected from a test vehicle. The fatigue cracking and rutting prediction models from the Mechanistic-Empirical Pavement Design Guide (MEPDG) were used to estimate the accumulated damage from distress; this was intended for use in initiating an early warning of pavement deterioration. However, according to the report, all vertical strain gages failed after five months, probably due to the harsh environment and excessive load (Xue et al. 2014).

Wireless sensor networks offer significant benefits for SHM applications. There are several different ways to build such networks, but using wireless systems for SHM in pavement is still in the study phase and there are still several challenges to be resolved. These challenges include a noisy wireless environment, limited bandwidth, low signal strength, hardware architecture, embedded software, energy consumption, battery life, the effects of weather on data collection, data aggregation, communication hops for large-scale structures, and other concerns.

FIELD INSTRUMENTATION AND EVALUATION OF COMMERCIAL OFF-THE-SHELF MEMS SENSORS AND WIRELESS SENSORS

This section describes a field demonstration of off-the-shelf MEMS sensors and wireless sensor system applications in actual in-service concrete applications. The specific objectives of the field demonstration are to:

- Evaluate the performance of commercially available off-the-shelf MEMS sensors and wireless sensors
- Identify current limitations of these MEMS sensors for SHM of pavement infrastructure
- Demonstrate how sensing data can be utilized to monitor concrete pavement behavior

Description of Site

In summer 2013, new jointed plain concrete pavement (JPCP) construction projects were carried out on US 30 under the supervision of the Iowa Department of Transportation (DOT). The project site was located near the southeast area of Ames, Iowa, as shown in Figure 10.

Figure 10. US 30 project location

To evaluate the performance of the off-the shelf MEMS sensors used for concrete pavement health monitoring, one section from this newly constructed highway pavement was selected for instrumentation to identify the requirements for a smart sensing system to advance SHM applications for concrete pavement systems.

Figure 11 illustrates the concrete pavement construction plan for this project.

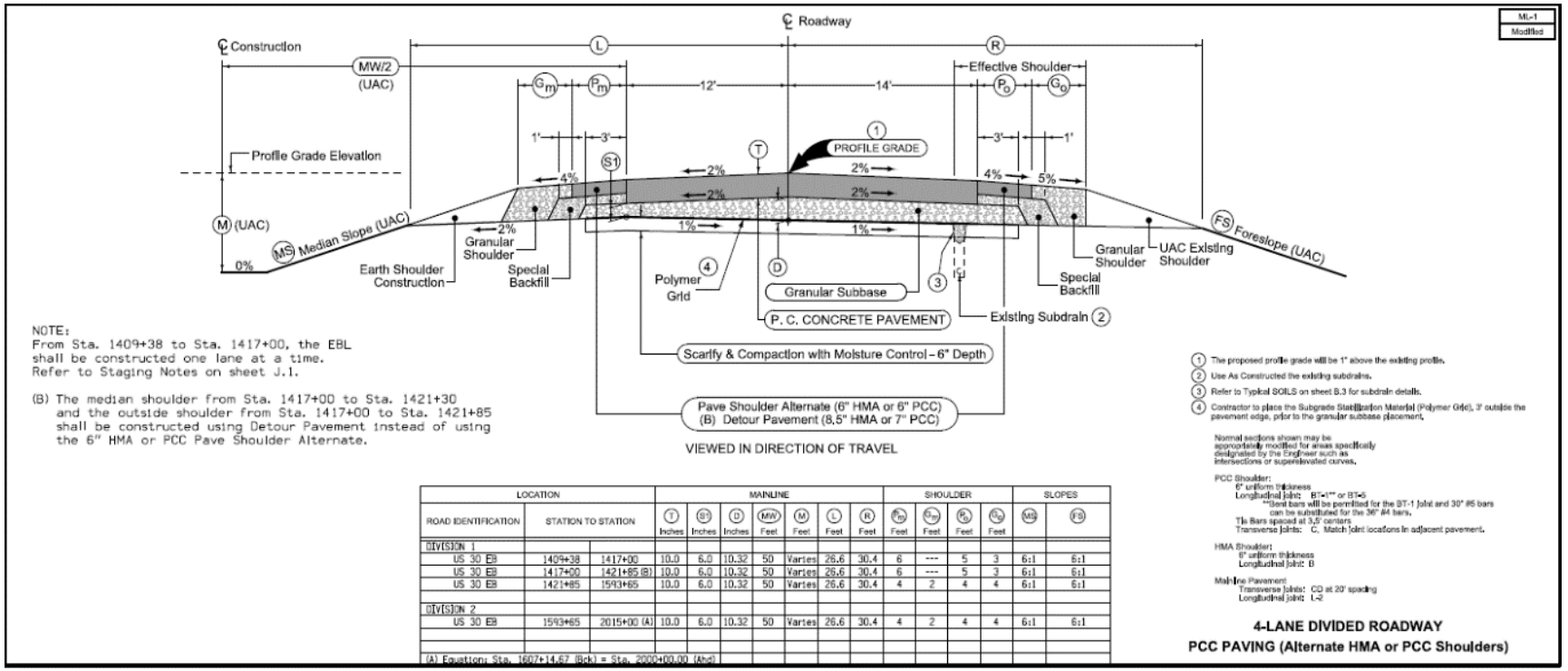

LOCATION			MAINLINE							SHOULDER				SLOPES	
ROAD IDENTIFICATION	STATION TO STATION		T Inches	ST Inches	D Inches	MW Feet	M Feet	L Feet	R Feet	P_m Feet	G_m Feet	P_o Feet	G_o Feet	MS	FS
DIVISION 1															
US 30 EB	1409+38	1417+00	10.0	6.0	10.32	50	Varies	26.6	30.4	6	---	5	3	6:1	6:1
US 30 EB	1417+00	1421+85 (B)	10.0	6.0	10.32	50	Varies	26.6	30.4	6	---	5	3	6:1	6:1
US 30 EB	1421+85	1593+65	10.0	6.0	10.32	50	Varies	26.6	30.4	4	2	4	4	6:1	6:1
DIVISION 2															
US 30 EB	1593+65	2015+00 (A)	10.0	6.0	10.32	50	Varies	26.6	30.4	4	2	4	4	6:1	6:1
(A) Equation: Sta. 1607+14.67 (Bck) = Sta. 2000+00.00 (Ahd)															

Figure 11. US 30 construction plan

The newly constructed pavement section was approximately 10 in. thick and constructed above a granular subbase with a thickness ranging from 6 to 10.3 in. The PCC pavement was crowned with a 2.0% transverse slope and had widths of 12 ft and 14 ft for the passing lane and travel lane, respectively. The transverse joint spacing was set at 20 ft, reflecting general practice in Iowa. Dowel bars with baskets were placed on the subbase before concrete paving.

Installation of sensors was conducted on May 23, 2013, one day before concrete paving commenced on US 30 at 8:00 a.m. on May 24, 2013. A slipform paver moved from west to east to pour fresh concrete on the subbase. A vibrator followed the paver to consolidate the fresh concrete using vibration tubes. Surface smoothing was performed manually. A slipform paver dragging a piece of burlap was used to create texture for the pavement surface, and a chemical curing compound was sprayed on the paving surface. Shoulder backfilling was conducted approximately 14 days after concrete paving; a 6 in. thick hot-mix asphalt (HMA) shoulder was then placed on June 10, 3 days after shoulder backfilling. One day later, a granular shoulder was added to the pavement. The constructed pavement was opened to traffic on June 14, 2013. Table 7 lists details of the construction timeline.

Table 7. US 30 construction timeline

Timeline	
Date	**Activities**
May 23, 2013	Sensor installation
May 24, 2013	Concrete paving
June 7, 2013	Backfilling for shoulder
June 10, 2013	HMA shoulder paving
June 11, 2013	Granular shoulder paving
June 14, 2013	Opened to traffic

Description of Sensors

Temperature and moisture are vital factors contributing to concrete properties such as strength and durability. Low temperatures and rapid loss of moisture can result in insufficient development of strength, and different temperature and moisture gradients in concrete can contribute to curling and warping behaviors that may result in cracks if the induced stress exceeds the concrete strength. A total of 30 sensors, including off-the-shelf MEMS-based temperature and moisture sensors and strain gages, were evaluated in this study. The sensors used were RFID temperature tags, Sensirion SHT71 digital humidity sensors, Thermochron iButtons, and Geokon model 4200 strain gages. A detailed description of each type of sensor is presented in the following sections.

RFID Temperature Tag

The wireless RFID tags from the HardTrack Concrete Monitoring System by WAKE, Inc. were selected for temperature monitoring due to their low cost, extensive communication range,

durability in concrete, and low power consumption. This active wireless RFID tag is a MEMS-based temperature sensor with advanced ultra-high frequency (UHF) RF technology that can provide real-time data collection and storage. This RFID system consists of an RFID transponder called i-Q32T and a portable handheld transceiver called Pro, which are shown in Figure 12 and Figure 13, respectively (Identec Solutions 2008, WAKE, Inc. 2014).

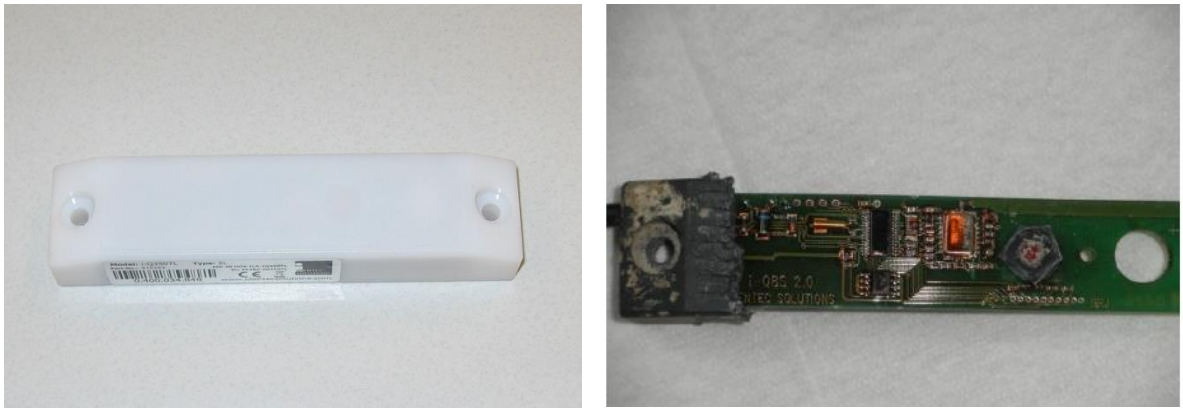

Figure 12. i-Q32T wireless RFID transponder

Figure 13. HardTrack portable handheld transceiver Pro

Figure 12 shows that the tag contains an internal temperature logger to capture the temperature of concrete at definable intervals and a battery for power (Identec Solutions 2008).

The antenna inside this tag enables the Pro to identify the tag and read/extract data or change the time interval. In this study, temperature readings were taken every 30 minutes. By communicating with the portable Pro, the collected temperature data could be imported into this handheld transceiver for data saving and for concrete maturity calculation using a PCC maturity concept. Consequently, this RFID tag was applicable to concrete temperature monitoring, and its excellent accuracy exceeded that of the ASTM C1074-93 requirement. This tag had a claimed capability of transmitting and receiving data within distances of up to 100 ft (30 m) from the

handheld device or up to 300 ft (100 m) from a fixed interrogator; its operational life could be greater than six years due to its low power consumption (Identec Solutions 2008).

Figure 14 illustrates the whole RFID system, including the portable handheld transceiver Pro.

Figure 14. RFID tag and portable Pro

In this system, the i-Q32T RFID tag can be divided into an embedded probe and an extended probe. The embedded probe is the tag the temperature logger installed inside of the i-Q32T tag, but when making deep pours the RFID tag can be equipped with a stainless steel temperature probe, referred to as an extended probe in this report, to enable it to penetrate deeper into large concrete structures. RFID extended probes are typically used in large-scale structures like dams to measure the temperature of concrete several feet below the concrete surface, but a i-Q32T tag with an antenna can still be placed at the surface to transmit data. The biggest advantage of the extended probe is that it can be removed from the tag so the tag can be recycled if there is no need to use the extended probe. Both the embedded probe and extended probe are shown in Figure 14.

MEMS Digital Humidity Sensor

The Sensirion SHT71 digital humidity sensor evaluated in this study is classified as a commercial multifunctional off-the-shelf MEMS sensor that can simultaneously measure relative humidity (RH) and temperature. Figure 15 shows the MEMS digital humidity sensor and the evaluation kit, respectively. The commercial MEMS digital humidity sensor, developed by Sensirion, Inc., is a metal pin-based sensor integrating both the sensing elements and signal processing circuitry on a silicon chip to provide fully calibrated digital output. In this sensor, a unique capacitive sensing element consisting of paired conductors is used to capture RH while another band-gap sensor measures temperature. The paired conductors are separated by a dielectric, a polymer that absorbs or releases water proportionally to the relative environmental

humidity. The capacitance change is measured by an electronic circuit to calculate RH (Sensirion, Inc. 2014). To simultaneously protect the sensor from interference, a micro-machined finger electrode system with different polymer-covered layers is used to produce the capacitance for this MEMS sensor.

The MEMS digital humidity sensors must be connected to evaluation kit EK-H4 (see Figure 15) at all times to continuously monitor temperature and RH.

Figure 15. Sensirion sensor system: Sensirion SHT71 sensor (left) and evaluation kit (right)

Moreover, it should also be pointed out that this evaluation kit does not have memory, so a laptop with related software must be connected at all times to store the measurements. Time intervals can be set through the laptop; in this study, measurements were performed at one-minute intervals.

Thermochron iButton

The Thermochron iButton from Maxim Integrated Products, Inc. is designed for temperature measurement and storage. This low-cost and reliable temperature sensor is equipped with a wide-temperature-range thermometer (14 to 185°F) and has a protected memory section. It is able to record time and temperature at user-defined intervals of up to 255 minutes, and a total of 2,048 temperature readings can be stored (Maxim Integrated 2014). Therefore, the monitoring period can be extended to 340 days based on the maximum measurement interval if the internal battery can guarantee a minimum of two years' working time at room temperature. Furthermore, this iButton sensor is protected by a durable stainless steel shield with a plastic cover to ensure that it is working properly in the concrete environment.

The main advantages of the iButton temperature sensor are large memory, long battery life, rugged packaging, and low cost. iButtons have been used in field projects for temperature monitoring of fresh concrete during construction. For example, the Texas Department of Transportation conducted a demonstration project in 1999 using a large number of iButtons, and the Des Moines International Airport utilized iButtons to monitor the temperature history of fresh concrete (Tully 2007). Figure 16 shows an iButton.

Figure 16. Thermochron iButton and USB cable

It can be seen in Figure 16 that the iButton requires a USB cable for data downloading. Unlike the MEMS digital humidity sensor, the iButton does not require a constant connection with the laptop because it has its own memory system. In this study, iButtons were used as reference sensors to measure the internal temperature of concrete at 30-minute measuring intervals.

Strain Gage

The strain gage evaluated in this project was the Model 4200 Vibrating Wire Strain Gage manufactured by Geokon, Inc., shown in Figure 17.

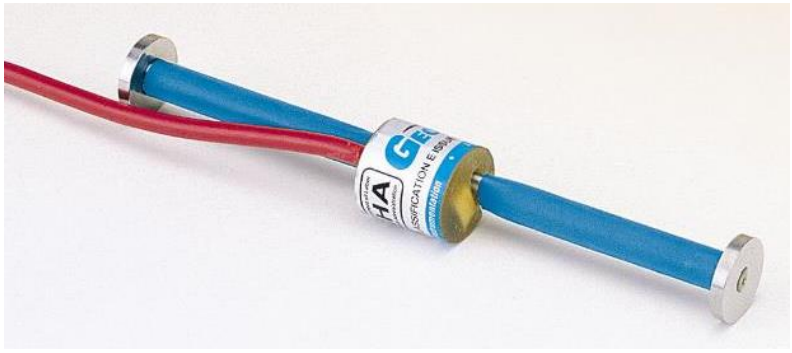

Figure 17. Geokon model 4200 strain gage

This is a 6 in. long static strain sensor designed for direct embedment in concrete; it makes measurements based on a vibrating wire principle.

When the gage is embedded in concrete, strain changes cause the two metal blocks to move relative to one another, and the resulting tension generated in the steel wire can be determined by plucking the wire and measuring its resonant frequency of vibration (Geokon, Inc. 2014).

The advantages of the Model 4200 Vibrating Wire Strain Gage claimed by its manufacturer include excellent long-term stability, maximum resistance to the effects of water, and a frequency output suitable for transmission over very long cables. Use of stainless steel ensures that it is waterproof and corrosion-free, but strain measurement is affected by temperature, so the Model 4200 strain gage incorporates an internal thermistor for simultaneous measurement of temperature.

Figure 18 shows the entire strain measurement system, including the Geokon Model 8002 data logger used for data collection.

Figure 18. Data logger and Model 4200 strain gage

This data logger can be conveniently powered either by widely available alkaline D cells or by an external 12 V source. It has an operating time ranging from eight days to two years, depending on the scan interval. However, in this study the strain reading was recorded every minute, so the estimated operational time was about two and a half days.

Installation of Sensors

The instrumented pavement section was located in the driving lane of US 30. A total of 30 sensors, including 14 RFID temperature tags (9 extended probes and 5 embedded probes), 4 MEMS digital humidity sensors, 5 iButtons, and 7 longitudinal strain gages were installed at different locations and at various concrete pavement depths and placed near a DAS for ambient temperature monitoring.

Location of Sensors

In general, concrete pavement edges and corners suffer more from load than other locations (Darestani 2007), so the locations selected for this project were the corners and mid-panels of the slab. Figure 19 shows the detailed instrumentation plan of this slab.

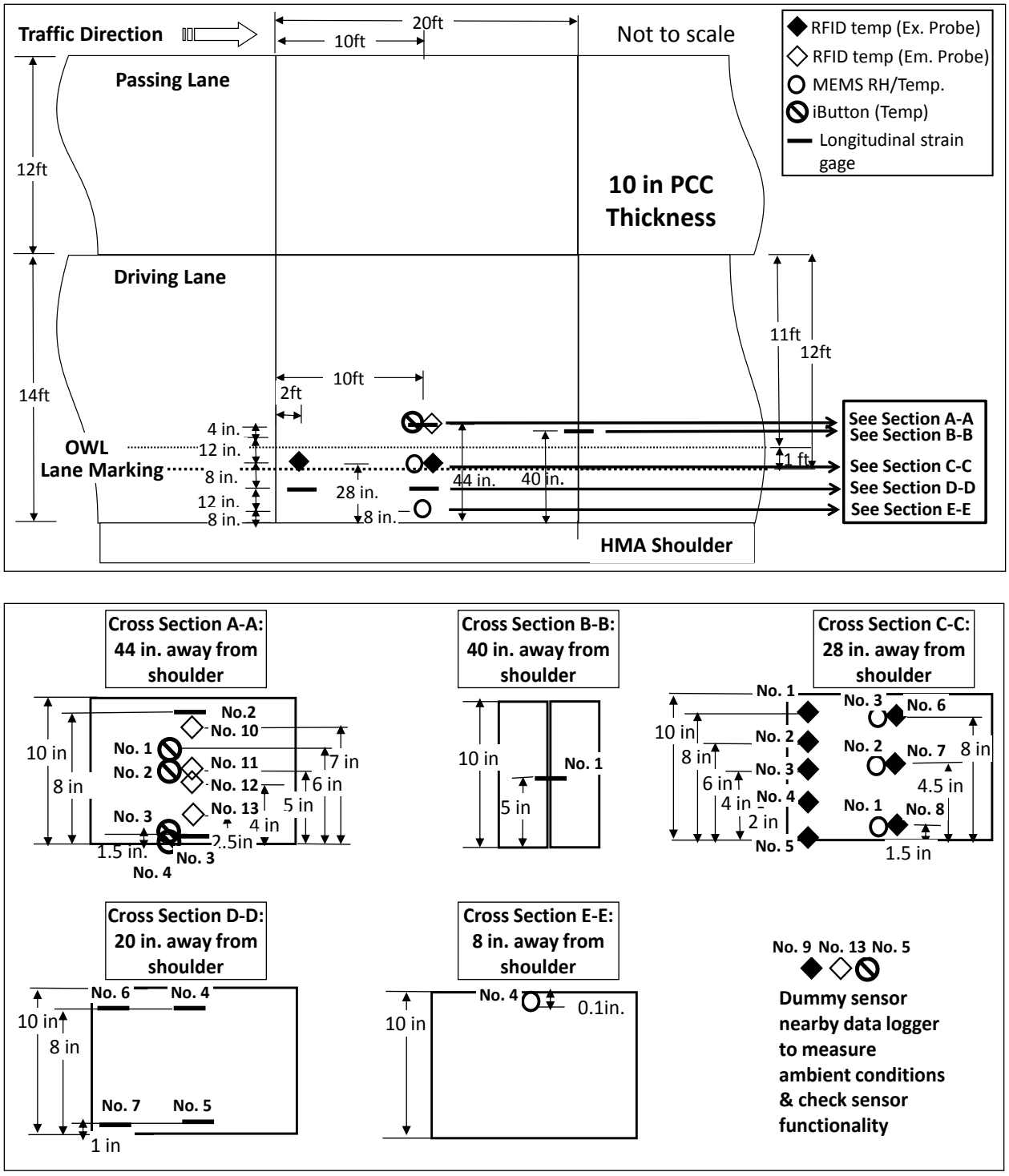

Figure 19. Sensor instrumentation plan: top view (top) and cross-section view (bottom)

Referring to these two views in the figure, five cross-sections (Sections A-A through E-E) were totally instrumented with these sensors. The distances from each section to the shoulder were all different. Among these cross-sections, Section A-A, 44 in. away from the HMA shoulder, was instrumented at mid-span using four RFID embedded probes, four iButtons, and two strain

gages. The RFID tags were installed at distances of 3, 5, 6, and 7.5 in. below the pavement surface, and the iButtons were installed at distances of 4, 5, 8.5, and 10 in. below the surface, respectively. Strain gages were embedded only at the top and bottom positions, 2 and 8.5 in. away from the pavement surface. Section B-B, located at the joint between two adjacent slabs, was 40 in. away from the HMA shoulder. It was instrumented using only one strain gage under a dowel bar, as shown in Figure 20.

Figure 20. Installation of strain gage at joint

Section C-C was 28 in. away from the shoulder. It was instrumented using eight RFID extended probes and three MEMS digital humidity sensors. Among these embedded RFID tags, five RFID extended probes were embedded in the corner at distances of 2, 4, 6, 8, and 10 in. below the surface, and three RFID extended probes were embedded in the mid-span at distances of 2, 5.5, and 8.5 in. below the pavement surface. The three MEMS digital humidity sensors were embedded at the same locations where the three RFID extended probes were installed. Section D-D, located 20 in. away from the HMA shoulder, was instrumented by strain gages only. In this section, two strain gages were embedded at the top and bottom in the corner at 2 and 9 in. below the surface. Another pair of strain gages was embedded at the top and bottom in the center, 2 and 9 in., respectively, below the surface. The last section, E-E, was 8 in. away from the shoulder and was instrumented using only one MEMS digital humidity sensor, located just 0.1 in. below the surface at the mid-span.

Processes of Installation

All sensors were pre-installed one day before concrete paving, with the installation of the sensors beginning in the subbase on the morning of May 23, 2013. Prior to installing the sensors, wooden bars were inserted in the subbase in accordance with the previous installation plan. The length of these wooden bars above the subbase surface was approximately 10 in., almost

equaling the thickness of the PCC slab. In the next step, all sensors were mounted to these wooden bars using zip ties to fix their positions during pavement construction, as shown in Figure 21.

Figure 21. Installation of sensors near the mid-span edge

As shown in the above two figures, two wooden bars were used to fix the location of the strain gages and RFID tags. While a wooden bar would not cause any issues related to thermal conductivity that might may affect strain and temperature measurement, it should be pointed out that the strain gages and RFID tags were placed in alignment with the traffic direction, which was the same as the direction of concrete paving. Additionally, the iButtons and MEMS digital humidity sensors were mounted on the back of the wooden bars to reduce the direct force of concrete paving. All of these strategies were applied to help the sensors survive during paving construction.

It should be noted that, during the installation of the sensors, the wires from the sensors needed extra attention because there was no way to repair them once inside the concrete if they were broken or had loose connection issues. In this project, all sensors deployed in the US 30 project were wired sensors except for the RFID tags, but even the RFID extended probe had a long cable between the temperature probe and the i-Q32T tag. To protect these wires, all were spliced and soldered to create connections and then placed in a polyvinyl chloride (PVC) pipe, as shown in Figure 22.

Figure 22. Wires in PVC pipe

The PVC pipes were then placed in a ditch dug in advance, and the wires were connected to the DAS, as shown in Figure 23.

Figure 23. PVC pipe in ditch with wires

Data Acquisition System (DAS)

Figure 24 shows the on-site DAS of the sensors used in the US 30 project.

Figure 24. Data acquisition system

It can be seen in Figure 24 that both the DAS and the batteries were stored in a plastic shield box. The laptop was used to collect data from the MEMS digital humidity sensors, and the rechargeable batteries were used to supply power to the laptop only. The box, located approximately 14 ft away from the HMA shoulder, was covered by an orange protective blanket. All devices were placed on a wooden board supported by two concrete caps, and a plastic bag was used to protect them from rain. These protective strategies were used to protect the DAS from animals, rain, wind, etc., because it was important to keep the DAS away from external disturbances. Additionally, ambient RFID tags (both extended probes and embedded probes) and iButtons were placed beside the shield box to capture ambient temperature conditions, as shown in Figure 25.

Figure 25. Ambient temperature sensors placed beside the shield box

Among the sensors deployed in the US 30 project, only the RFID tags and iButtons were equipped with internal batteries. The MEMS digital humidity sensors and strain gages, as well as the DAS, required batteries to make them function during the monitoring period. However, the batteries could only provide three days' power for the laptop, so data acquisition and battery replacement were scheduled every two days to achieve continuous data collection during the initial stages until June 28, 2013. However, these procedures were time- and labor-intensive, so different summer and winter data acquisition times were scheduled due to traffic and environmental conditions.

Concrete Paving

Concrete paving for the instrumented pavement section started at 7:45 a.m. on May 24, 2013. Before concrete paving, dowel bars with baskets were placed above the subbase. The average water-cement ratio for the concrete ranged from 0.4 to 0.43. The times of initial and final set were determined to be 4.84 and 7.17 hours, respectively, in accordance with ASTM C 403 (Appendix B). During road construction, both a paver and a vibrator were used. A large amount of fresh concrete first poured on the subbase was spread by the passing paver, as shown in Figure 26.

Figure 26. Concrete paving

A vibrator with vibration tubes followed the paver to produce consolidated concrete. The vibrator leveled off the concrete as it passed through, and the workers behind the vibrator then smoothed the surface. Finally, the surface was textured by dragging a piece of burlap in the longitudinal direction. Water was sprayed onto the pavement surface after texturing, followed by the spraying of chemical components for curing purposes.

However, both the paver and vibrator were potential threats to the sensors due to the auger and vibration forces that the paver and vibrator produced during pavement construction, which might break either the sensors or the wires. Moreover, dropping a heavy mass of concrete could crush the sensors and tear the wires. Therefore, to protect the sensors as much as possible, fresh concrete was carefully pre-poured on the top of sensors to mitigate the force from the paver, vibrator, and dropped concrete, as shown in Figure 27.

Figure 27. Sensor protection during road construction: obtaining fresh concrete from the paver (top) and pouring concrete on the sensors (bottom)

After concrete paving, a MEMS digital humidity sensor was embedded 0.1 in. below the pavement surface at cross-section E-E, as shown in Figure 28.

Figure 28. Embedment of MEMS digital humidity sensors

The temperature probes of the RFID tags (extended probes) were mounted on wooden bars, and the i-Q32T tags (transponders) were placed in a protective wooden box beside the concrete slab, as shown in Figure 29.

Figure 29. RFID extended probe in wooden box

This box was used to protect the tags during shoulder construction, as shown in Figure 30.

Figure 30. Shoulder construction: backfilling (top) and HMA shoulder paving (bottom)

As a result, the data measured inside the concrete could be successfully transmitted from the transponders in the box. Figure 31 shows the opening to traffic on June 14, 2013; the protective wooden box for the RFID tags can be seen at the bottom of the figure.

Figure 31. Opening to traffic

Sensor Performance Evaluation

This section provides detailed descriptions of both the quantity and quality evaluation of the sensor performance. Because JPCP behavior before traffic opening is largely affected by environmental conditions, the effects of temperature and moisture are discussed. Temperature, moisture, and strain profiles obtained by the sensors used in this research are provided in Appendix A.

In concrete pavement, knowledge of the temperature profile is essential for stress analysis. Different temperature gradients throughout the entire concrete depth and excessively high ambient temperatures, such as those during heat waves, can result in structural failure. In this study, temperature measurements were mainly captured by the RFID tags, MEMS digital humidity sensors, and iButtons embedded throughout the entire depth of the PCC pavement. The measurements from the iButtons were used as reference temperatures to be compared to the other two types of temperature sensors. Moisture content plays a significant role in cement hydration because concrete may not develop properly under low-moisture conditions. Moisture gradient changes inside the concrete, just like temperature gradient changes, can lead to concrete deformation. Moisture content distribution is also crucial to evaluating the severity of shrinkage during the setting and hardening processes. However, the moisture content measured in concrete is usually represented by the humidity level. Moisture typically refers to the amount of water present in a material, but humidity is the amount of water vapor present in the air and can be represented as either absolute or relative humidity (Das 2010, Ye et al. 2006). Absolute humidity is the ratio of the mass of water vapor to the volume of air or gas, while relative humidity refers to the percent of water content in the air compared to the saturated moisture level at the same temperature and pressure (Ye et al. 2006).

Monitoring Period Overview

The entire monitoring period extended from May 24, 2013 to April 1, 2014, approximately 10 months after traffic opening. However, to obtain continuous data, data acquisition had to be

scheduled every two days. This was an unrealistic requirement over the entire period due to the remote location of the DAS, the sometimes harsh climate, and the limited labor available. As a result, the longest continuously monitored period actually used is described and discussed.

RFID Tags (Extended Probe)

Figure 32 illustrates the temperature profiles captured by the RFID extended probes at the slab corner and center.

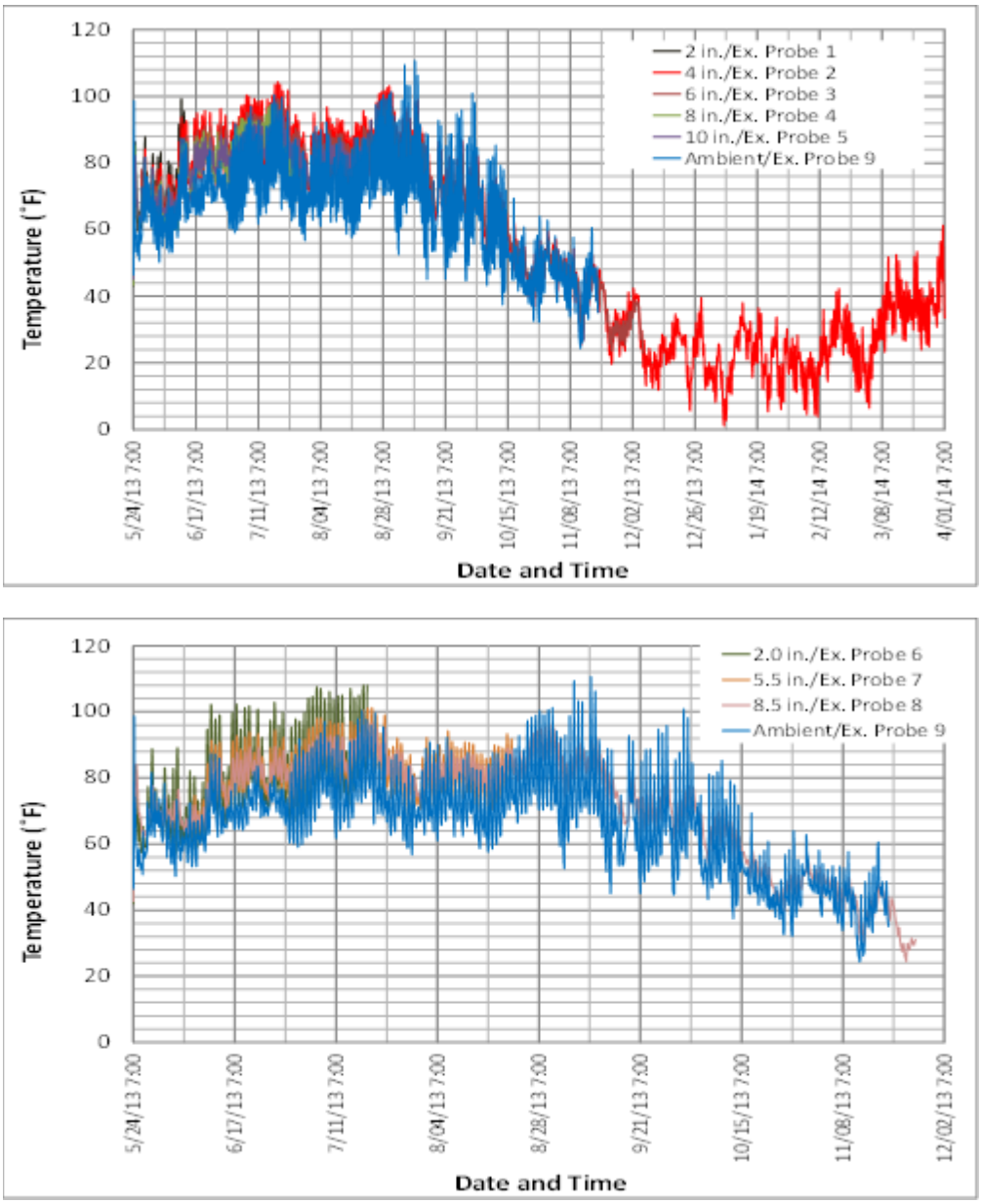

Figure 32. RFID extended probe measurement: in the corner (top) and in the center (bottom)

Probes 1 through 5 were 2, 4, 6, 8, and 10 in., respectively, below the pavement surface, and Probe 9 was an ambient temperature sensor. Probes 6 through 8 were located 2, 5.5, and 8.5 in., respectively, below the surface. As seen in Figure 32, a maximum temperature of 111°F and a minimum temperature of 0°F were observed during the monitoring period. The average temperature rose to 80°F in summer and rapidly fell to 20°F in winter. However, the sensors embedded in the center were not functional after December 2013.

RFID Tags (Embedded Probe)

Figure 33 illustrates the temperature profile captured by the RFID embedded probes in the mid-span 44 in. away from the shoulder. RIFD extended probes 10 through 13 were embedded 3, 5, 6, and 7.5 in., respectively, below the pavement surface, and Probe 14 was an ambient temperature sensor. As seen in Figure 33, the temperature ranged from 20°F to 108°F before December 6, 2013, similar to the temperature captured by the RFID extended probes embedded in the center. However, fewer and fewer RFID embedded probes remained functional as time passed, and no embedded probes were functional after December 7, 2013. Note that the ambient temperature probe (14) was removed on July 19, 2013. Furthermore, based on observation, it was found that the temperature difference between the top and bottom of the concrete was in the range of 4°F to 12°F.

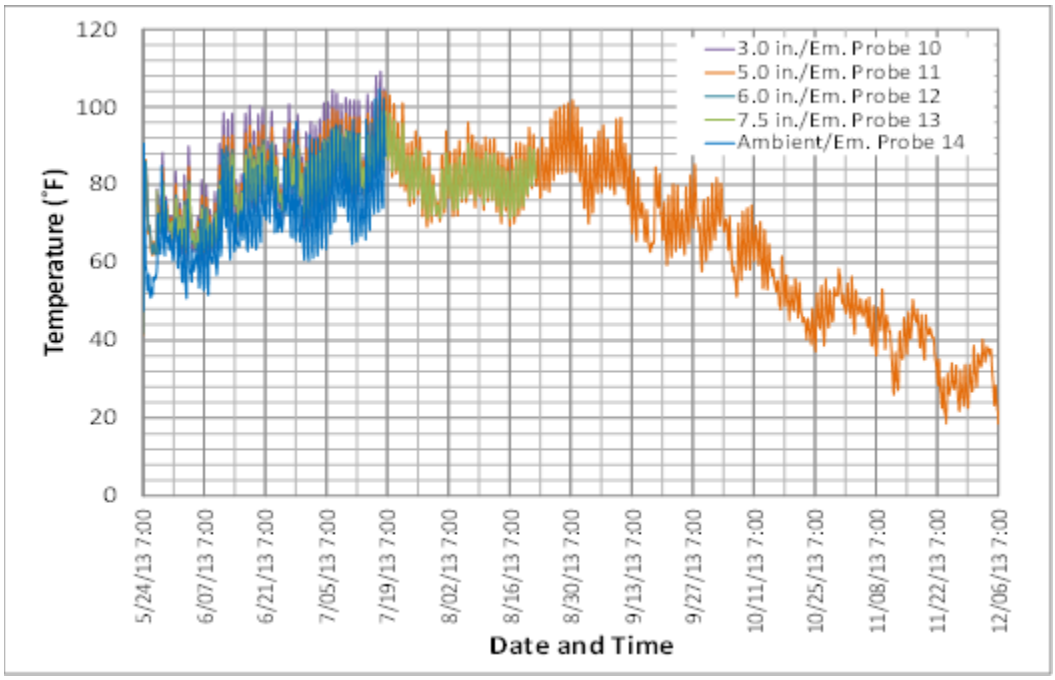

Figure 33. RFID embedded probe measurement in the mid-span

MEMS Digital Humidity Sensors

Four MEMS digital humidity sensors were embedded in US Highway 30. Sensors 1 through 3 were embedded 8.5, 5.5, and 2 in., respectively, below the pavement surface, and Sensor 4 was

just 0.1 in. below the pavement surface. However, Sensors 1 and 2 were unable to collect data within just a few hours after concrete paving. This could probably be attributed to wire damage or loose connections caused by the concrete paver, the vibrator, or the high-alkali environment prevailing during concrete hydration. Note also that data could not be acquired in the period from May 26 through May 28, 2013 because the battery (power supply) for the DAS was not recharged. Figure 34 and Figure 35 show the temperature and RH profiles captured by the MEMS digital humidity sensors.

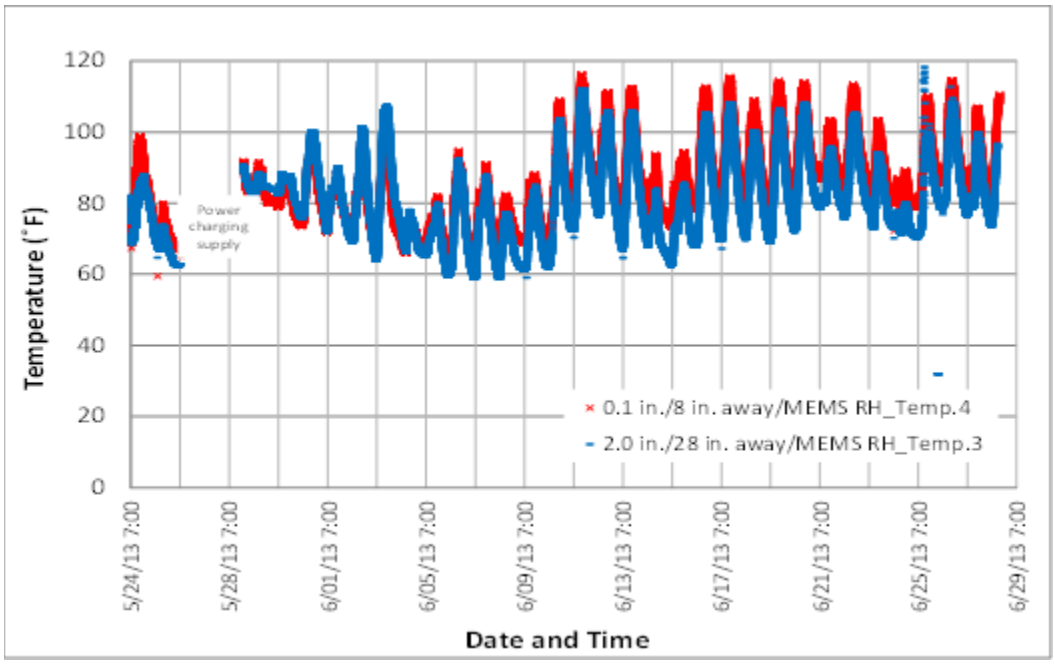

Figure 34. Temperature measurements from the MEMS digital humidity sensors

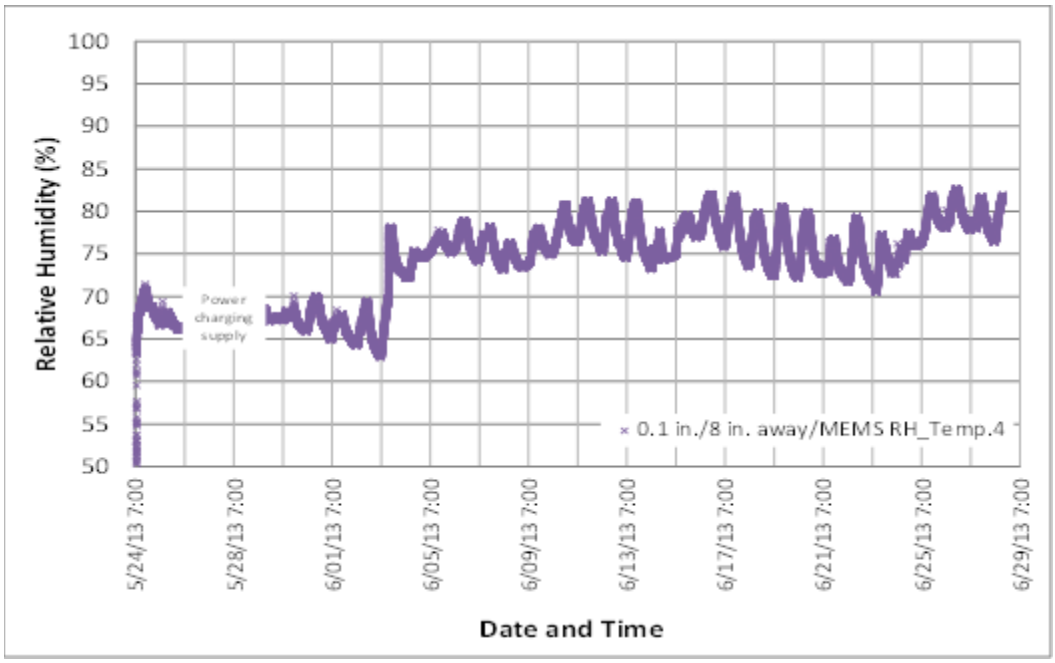

Figure 35. RH measurements from the MEMS digital humidity sensor

According to Figure 34, the temperature before June 29 ranged from 60°F to 120°F. It can also be seen that Sensor 4 in its initial stage reflected higher temperatures in the daytime and lower temperatures at night. This is because Sensor 4 was closer to the pavement surface, so it was more easily affected by ambient environmental conditions such as solar radiation. Meanwhile, the temperature at the pavement top dropped more rapidly than that at the bottom. However, in later stages, Sensor 4 also exhibited higher temperatures at night; this was probably due to a heat wave reported in June 2013. According to Figure 35, the RH was about 67% in the beginning of the monitoring period followed by a sharp increase in RH from 63% to 78% observed on June 3, 2013, due to a serious thunderstorm occurring on June 3 and 4, 2013. Following that, the RH fluctuated between 70% and 80% most of the time.

iButtons

Figure 36 illustrates the temperature measurements taken from the iButtons between May 24 and August 22, 2013.

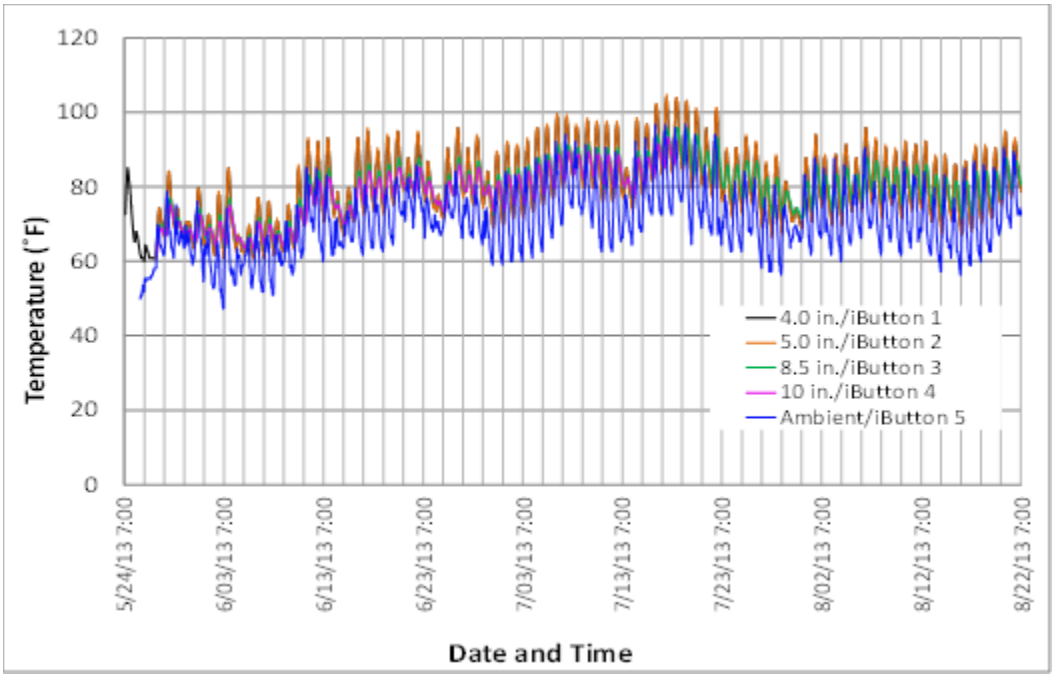

Figure 36. Temperature measurements from the iButtons

iButtons 1 through 4 were embedded 4, 5, 8.4, and 10 in., respectively, below the pavement surface, and iButton 5 was an ambient temperature sensor. Among these sensors, only one iButton (4) stopped functioning (on July 18, 2013). It can be seen that the temperatures measured by the iButtons ranged from 47°F to 105°F, lower than the values captured by the RFID tags. This was because the highest temperature was captured by iButtons 1 and 2 installed at the midpoint of the pavement depth, so their readings were lower than the values captured by the RFID tags and the MEMS digital humidity sensors located near the top of the pavement. However, comparing ambient temperature measurements, the ambient RFID extended probe and embedded probe had the same reading, approximately 2°F higher than the ambient iButton's measurement.

Strain Gages

Strain is a significant indicator of concrete structural quality. Figure 37 illustrates the strain change captured in the period between May 24 and June 29, 2013.

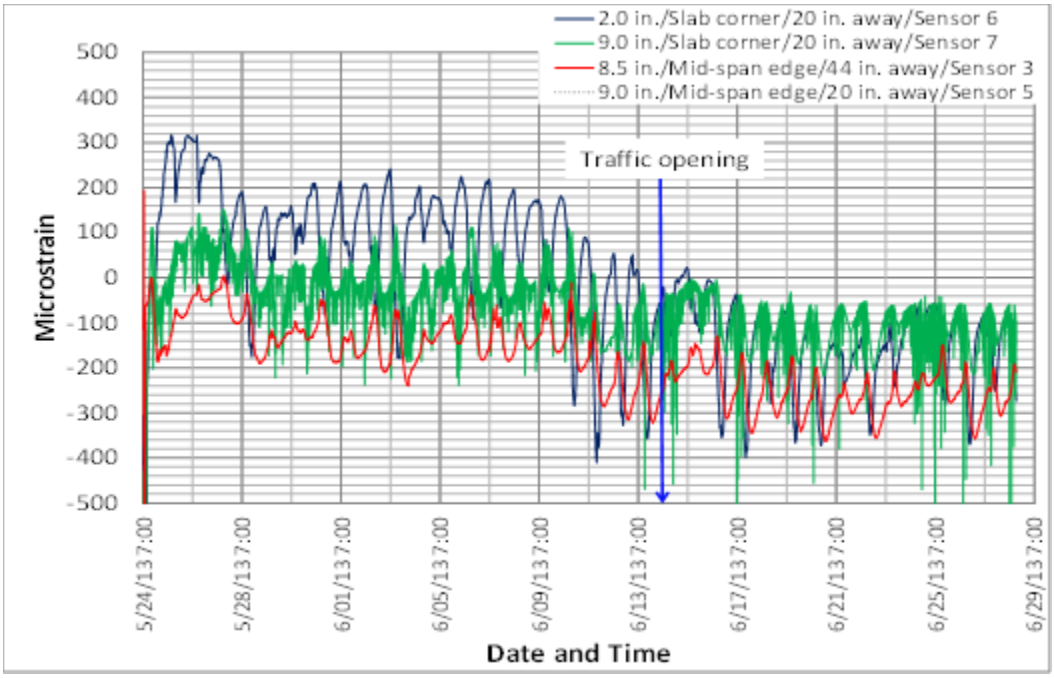

Figure 37. Strain measurement

Strain Gages 3 and 5 were embedded 8.5 and 9 in., respectively, below the pavement surface at the slab corner, while Strain Gages 6 and 7 were embedded 2 and 9 in., respectively, below the pavement surface at the mid-span edge. The other strain gages, Strain Gages 1, 2, and 4, stopped functioning immediately, probably due to wire issues. In Figure 37, positive and negative microstrain represents tension and compression, respectively. However, after opening to traffic, the strain readings were greatly affected by the traffic load. The strain behavior after traffic activity began was not in the research scope and is therefore not discussed in this section. A detailed description of strain behavior before opening to traffic is provided in the next section.

Before Opening to Traffic (May 2013 to June 2013)

Performance of Sensors

The overall monitoring period was divided into three periods: before opening to traffic, two months after opening to traffic (summer), and six months after opening to traffic (winter). The pavement was opened to traffic on June 14, 2013, and there was therefore no vehicular effect on pavement properties before that date. The strain behavior of the pavement associated with environmental effects from temperature and moisture could be analyzed for this period. Figure 38 through Figure 42 illustrate temperature, RH, and strain captured by the sensors.

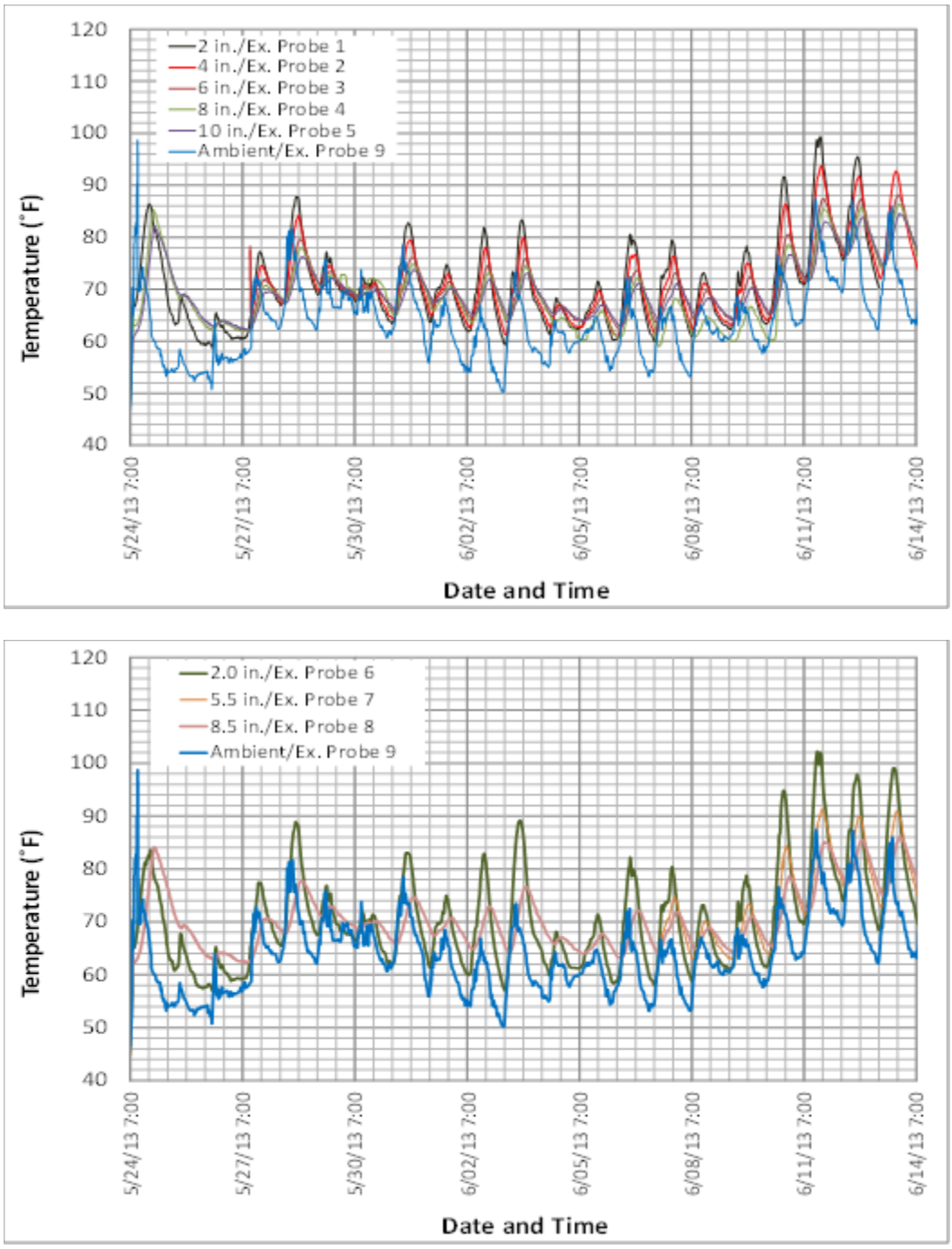

Figure 38. Measurements from the RFID extended probes before opening to traffic: in the corner (top) and in the center (bottom)

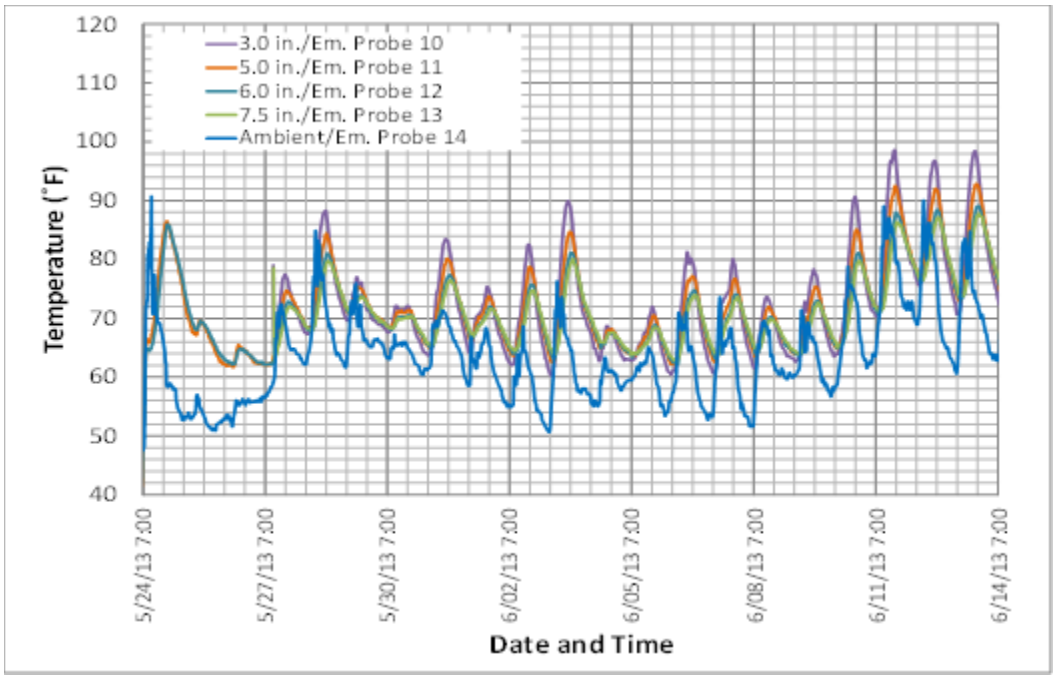

Figure 39. Measurements from the RFID embedded probes before opening to traffic

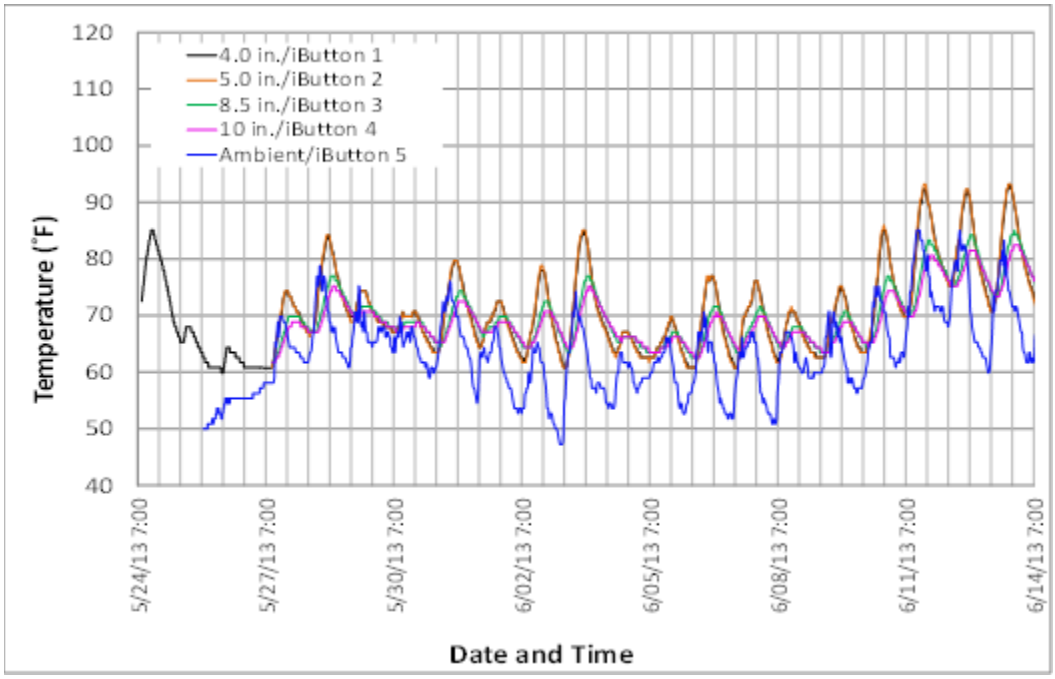

Figure 40. Measurements from the iButtons before opening to traffic

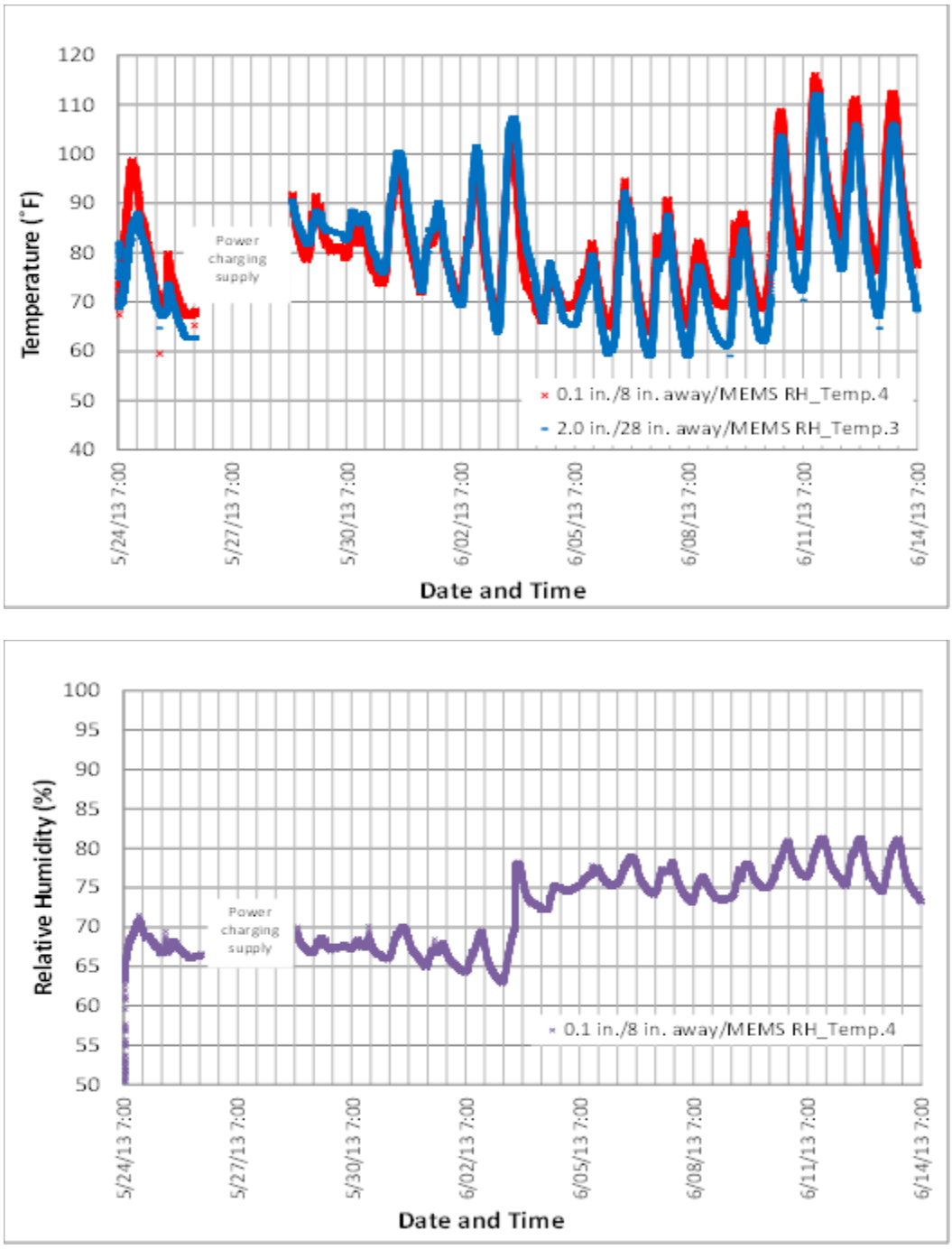

Figure 41. MEMS digital humidity sensor measurements before opening to traffic: temperature measurements (top) and RH measurements (bottom)

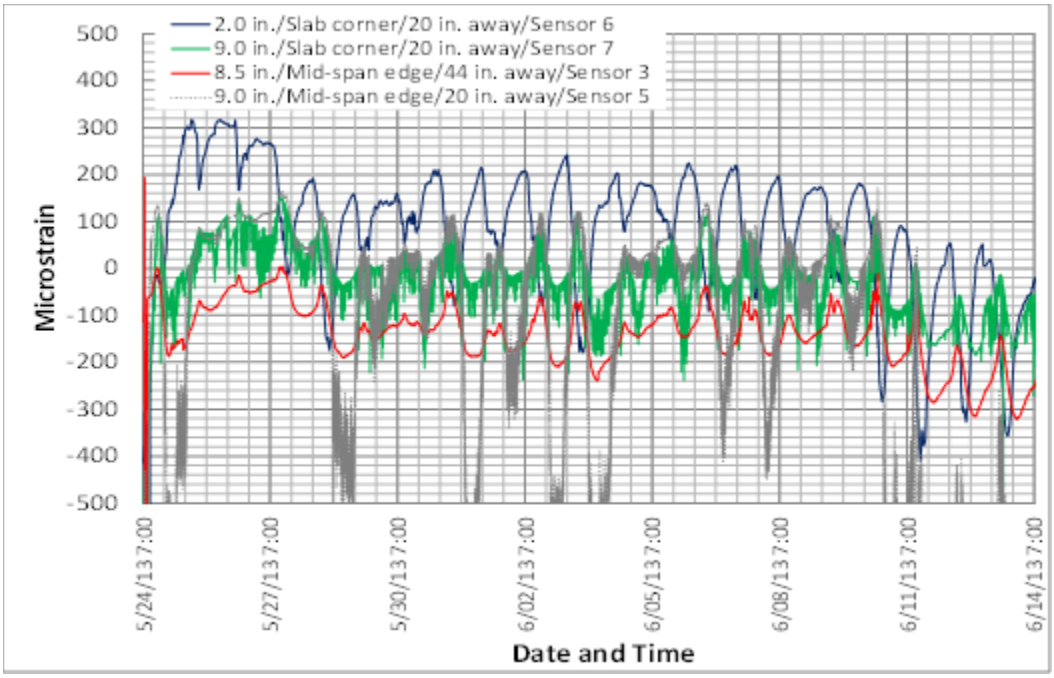

Figure 42. Strain profile before opening to traffic

Figure 38 through Figure 41 illustrate that the temperature measurements from the RFID tags (extended and embedded probes) and iButtons, as well as from the MEMS digital humidity sensors, show similar temperature trends. All sensors captured the sharp increase in temperature due to the cement hydration reaction at the beginning of concrete paving. Furthermore, these figures also show that the temperature at the concrete top was usually higher than the temperature at the bottom during the daytime, but the temperature at the top became lower during the nighttime. This is due to the fact that the top of the PCC pavement is mainly influenced by daily ambient temperature while the bottom is mainly influenced by seasonal weather (Wells 2005). During the daytime, the temperature at the pavement top was relatively high because of ambient temperature and solar radiation, and the temperature dropped quickly at night. However, the bottom of the concrete is not as sensitive to ambient temperature, so its temperature variation was much lower than that of the concrete top throughout the day. It was also observed that when the concrete was thicker, the peak temperature occurred later because it takes more time for thicker concrete to reach its peak temperature caused by ambient temperature change.

The RH measurements exhibited a trend similar to that of temperature, i.e., RH increased as temperature increased, as seen in Figure 41. At the beginning of concrete paving, RH built up rapidly, and then the value was maintained between 65% and 70% until a thunderstorm on June 3, 2013 caused a sharp increase in RH. After that, RH reached 78% and then fluctuated between 75% and 80%. However, only one moisture sensor remained operational, so the RH profile at various depths could not be developed. Nevertheless, RH generally increases as pavement depth increases (Asbahan 2009).

Figure 42 illustrates the strain measurements captured by the strain gages before opening to traffic. It was found that the strain value was mainly in the range of -200 to +200 microstrain except for Strain Gage 5, which may have suffered from disturbance problems. The value captured was similar to those found in studies by Wells (2005), Asbahan (2009), Qin (2011), and Nassiri (2011), who found typical strain values in response to environmental loads to range from -150 to +150 microstrain. However, according to Figure 42, the curve patterns of Strain Gages 3, 5, and 7 agreed but were totally opposite to that of Strain Gage 6 because the pavement experienced different deformation behavior in the bottom and the top sections under environmental loads. In the instrumented section, Strain Gages 3, 5, and 7 were at the bottom of the pavement and Strain Gage 6 was at the top. When tension was induced at the top (Strain Gage 6), compression was induced at the bottom. This phenomenon is referred to as the curling and warping behavior of concrete and is explained in the following section. While Strain Gage 5 exhibited a noisy signal, it still provided a clear curve pattern.

Curling and Warping

Curling and warping are common concrete behaviors that have been extensively investigated. In general, conventional concrete pavement deteriorates under the influence of repeated traffic and environmental loads. In terms of environmental load, two well-known factors, temperature and moisture, produce significant effects called curling and warping. Curling and warping stresses develop as a result of temperature and moisture gradients. When a non-uniform temperature or moisture gradient is induced in a PCC slab, the differential strain response throughout the slab depth leads to curvature. Generally, when the top of the PCC slab has a higher temperature or moisture content, a positive gradient is induced and the top part of the PCC slab expands more than the bottom, resulting in downward slab curling or warping. Conversely, if the bottom of the PCC slab has a higher temperature or moisture content than the top, a negative gradient occurs and the bottom part of the slab expands more than the top, resulting in upward curling or warping of the slab.

The curling and warping behavior of a PCC slab may influence the degree of support offered by the subgrade and the stiffness along the joint. When curling and warping occurs in the PCC slab, the self-weight of the slab tends to exert tensile stresses resisting the deformation caused by the curvature, as shown in Figure 43.

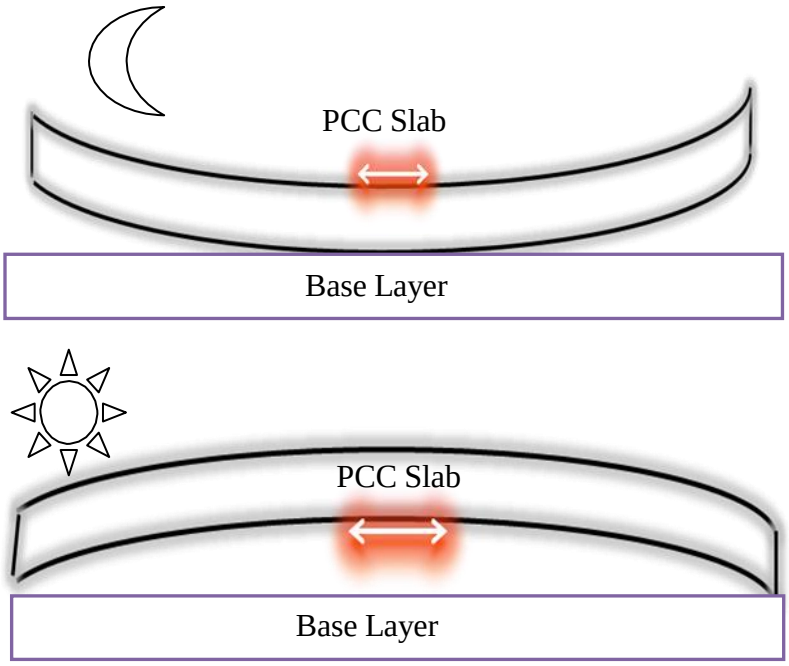

Nassiri 2011

Figure 43. Stresses exerted due to PCC curling and warping: tensile stress exerted at the top of the PCC slab with upward curvature (top), and tensile stress exerted at the bottom of the PCC slab with downward curvature (bottom)

Additionally, internal tensile stresses in a PCC slab can develop due to restraints to deformation such as dowel bars and friction between the PCC slab and the base course (Wells 2005). The induced tensile stresses are further magnified under repetitive vehicle loading and can easily lead to transverse cracking. In addition to temperature and moisture gradients in a PCC slab, the curling and warping behavior of early-age concrete is also affected by early-age curing, temperature conditions during pavement construction, and other factors such as solar radiation, base layer type, slab geometry, degree of built-in slab curvature, concrete mixture, dry shrinkage, and creep (Ceylan et al. 2013).

To minimize the effects of slab curling and warping, the time at which the concrete is placed should be adjusted to avoid weather conditions that may lead to the development of built-in temperature gradients. A good curing method, including covering the entire concrete surface, should also be used. Like the curling and warping behavior of a PCC slab, the contraction and expansion behavior in response to temperature and moisture is also related to cracks in the slab. However, curling and warping are more complicated phenomena than contraction and expansion because the former involve variations and non-uniform volume changes at different slab depths and locations. Compared to curling and warping, the contraction and expansion behavior of concrete mainly involves horizontal volume changes of the PCC slab, which is more related to joint spacing design.

In summary, curling and warping develop as a result of induced non-uniform temperature or moisture gradients that generate differential strain responses throughout the slab depth, leading to slab curvature. Curling and warping are illustrated in Figure 44.

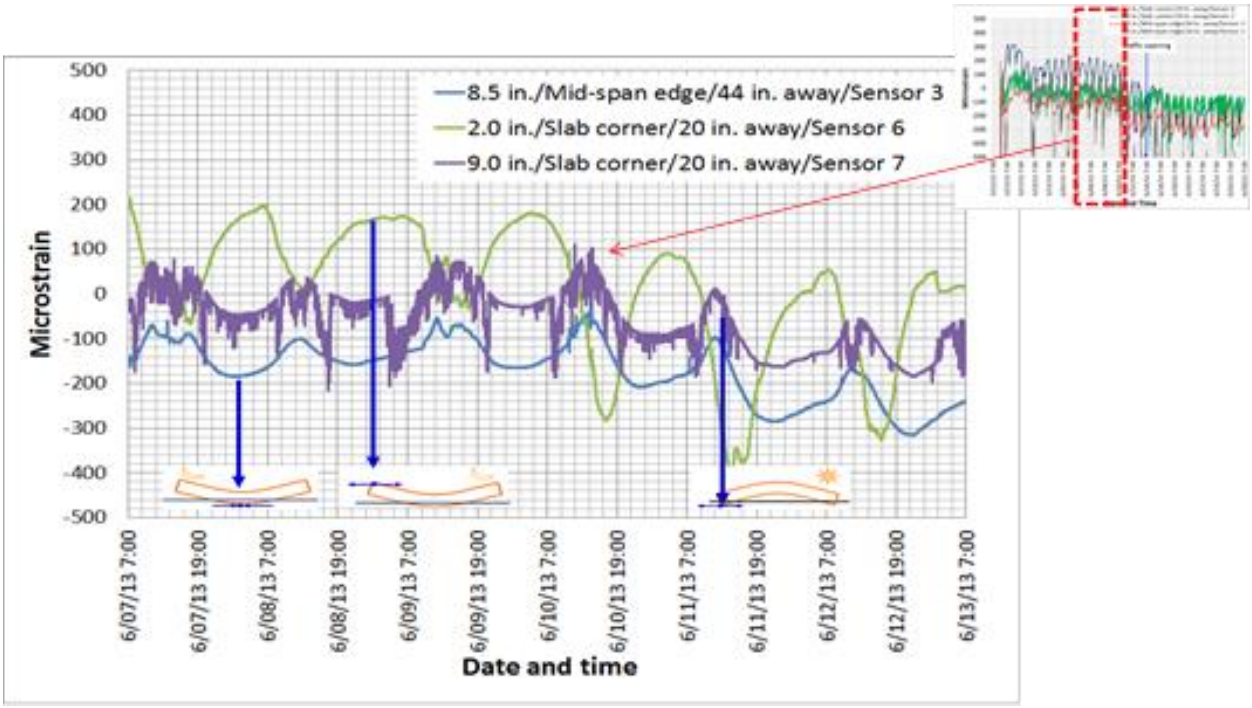

Figure 44. Strain measurement: curling and warping

According to Figure 44, when the concrete curled upward, the top of the concrete (Strain Gage 6) had a maximum of 200 tensile microstrain at 2:00 a.m. on June 8, 2013. Meanwhile, the bottom of the concrete (Strain Gage 3) had a maximum of 200 compressive microstrain. Comparing these observations with the temperature measurements shown above in Figure 38 through Figure 41, it can be observed that the top of the concrete had an approximate temperature of 60°F while that of the bottom of the concrete was 65°F. As a result, the top of the concrete was cooler than the bottom and therefore the slab curled up, in agreement with the strain readings in Figure 44.

Two Months after Opening to Traffic (June 2013 to July 2013)

Figure 45 through Figure 50 illustrate the temperature and RH behavior two months after opening to traffic, i.e., from July 25 through July 27, 2013.

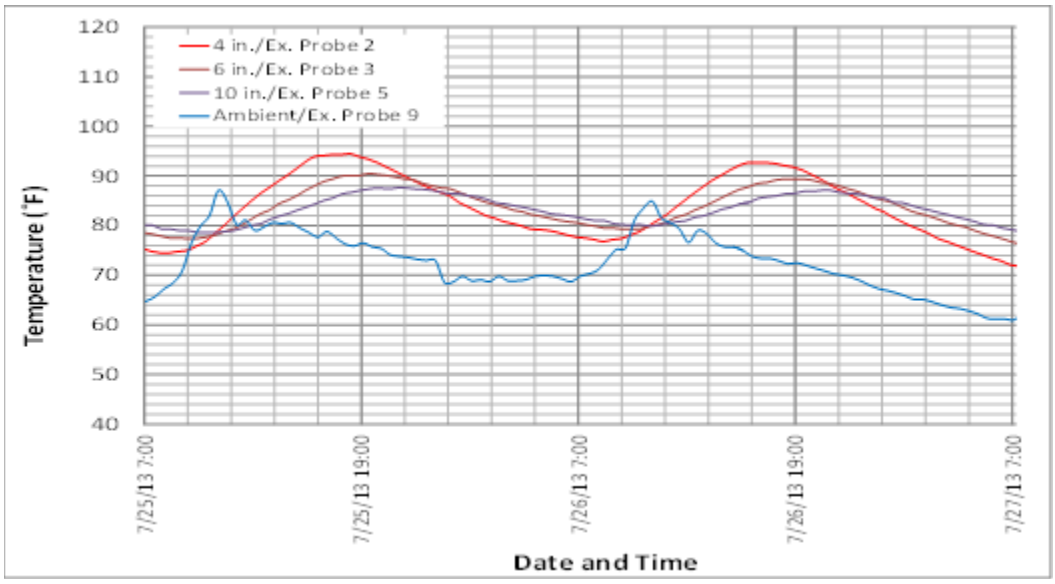

Figure 45. Measurements from the RFID extended probes in the corner two months after opening to traffic

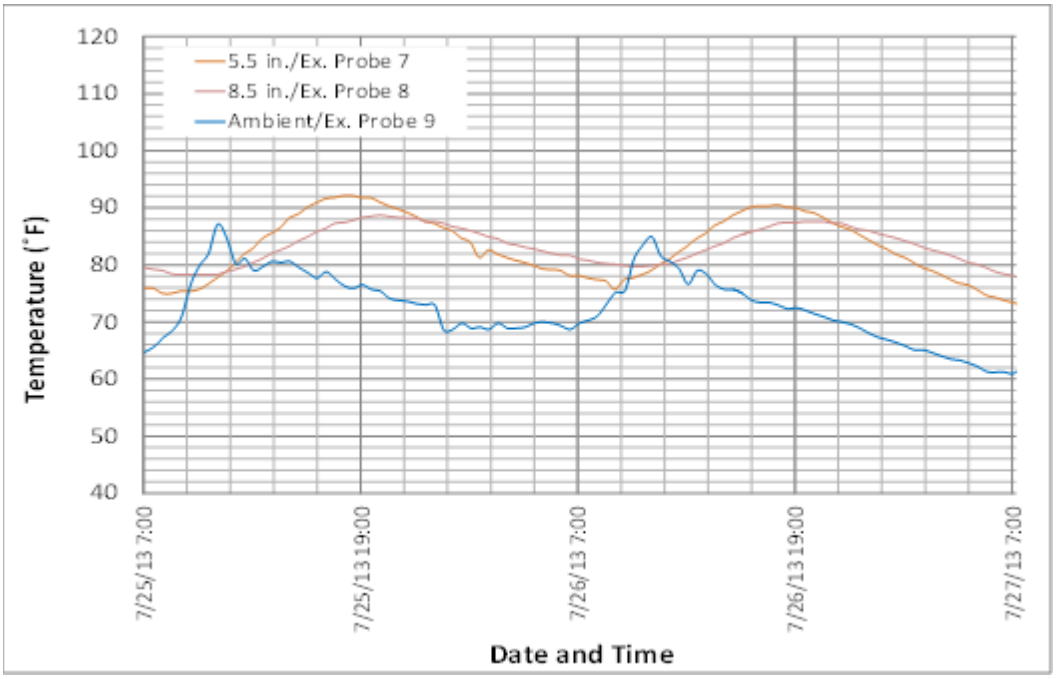

Figure 46. Measurements from the RFID extended probes in the center two months after opening to traffic

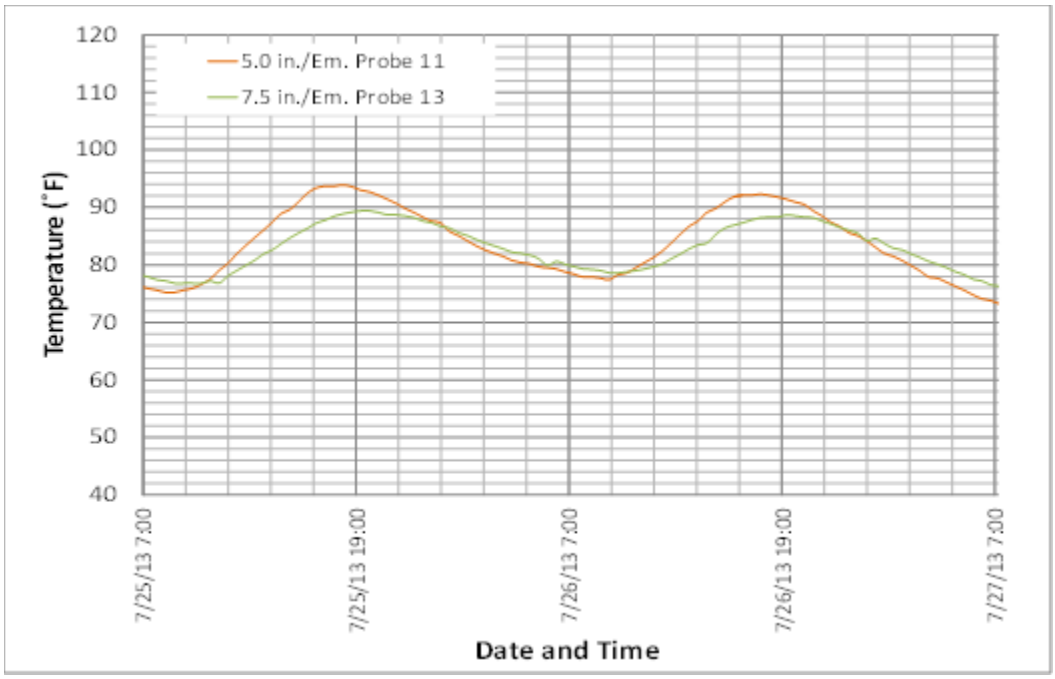

Figure 47. Measurements from the RFID embedded probes two months after opening to traffic

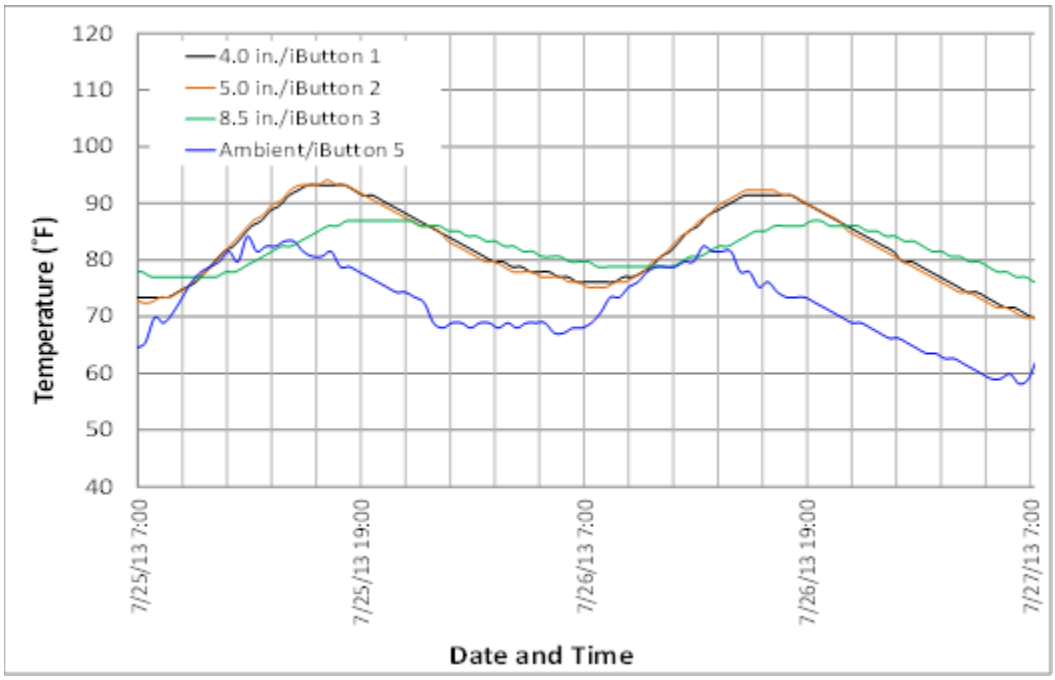

Figure 48. Measurements from the iButtons two months after opening to traffic

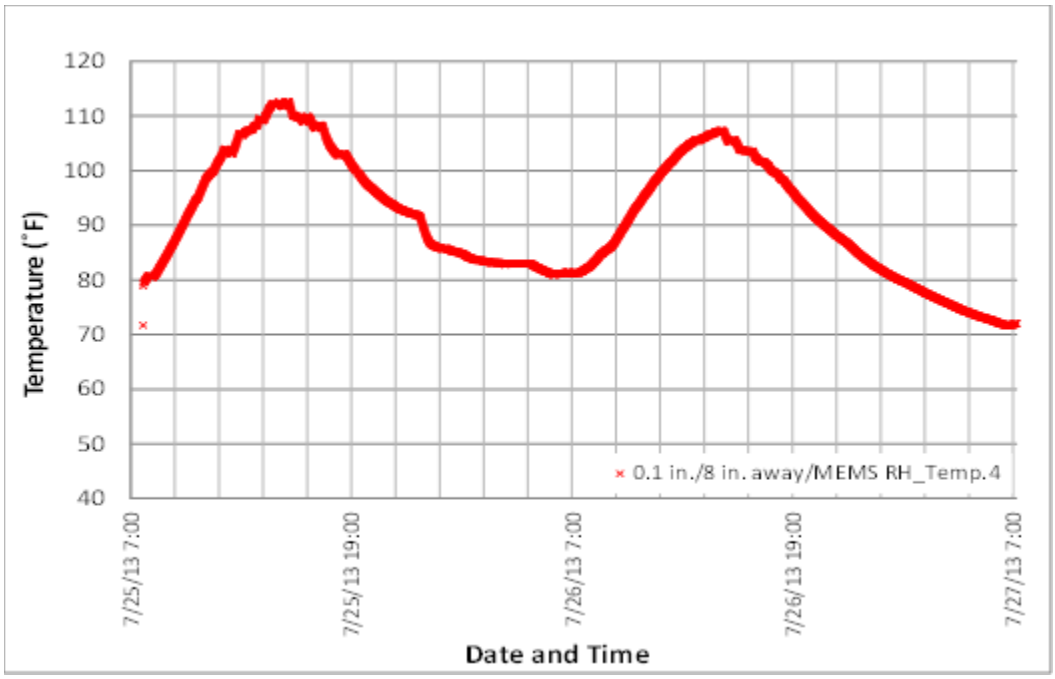

Figure 49. Temperature measurements from the MEMS digital humidity sensor two months after opening to traffic

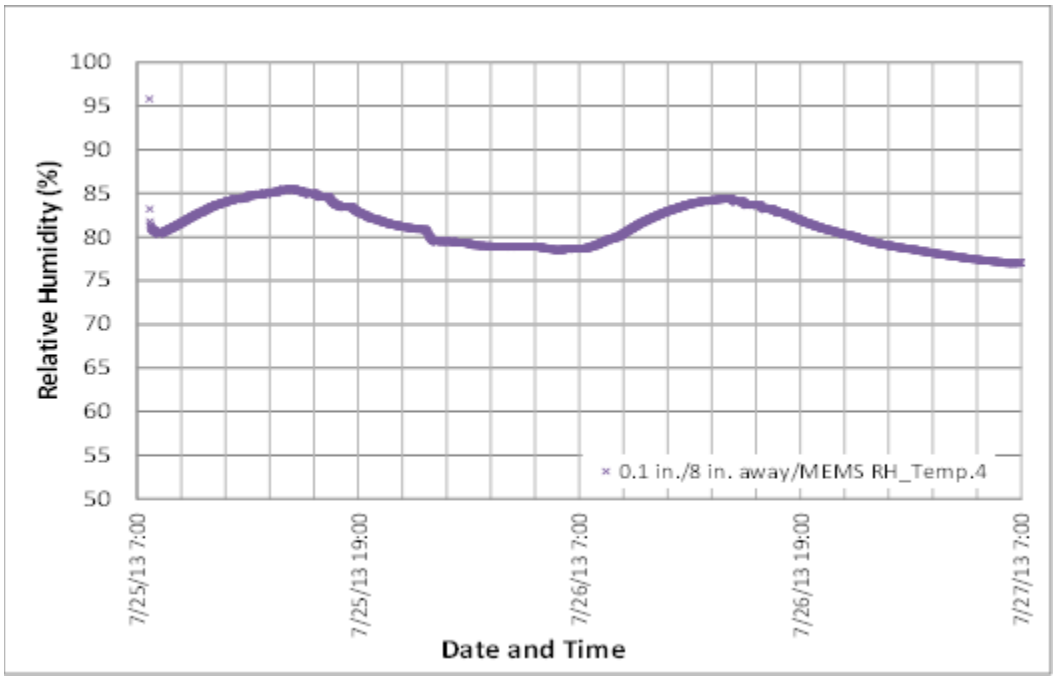

Figure 50. RH measurements from the MEMS digital humidity sensor two months after opening to traffic

It was discovered that an additional 26% of the sensors were not functional at the end of July 2013. These sensors were RFID extended probes 1, 4, and 6; embedded probes 10 and 12;

iButton 4, MEMS digital humidity sensor 3; and strain gage 5. Furthermore, these sensors were distributed everywhere throughout the slab, so there was no concentrated location where the sensors stopped functioning.

Figure 45 through Figure 48 show that the average temperature mainly ranged from 74°F to 94°F. According to Figure 49, the MEMS digital humidity sensor exhibited a higher temperature than other sensors, ranging from 80°F to 110°F, probably due to strong solar radiation at noon because the MEMS digital humidity sensor was just 0.1 in. below the pavement surface. Furthermore, it is obvious that the ambient temperature was lower than that of the concrete, and ambient temperature reached its peak earlier, as previously discussed.

Six Months after Opening to Traffic (December 2013)

Figure 51 through Figure 55 illustrate the temperature and RH measurements in winter.

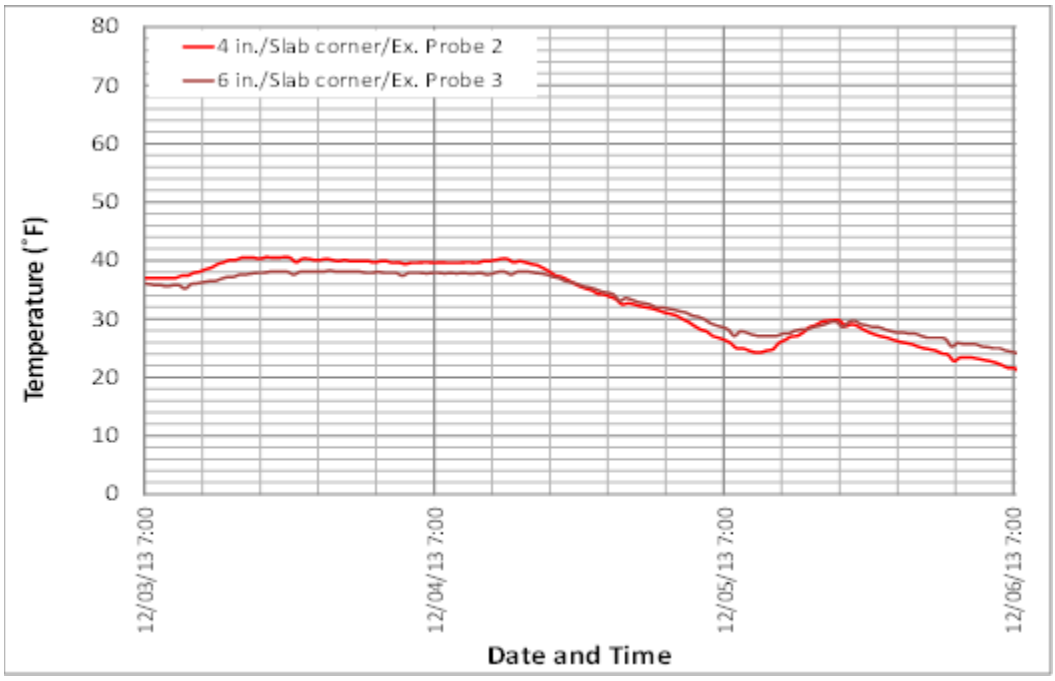

Figure 51. Measurements from the RFID extended probes in the corner six months after opening to traffic

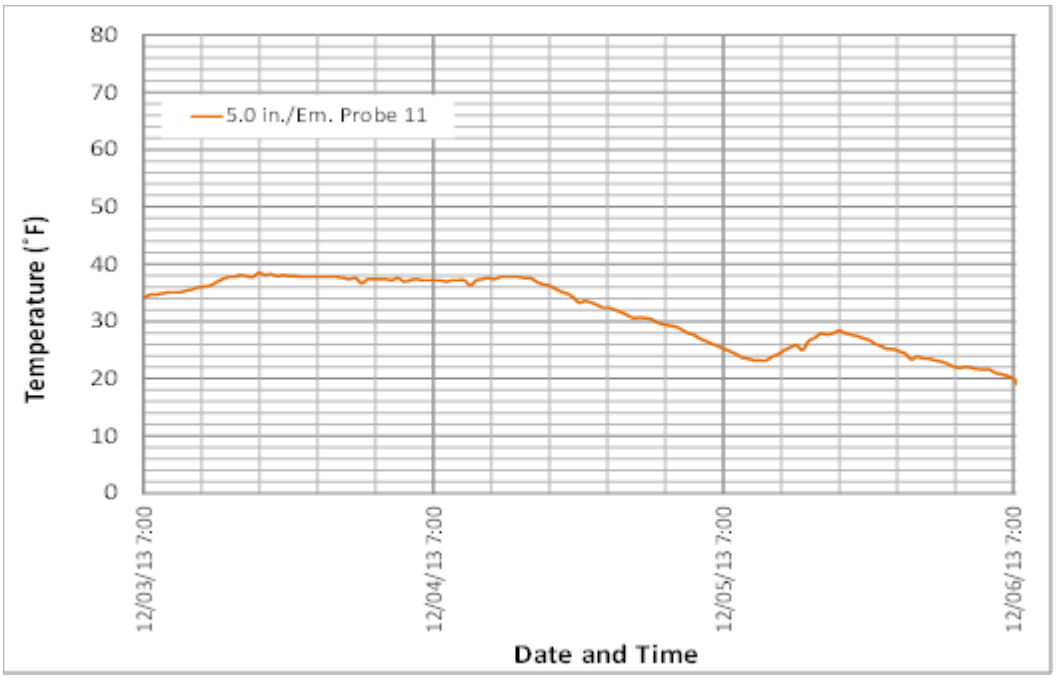

Figure 52. Measurements from RFID embedded probe six months after opening to traffic

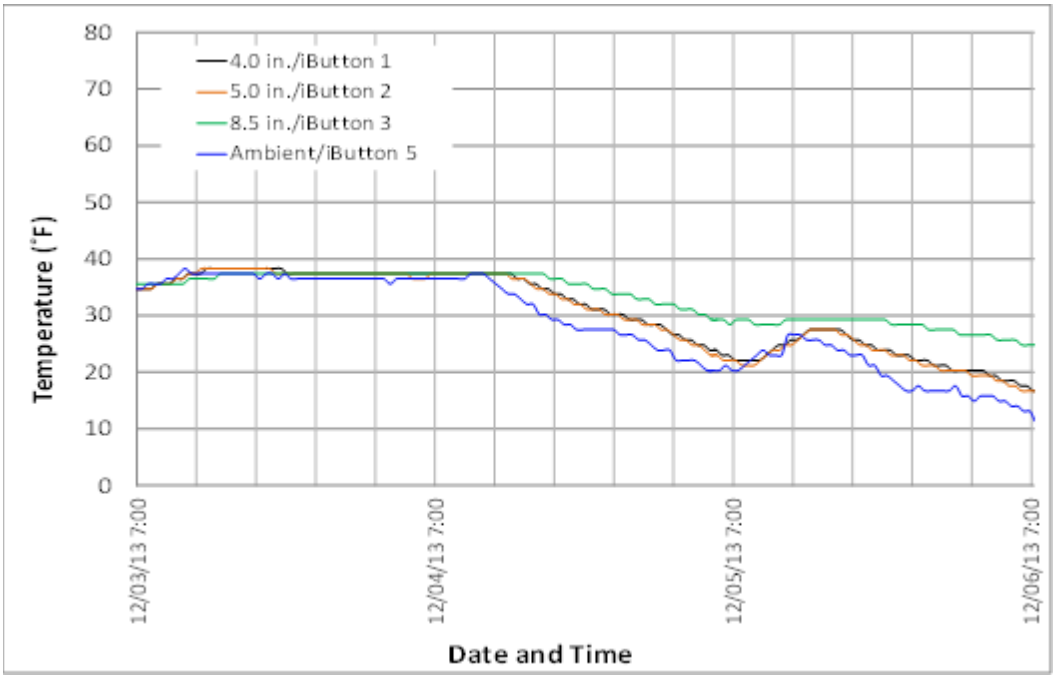

Figure 53. Measurements from the iButtons six months after opening to traffic

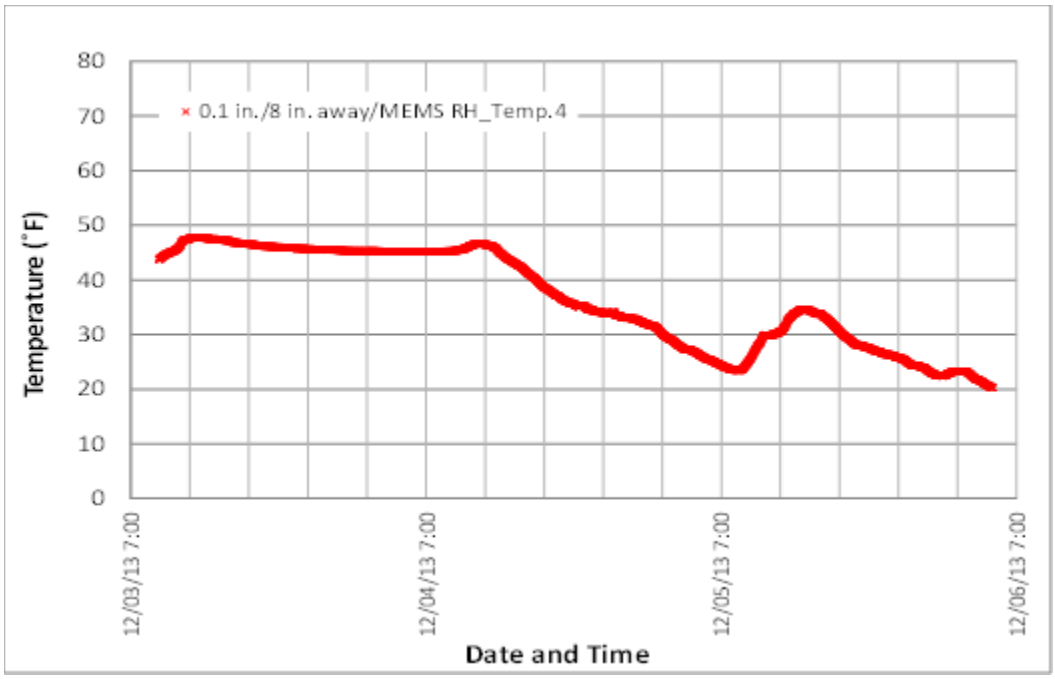

Figure 54. Temperature measurements from the MEMS digital humidity sensor six months after opening to traffic

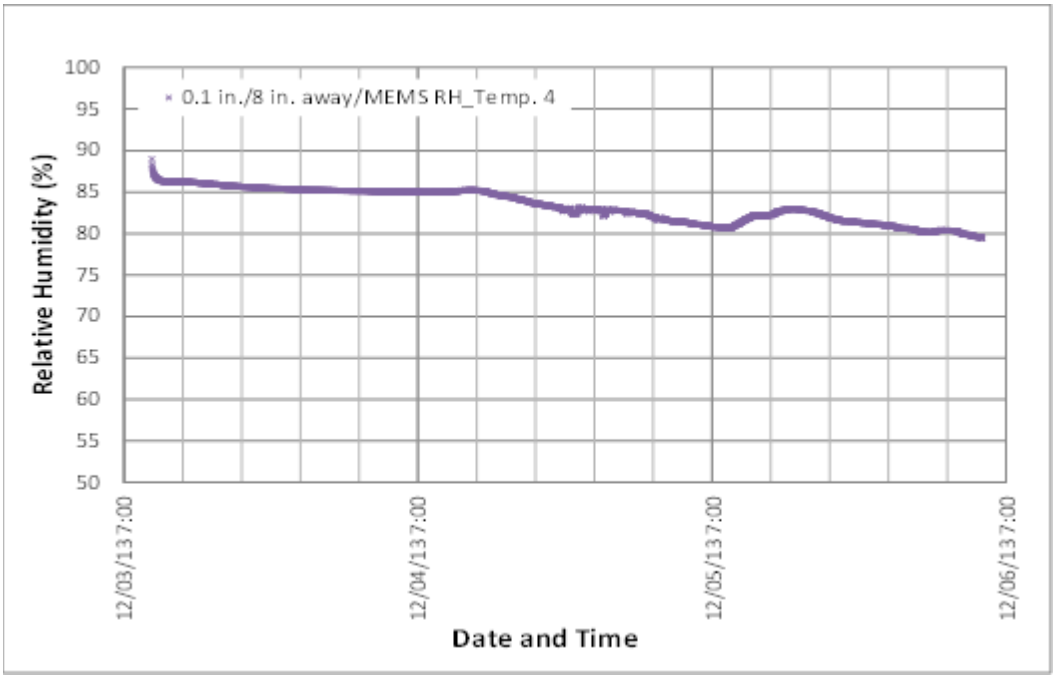

Figure 55. RH measurements from the MEMS digital humidity sensor six months after opening to traffic

By the end of December 6, 2013, RFID extended probes 5, 7, 8, and 9 and RFID embedded probe 13 had stopped functioning. According to Figure 51 through Figure 55, the MEMS digital humidity sensor also reported a temperature more than 50°F higher than the RFID tags, and the iButton reported maximum temperatures of approximately 40°F. The RH value in winter was maintained between 80% and 90%, and that sensor showed a similar temperature pattern.

Concrete Maturity

Laboratory Tests

During concrete construction, a total of 72 cylinders (4 in. × 8 in.) were collected from the project site, and 63 of these were used in laboratory concrete tests, including a compressive strength test, a split tensile strength test, an elastic modulus test, and a coefficient of thermal expansion (CTE) test. Table 8 and Figure 56 through Figure 59, respectively, illustrate the detailed testing plan and the test results.

Table 8. Concrete testing plan summary

Type of Test	Age	Repeatability	Standards
Compressive strength	1, 3, 7, 14, 28, and 90 days	3	ASTM C39
Split tensile strength	1, 3, 7, 14,28, and 90 days	3	ASTM C496
Elastic modulus	1, 3, 7, 14, 28, and 90 days	3	ASTM C469
CTE	7, 28, and 56 days	3	AASHTO T336-11

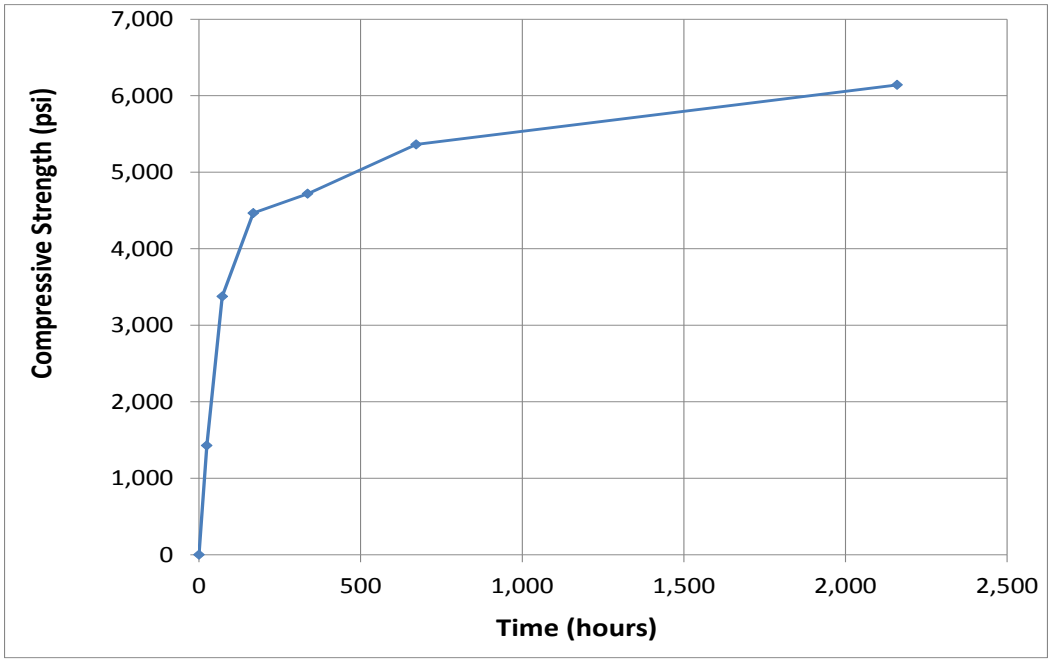

Figure 56. Compressive strength test results

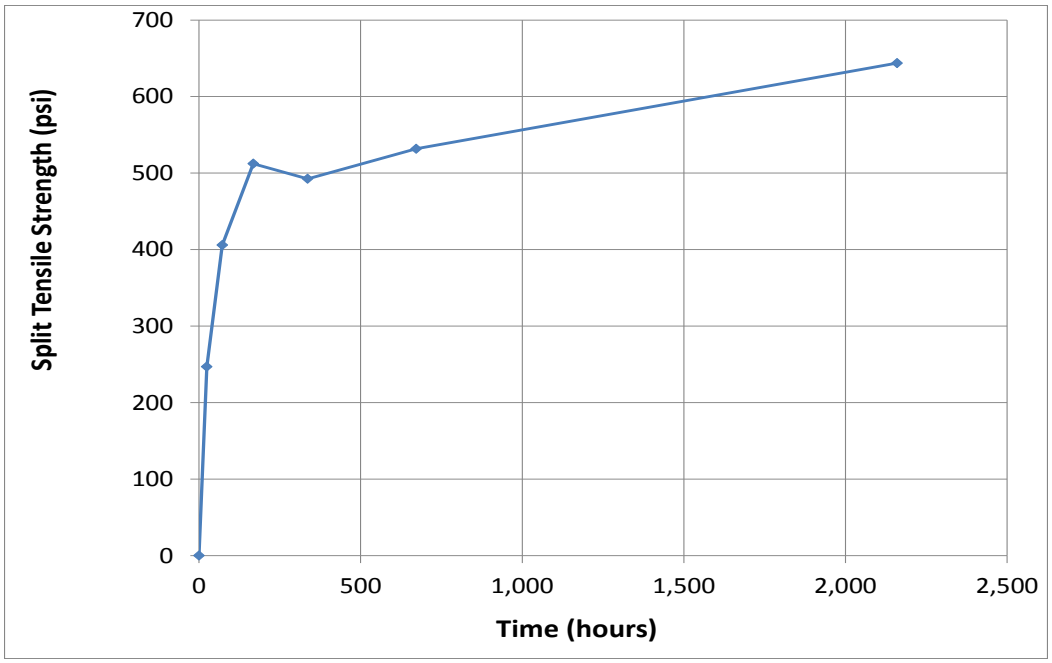

Figure 57. Split tensile strength test results

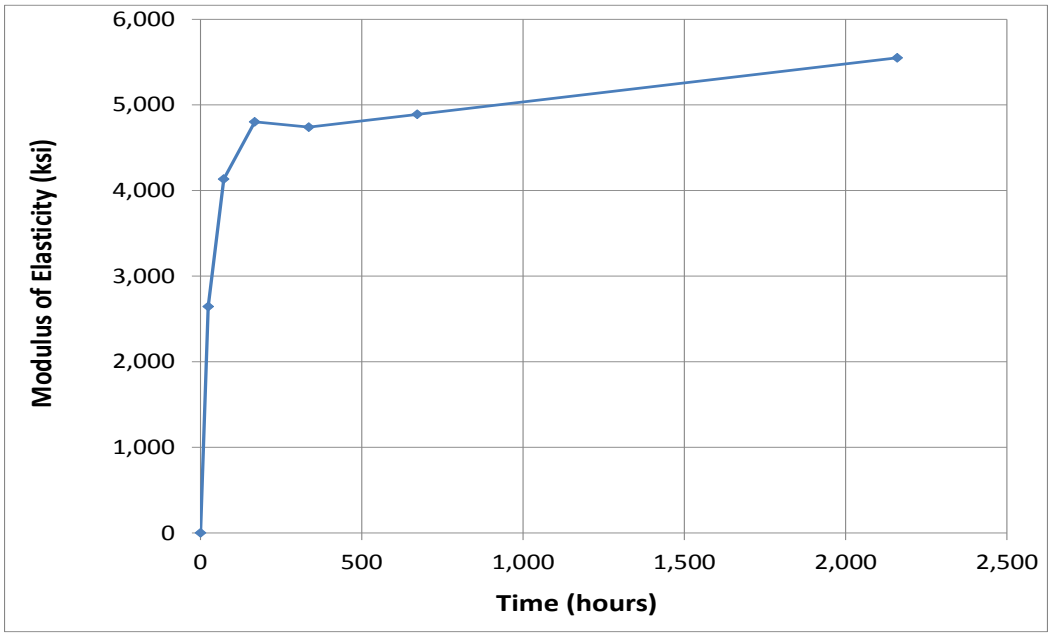

Figure 58. Modulus of elasticity test results

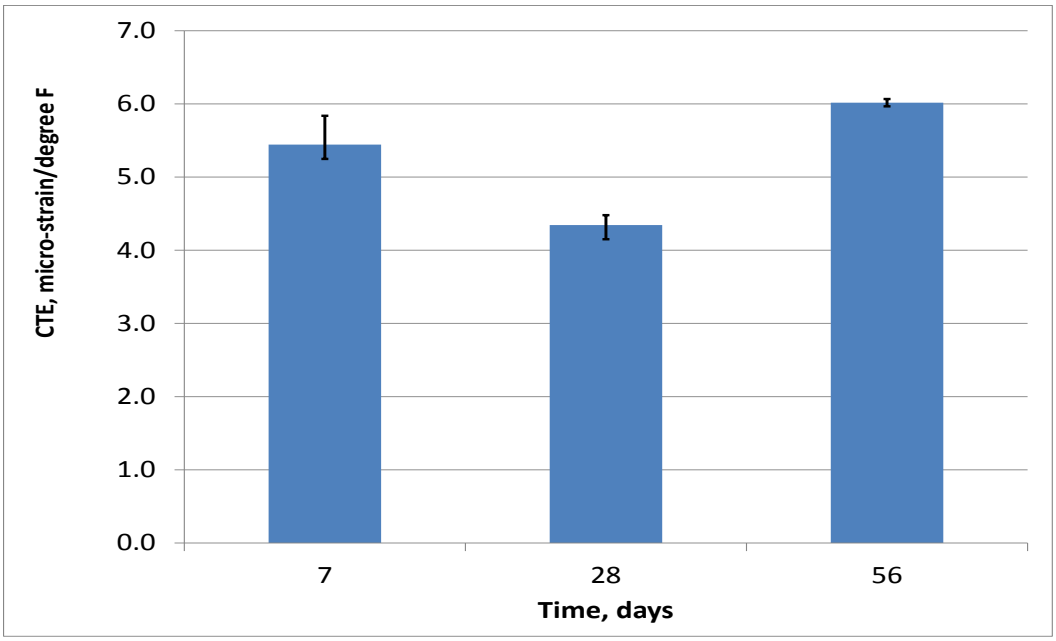

Figure 59. Coefficient of thermal expansion test results

Figure 56 through Figure 59 illustrate the results of common laboratory concrete tests conducted in accordance with the corresponding related standards. It can be seen that the strength increased rapidly during an initial period of 7 days, after which the speed of the strength increase became slower. However, a slight decrease in split tensile strength and modulus of elasticity were recorded by the 14-day test, and the results of the 28-day CTE test exhibited a slight decrease as well. These differences were probably due to variations among the different concrete specimens and machine calibration errors. Nevertheless, all the test data were in a reasonable range and met the minimum construction requirements. Estimated initial set time and final set time were also obtained in accordance with ASTM C403. The detailed test results are shown in Appendix B.

Maturity Calculation

The concrete maturity method is a simple and reliable quality control approach for estimating in-place concrete strength. This method accounts for the effects of both time and temperature on strength development. According to ASTM C1074 (2011), the maturity method is defined as "a technique for estimating concrete strength that is based on the assumption that samples of a given concrete mixture attain equal strengths if they attain equal values of the maturity index." The method can help engineers determine appropriate times for form removal, opening to traffic, and joint sawing so that money can be saved through more efficient construction.

ASTM C1074 provides two alternative equations for maturity index calculation: the temperature-time-factor–based Nurse-Saul function and the equivalent age-based Arrhenius function. The Nurse-Saul function assumes a linear relationship between the rate of strength development and temperature, while the Arrhenius function assumes an exponential relationship between the rate of strength development and temperature. This study adopted the Nurse-Saul function, which can be expressed as follows:

$$M = \sum_0^t (T - T_0)\Delta T \quad (1)$$

where M is the maturity index (°C-hours or °C-days), T is the average concrete temperature (°F, during time interval ΔT), T_0 is the datum temperature, and ΔT is the time interval (hours or days).

Equation (1) can be used to calculate the maturity index by utilizing monitored temperature history. The maturity index is an indicator of concrete maturity that can be used to estimate the corresponding in-place strength. The datum temperature is 10°C, based on the recommendation given in ASTM C1074. The in-place strength estimation can be calculated from the following:

$$S = S_u \frac{K(t-t_0)}{1+K(t-t_0)} \quad (2)$$

where S is the in-place compressive strength at age t, t is the test age, S_u is the limiting strength, t_0 is the age when strength development is assumed to begin, and K is the rate constant.

According to equation (2), in-place strength can be calculated by using the estimated limiting strength, the rate constant, the test age, and the assumed age at which cement hydration began. The limiting strength and the rate constant can be found by developing the plots described in ASTM C1074. Equation (3) shows how to calculate the A-value for the y-axis in the plot to determine the K-value, and Figure 60 and Figure 61, respectively, show the concrete maturity curve and the relationship between the estimated in-place strength and the maturity index.

$$A = \frac{\mathrm{s}}{(S_u - \mathrm{s})} \quad (3)$$

where s is the compressive strength from the laboratory test.

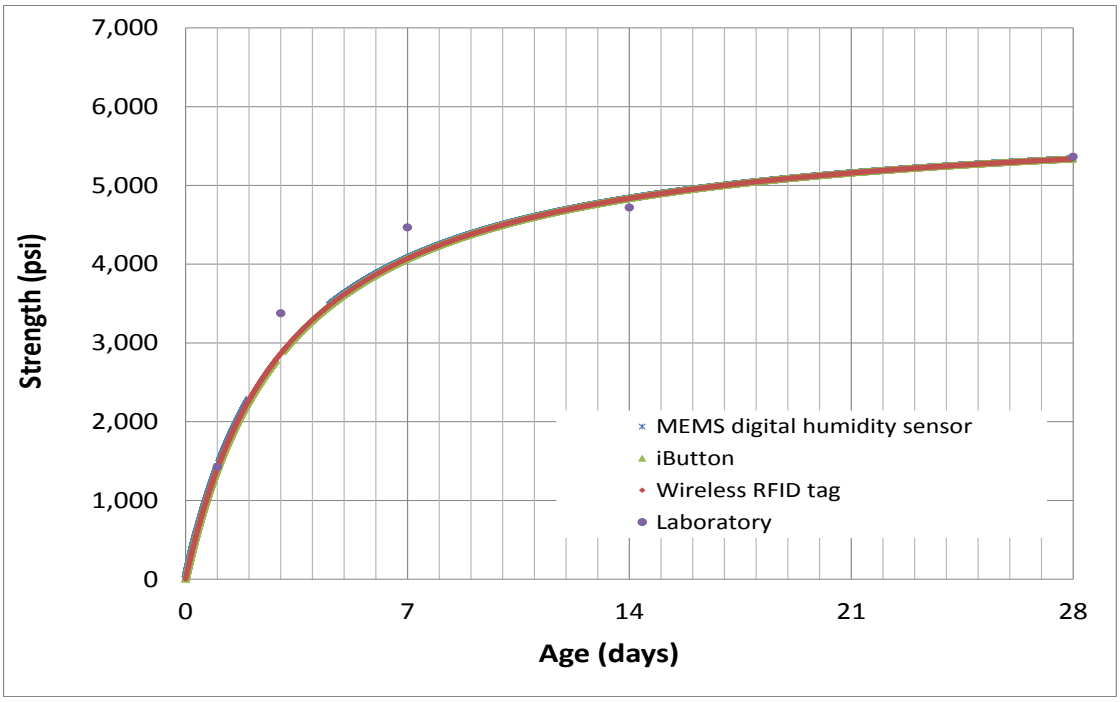

Figure 60. Concrete maturity curve

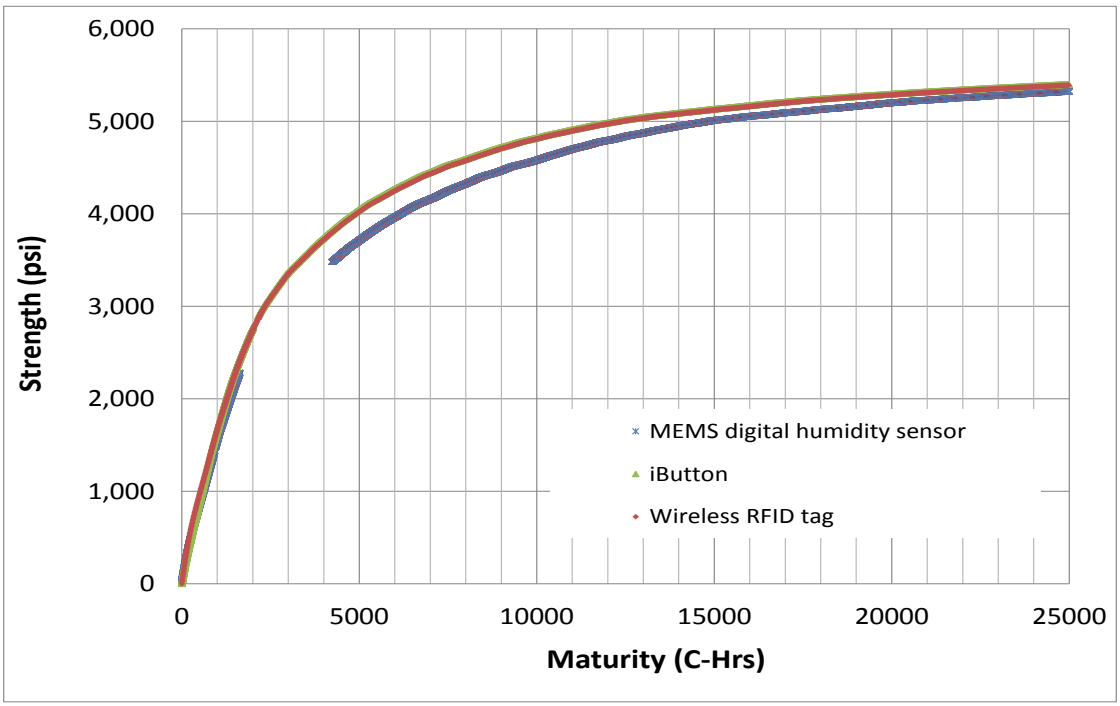

Figure 61. Relationship between in-place strength and maturity index

The concrete maturity curves shown in Figure 60 were derived from the sensor data and compressive strength data described above. Figure 61 shows the relationship between the in-place strength and maturity index derived from different sensors. However, the RFID tags and

the iButtons showed similar average temperature readings, so their curves overlap one another. The MEMS digital humidity and temperature sensors indicated higher average temperatures due to different sensor positions and temperature measurement methods, so they produced a relatively lower curve. It should be noted that the MEMS digital humidity and temperature sensors that survived were originally embedded near the top surface of the PCC slab. The gap shown in the curve for the MEMS digital humidity sensor is due to power recharging.

Discussion

As stated above, this project was conducted to evaluate the performance of MEMS sensors and wireless sensors that had shown promise in helping to achieve Smart Pavement SHM and overcome the limitations of traditional wired sensor–based SHM. The MEMS sensors nicely captured temperature variations for different pavement depths, weather conditions, and seasons and produced results consistent with early-age curling and warping behaviors of concrete pavement. However, as in earlier projects, some embedded sensors stopped functioning both during road construction and during the pavement monitoring period. Table 9 shows the number of embedded sensors surviving at various times throughout the entire monitoring period.

Table 9. Sensor survivability evaluation

	Number of Surviving Sensors					
Sensor	**May 23, 2013**	**May 24, 2013**	**Jun. 14, 2013**	**Aug. 22, 2013**	**Dec. 6, 2013**	**Apr. 1, 2014**
RFID temp (Ex. probe)	8	8	7	3	2	1
RFID temp (Em. probe)	4	4	4	2	1	0
EMS RH/Temp.	4	2	2	1	1	1
iButton (Temp)	4	4	4	3	3	3
Longitudinal strain gage	7	4	4	3	3	0
Total	**27**	**22**	**21**	**12**	**10**	**5**

According to this table, it can be seen that 19% of the sensors had stopped functioning after concrete paving and approximately 63% of the sensors gradually stopped functioning during the 10 months after opening to traffic. Possible reasons for these malfunctions can be attributed to the following:

- Damage of sensors due to the high-alkali environment in concrete
- Damage of sensors and wires incurred by the paving and vibration operations of the concrete paver
- Corrosion of wires in the concrete
- Battery issues
- Harsh climate and slab movement

High temperature and moisture and adverse pH values all represent challenges to embedded sensor survivability in plastic concrete. The high-alkali environment in concrete is critical to

sensors, especially moisture sensors, because their operation requires the exposure of their sensing elements to the water vapor in the concrete. During construction of this segment of US 30, two of the four MEMS digital humidity sensors directly failed, and another MEMS digital humidity sensor could measure temperature only after concrete paving, probably due to the high-alkali environment and extreme moisture content (liquid water) in the concrete.

In addition to the high-alkali environment, other road construction activities can be considered to be primary sources of sensor malfunction, as was observed in the construction of MnROAD sections. The paving and vibration operations of concrete pavers generate large lateral forces that can damage a sensor, loosen wire connections, and change the sensor position; the spreading plow or auger used to spread concrete at the front of the paver might also damage the sensor or cut its wiring, as shown in Figure 26. Wire also has the potential to corrode due to the chemical environment inside the concrete.

Figure 62 shows the winter data acquisition process for RFID tags.

Figure 62. Data acquisition from RFID extended probes in winter

During this process, the portable handheld transceiver "Pro" was generally able to identify tags but could not download data from some tags. Even though the distance between the "Pro" and the RFID extended probes was only 2 ft, downloading data was still difficult despite the nominal range of 300 ft claimed by the manufacturer. This difficulty may have been related to battery issues, such as the reduction of battery capacity and battery life in severe temperatures, and harsh

climate conditions, such as repeated freezing-thawing cycles that might lead to sensor malfunction or low signal strength. Even the ambient RFID tags stopped functioning during wintertime. Slab movement may also be a source of sensor damage.

Although several sensors malfunctioned after road construction, the 81% sensor survival rate at the beginning of opening to traffic can still be regarded as successful instrumentation in comparison to previous pavement instrumentation efforts (Sebaaly et al. 1991). Furthermore, the results of the concrete maturity calculation show the benefit of using pavement SHM. By using MEMS sensors, maturity can be directly calculated on-site and immediately generated as one of the sensor system outputs. However, the performance of the off-the-shelf MEMS sensors deployed on US 30 illustrated their current limitations, i.e., packaging, wires, signal strength, etc., when used in pavement health monitoring systems. A wireless communication system with robust packaging for the MEMS digital humidity sensor was therefore implemented to demonstrate a preliminary design for a wireless sensor system.

INTEGRATION OF WIRELESS COMMUNICATION SYSTEM WITH MEMS SENSORS

Implemented Wireless System Overview

The wireless system discussed in this report is a preliminary design mainly focusing on the wireless transmission function and was motivated by field instrumentation in US 30. In this study, an IEEE standard–based wireless system was utilized because of both its low price and low power consumption. A MEMS digital humidity sensor was used as the sensing unit; this pin-based sensor had no packaging for its sensing element, so additional robust packaging was required.

This wireless system can be subdivided into transmitter and receiver. The transmitter was interfaced with a MEMS digital humidity sensor to transfer the data captured, while the receiver received transmitted data and downloaded it to a computer through a USB port. Microcontrollers and XBee-PRO modules were used for both the transmitter and the receiver.

Wireless Protocols

As described above, wireless network protocols are used to define or standardize the rules and conventions for communication between devices (Lee et al. 2007). The wireless protocol implemented in this design was ZigBee, which is used to construct a decentralized self-healing wireless mesh network. In this mesh network, nodes can find a new route when an original route fails (Texas Instruments 2013). ZigBee is the standard IEEE 802.15.4-based protocol (Digi 2014); in addition to ZigBee, there are also other possibilities, including Bluetooth, Wi-Fi, cellular, and other protocols. Table 10 presents a comparison between different wireless technologies in terms of their total scores derived from weighted scores considering various aspects such as data rate, range, energy consumption, and other factors.

Table 10. Comparison of wireless technologies

Aspects		Score (0 to 10)			
Factors	***Weight***	*Bluetooth*	*ZigBee*	*Wi-Fi*	*Cellular*
Multi-node network support	**100**	5	10	10	10
Throughput	**60**	7	6	8	3
Data rate	**60**	7	6	10	10
Range	**50**	6	5	7	10
Ease of implementation	**50**	6	8	6	4
Power consumption	**-80**	6	2	8	6
Cost	**-100**	5	3	7	8
Total Score		**460**	**910**	**390**	**200**

Source: Al-Khatib et al. 2009

In Table 10, the weighted score of each aspect is calculated by multiplying its weight by the score of each specific wireless technology; a higher total score represents a better wireless technology for this application. Based on this table, it can be seen that ZigBee is more energy-efficient and cost-effective and is easier to work with than the other technologies.

Microcontrollers

An Arduino board is a single-board microcontroller consisting of an Atmel AVR 8-bit or 32-bit microcontroller, which can be wirelessly programmed by a device utilizing the ZigBee protocol (Atmel Corporation 2014). In this study, Arduino Uno and Arduino Mega 2560, shown in Figure 63, were used for the wireless transmitter and receiver, respectively.

Figure 63. Microcontrollers: Arduino Uno for wireless transmitter (left) and Arduino Mega 2560 for wireless receiver (right)

The Arduino Uno is a microcontroller using an ATmega328 processor with 32 KB of flash memory, 2 KB of static random-access memory (SRAM), and 1 KB of electrically erasable programmable read-only memory (EEPROM). The board has 14 digital input/output pins, 6 analog inputs, a 5-volt linear regulator, a 16 MHz ceramic resonator, a USB connection, a power jack, an in-circuit serial programming (ICSP) header, and a reset button. The Arduino Mega 2560 is similar to the Arduino Uno but has an ATmega2560 processor with 54 digital input/output pins, 16 analog inputs, 4 hardware serial ports (UARTs), and a 16 MHz crystal oscillator. The Arduino Mega 2560 is compatible with most shields designed for the Arduino Duemilanove or Diecimila and has 256 KB of flash memory, 8 KB of SRAM, and 4 KB of EEPROM for storing code and data. These two microcontrollers were selected because of their high reliability and low cost. Furthermore, Arduino 1.0.4 (open-source software) can be used for programming the time interval, changing the format of exported data, and specifying other functions to control both the Arduino Uno and the Arduino Mega 2560 (Arduino 2014).

XBee-PRO Modules

The XBee-PRO RF module (series 1), shown in Figure 64, is a wireless device that offers low-cost wireless connectivity in ZigBee mesh networks.

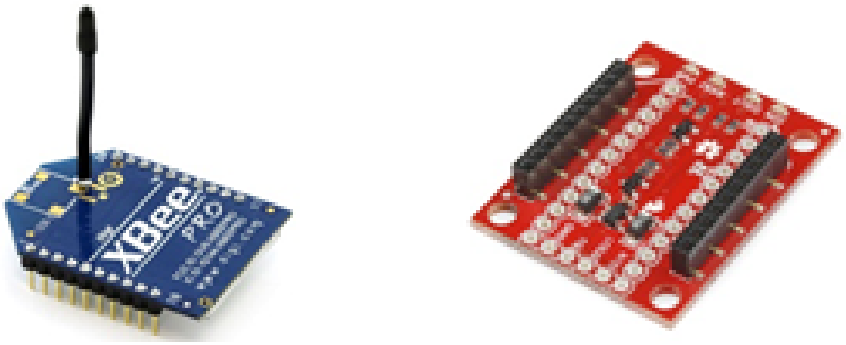

Figure 64. XBee devices: XBee-PRO module (left) and XBee Explorer Regulated (right)

The XBee-PRO module is reliable in point-to-point, multipoint wireless transmission and is designed to conform to the IEEE 802.15.4 standard. Furthermore, the XBee-PRO module has an easy setup process; its software is called X-CTU, and it can adjust frequency, signal strength, energy consumption, etc. An XBee Explorer Regulated board can also be used to help regulate the voltage input.

Wireless Transmitter

The wireless transmitter, shown in Figure 65, consists of a MEMS digital humidity sensor, an XBee-PRO module, an XBee Explorer Regulated, an Arduino Uno microcontroller, and 12 1.5V AA batteries.

Figure 65. Wireless transmitter

Among these devices, the XBee Explorer Regulated is a board that can be pinned onto the XBee-PRO to help it regulate the voltage input. At the wireless transmitter, both a SHT71 sensor and an XBee-PRO with XBee Explorer Regulated were pinned to the digital port and power port on the Arduino Uno board. Meanwhile, 12 1.5V AA batteries were placed in a plastic holder and connected to the microcontroller to power the entire wireless transmitter through the board's voltage output pin. Because the entire wireless transmitter was to be buried in concrete, a robust packaging framework was needed, as discussed below.

Wireless Receiver

Figure 66 shows the wireless receiver; it consists of an XBee-PRO module, an XBee Explorer Regulated, and an Arduino Mega 2560 microcontroller.

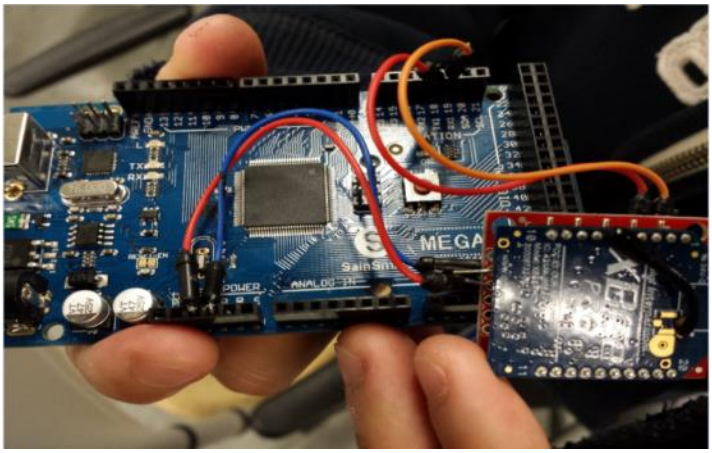

Figure 66. Wireless receiver

The XBee Explorer Regulated used for the wireless receiver plays the same role as in the wireless transmitter. However, no battery was used on the Arduino Mega 2560 because it is powered by the computer through a USB cable. The XBee-PRO on the Arduino Mega 2560 was paired with the other XBee-PRO used on the Arduino Uno for the wireless transmitter to receive the transmitted data. The data were then stored on the Arduino Mega 2560 in a data storage module with 4096 bytes of non-volatile memory.

Packaging

Robust packaging is required to protect both the sensor and wireless transmission devices like the XBee-PRO module and the microcontroller to ensure that they can work properly inside the concrete. The packaging functions include protecting the wireless transmitter during the sensor installation and pavement construction processes, protecting the sensor from the alkali-cement hydration reaction, and protecting the wireless transmitter under harsh climate and traffic conditions.

Two types of in-house packaging were designed to protect the sensor, the microcontroller, and the XBee-PRO module. For the MEMS sensor, a piece of adhesive tape, a protection filter cap, and steel wool comprised a protective package to prevent direct contact between the raw sensor and the fresh concrete, as shown in Figure 67.

Figure 67. MEMS sensor with packaging

In this packaging, a filter cap was attached to the top of the MEMS sensor using adhesive tape, and steel wool was used to attach the sensor. For the microcontroller and the XBee-PRO module, a small box with an open bottom was prepared; the bottom consisted of a 0.5 in. thick wooden board nailed to a 7.1 in. long sharp-edged wooden stick. A hole was drilled through the bottom board to permit a sensor cable to pass through and be connected to the Arduino Uno microcontroller, which was to be placed inside the box. The size of the box was 6.3 in. × 4.1 in. × 3.5 in., which was sufficient to contain the entire wireless transmission system, as shown in Figure 68.

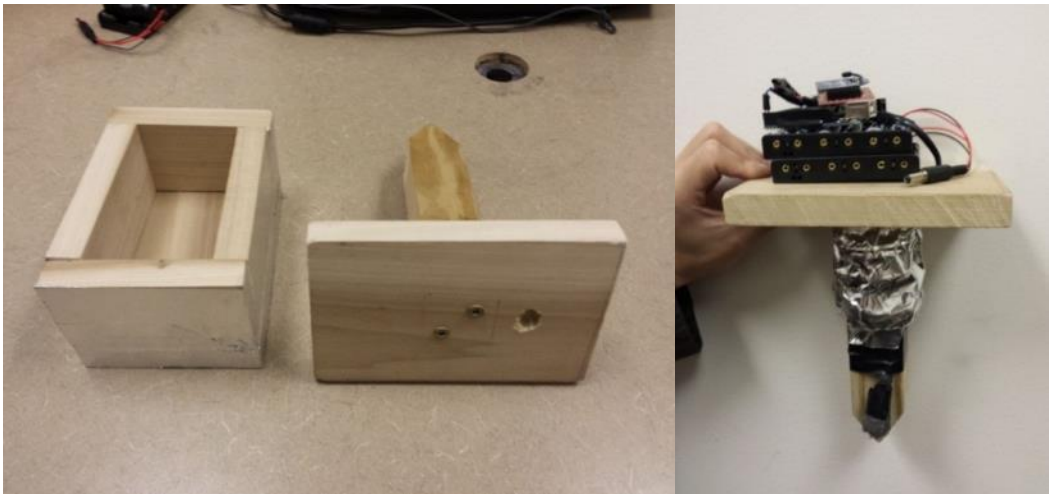

Figure 68. Packaging for wireless transmitter

Silicon glue and adhesive tape were used to seal the small gaps in the box. However, it should be noted that the basic design concept of the packaging for the moisture sensor was to use the material like a filter to allow only water vapor to pass through. An additional eight sensors packaged in the same way were first tested in mortar specimens, and seven out of the eight were able to continuously capture data, indicating that this packaging was successful.

Evaluation of Implemented Wireless Communication System

Working Principle of Implemented Wireless System

The data exchange principle of this wireless system is based on the ZigBee protocol. This system requires no external cables. When activated, the MEMS sensor measures temperature and RH and transfers those data to the XBee-PRO through the Arduino Uno microcontroller. Then the XBee-PRO at the wireless transmitter transmits the data to the paired XBee-PRO at the wireless receiver through an antenna; these data are stored in the Arduino Mega 2560, and therefore the wireless receiver and a computer must be placed nearby because only the Arduino Mega 2560 microcontroller is used to store data in this wireless system. The data can finally be downloaded to the computer through software called "CoolTerm," a simple freeware serial port terminal application without terminal emulation that supports data exchange with hardware connected through serial ports (CoolTerm 2014, Sparkfun Electronics 2014). Temperature, RH, and dew point are the data elements exported from the system.

Comparison between Wired MEMS System and Implemented Wireless MEMS System

Figure 69 provides an overall system-level comparison between a wired MEMS system and the wireless MEMS system developed for this study.

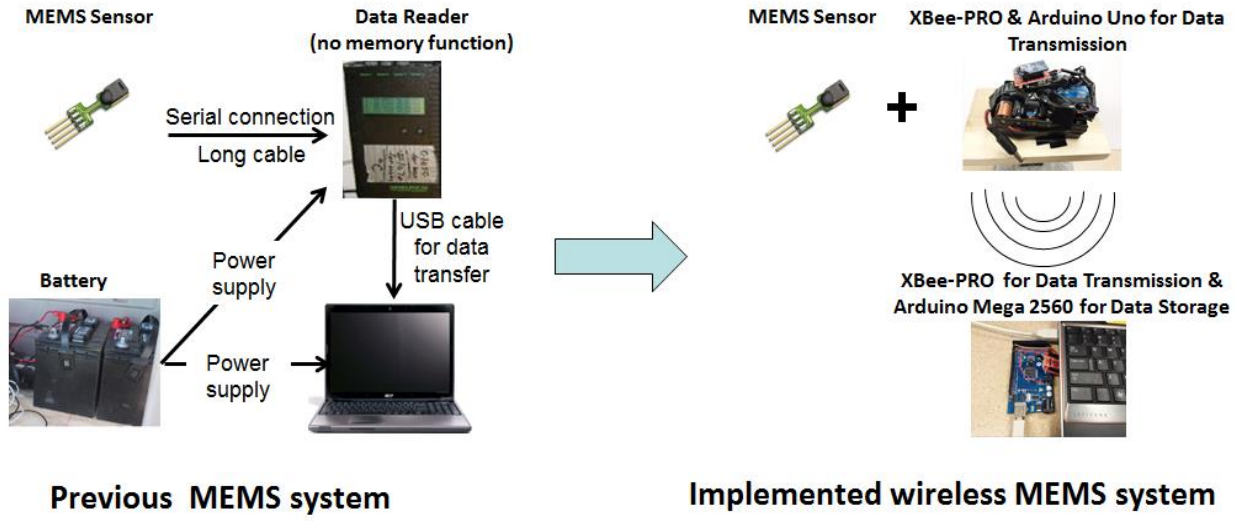

Figure 69. Comparison between a wired system and the implemented wireless system

In the wired MEMS system, the sensor must be connected to the data reader and the computer through cables to continuously monitor the concrete properties and data. As a consequence, both the data reader and the computer require an electrical power supply. However, the implemented wireless system requires no external cables and can thereby save installation time and reduce the risk of sensor malfunction.

Evaluation of Wireless Communication Capability

To test the reliability and survivability of the wireless communication system inside the concrete, both the wireless transmitter and receiver were embedded in the concrete as shown in Figure 70 to conduct a success rate test. Success rate refers to the amount of data transmitted from the transmitter that successfully reaches the receiver. The higher this rate, the more reliable the system.

Figure 70. Wireless MEMS system inside concrete

The success rate test was conducted for the wireless MEMS system by burying the concrete containing the wireless MEMS system underground and gradually increasing the horizontal and vertical distances between the wireless transmitter and receiver, as shown in Figure 71.

Figure 71. Success rate test: wireless MEMS system inside concrete buried underground (left) and horizontal distance measurement for data transmission (right)

The test results indicated that the wireless communication system was able to successfully transmit temperature and RH measurements with a nearly 100% success rate when the receiver

was horizontally positioned approximately 150 ft away from transmitter. The results of the success rate test are provided in Appendix C.

Future Improvement

The objective of this study was to investigate the feasibility of implementing a wireless-based MEMS system for concrete pavement SHM. The requirements for the wireless MEMS system were derived from field experience with the wired MEMS system used in US 30. In the design of the wireless system, a wireless communication system was integrated with off-the-shelf MEMS sensors originally designed to be wired. The wireless MEMS system developed was capable of providing reliable temperature and RH data over a distance of more than 150 ft from the receiver when the sensor was embedded in concrete. However, the entire system was still energy consuming and had a limited energy source. It could work for just a few days at a reasonable data sampling rate using 12 1.5V AA batteries. The lifetime of these batteries could easily be diminished by harsh environmental factors such as the high temperatures occurring during concrete hydration; extremes of both temperature and humidity can reduce the lifetime and capacity of such batteries. Future research should focus on increasing memory capacity and making the whole system smaller. Some recommendations for resolving the aforementioned issues are as follows:

- A power management circuit, such as the Texas Instruments TPL5000 power timer, can be used to control the power output of the battery; this device can possibly extend the current working time to as much as several years under ideal conditions (Texas Instruments 2014).

- A microSD card or QuadRam Shield can be added to the microcontroller to tremendously increase its memory capacity.

- A smaller microcontroller called an Arduino Fio with an XBee plug, shown in Figure 72, can be used to replace the original microcontroller to reduce overall system size.

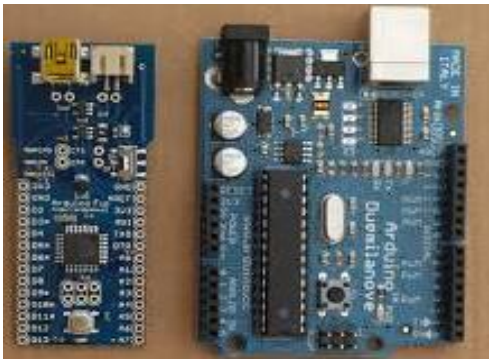

Figure 72. Arduino Fio (left) and Arduino Mega 2560 (right)

REQUIREMENTS FOR STRUCTURAL HEALTH MONITORING SYSTEM USING SMART SENSING TECHNOLOGIES

This chapter summarizes the issues involved in using MEMS and wireless sensors in pavement health monitoring systems based on a literature review, field instrumentation, and implementation of a wireless communication system. The requirements for advanced pavement SHM systems are addressed to generate some ideas regarding the strategies that can be effectively used to resolve the identified issues. A cost evaluation of pavement SHM systems and the architecture of advanced pavement SHM systems are presented.

Issues regarding SHM of Pavement Systems

Based on decades of pavement instrumentation, the general issues related to pavement SHM systems can be mainly divided into four categories: sensor selection, sensor installation, sensor packaging to prevent damage from road construction, and monitoring. These issues are present from the planning of a pavement SHM system to the end of the monitoring period. Each of these categories can be crucial to pavement SHM, so relative strategies must be identified to develop MEMS-based smart wireless sensing technologies for concrete pavement SHM. Table 11 summarizes the issues related to each category.

Table 11. Issues regarding SHM of pavement systems

Category	Issues
Sensor selection	Effects of asphalt/concrete medium, temperature and moisture effects, battery life (measurement frequency), placement, sensor specifications and operating characteristics, cost, hardware architecture, packaging, delivery time
Sensor installation	Optimal number of sensors, optimal locations to capture critical responses, orientation/direction, read/write range (placement depth), repeatability and reproducibility, installation methods (embedded or surface-mounted), training of sensor instrumentation personnel off-site
Road construction	Design and cost of durable sensor packaging, packaging for moisture sensors
Monitoring	Monitoring period, data measuring interval, frequency of data collection, data signal interference, wireless communications (“hop” network architecture), off-site power, data transfer and storage, protection of equipment, data acquisition systems, embedded software

The corresponding requirements for advanced pavement SHM systems are discussed in the latter part of this chapter.

Cost Evaluation of Pavement SHM Systems

The cost to implement SHM systems in similar projects can vary a great deal because the cost is associated with design, materials, labor, the scale and type of the structure to be monitored, the number and types of sensors, site location, monitoring period, and other factors. There is therefore no standard cost for a typical pavement SHM system at this time. However, the following factors typically contribute to the total SHM cost:

- Type and number of sensors (traditional sensors versus MEMS-based sensors, wired/wireless, static/dynamic, active/passive, etc.)
- DAS (automatic or manual)
- Sensor and DAS installation costs
- Travel costs (site investigation, sensor installation, data collection, etc.)
- Software
- Protective equipment (cabinet for DAS, safety vests, helmets, etc.)

Table 12 shows a unit sensor cost comparison between traditional sensors and MEMS sensors.

Table 12. Sensor unit cost comparison as of 2014

	Traditional Sensors		MEMS Sensors	
Category	**Manufacture (Model)**	**Price ($)**	**Manufacture (Model)**	**Price ($)**
Strain or Soil Pressure	Geokon (4000 series)	120~600	Melexis (90809)	7~8
	Geokon (3900 series)	605		
	Vishay (EGP)	44		
	Tokyo Sokki (PML)	143		
	Encardio Rite (EDS)	65~90		
	Endevco Corp.	5~10		
	Marton Geotechnical Services	150~500		
	Micron Optic (os3600)	649		
	RST Instruments	70~90		
	Smartec	65~90		
	Omega (KFH)	110~290		
	LTD	150~500		
	Applied Geomechanics	150~500		
	CTL (ASG)	500		
Temperature	Omega (Thermocouple)	65~260	Analog Device (ADT7320)	3
	Geokon (Vibrating Wire Temperature Sensor)	200	iButton (DS1921)	15~23
	Applied Geomechanics	200	MEMS VISION (MVH3000D)	N/A
	Slope Indicator	200	RFID tag Q350 series*	30~50
	Omega (RTD)	50~110	Sensirion (SHT71)	25
	Omega (Infrared temperature sensors)	65~260	STMicroelectronics (HTS221)	4~3
	Omega (TT-K-24-100)	78	MEMS VISION (MVH3000D)	N/A
Moisture	Vaisala Inc. (SHM40)	635	Hygrochron iButton	4~3
	Decagon Devices (GS3)	260	Sensirion (SHT71)	25
	Irrometer Watermark (200SS)	90	STMicroelectronics (HTS221)	4~3
	Campbell Scientific (CS616-L25)	140		
	Stevens (Hydraprobe II)	360	MEMS VISION (MVH3000D)	N/A
	Hydronix (Hydro-Probe II)	5,000		
	Innovative Sensor Technology (MK33)	32~50		

Note: * indicates wireless sensors; all other sensors shown in the table are wired sensors.

In general, unit sensor cost depends on the number of sensors procured; a larger number of sensors is typically associated with a lower per-unit cost. According to Table 12, MEMS sensors generally have a lower unit cost, varying perhaps from $3 to a few tens of dollars per sensor. Traditional sensor prices usually range from $50 to $500. However, the cost of a DAS is much higher than that of a sensor. Table 13 illustrates the cost of a DAS (computer cost not included) for some of the sensors from Table 12.

Table 13. DAS cost comparison as of 2014

	Traditional Sensors		MEMS Sensors	
Category	**Sensor Type**	**DAS Cost ($)**	**Sensor Type**	**DAS Cost ($)**
Strain or Soil Pressure	Geokon strain gage	1,760	Melexis (90809)	N/A
	Micron Optic (os3600)	24,000		
	Tokyo Sokki (PML)	3,000		
	Vishay (EGP)	708		
Temperature	Omega (Thermocouple)	549	Analog Device (ADT7320)	45~60
			iButton	40
			MEMS VISION (MVH3000D)	N/A
			RFID tag Q350 series	2,000
	Omega (TT-K-24-100)	450	Sensirion (SHT 71)	640
			STMicroelectronics (HTS221)	32
Moisture	Campbell Scientific (CS616-L25)	1,465	Hygrochron	40
			MEMS VISION (MVH3000D)	N/A
	Stevens (Hydra probe II)	3,270	Sensirion (SHT 71)	640
			STMicroelectronics (HTS221)	32

It can be seen that the DAS is much more expensive than the sensors and may cost $500 to $3,000 per unit. Furthermore, a DAS using wired sensors usually has a limited number of connection ports, so a more comprehensive DAS must be purchased if a large number of sensors is needed. For MEMS sensors, the cost of a DAS is relatively lower because many MEMS sensors can use an evaluation kit/board equipped with a USB cable to read and transmit data to a computer, usually resulting in a relatively lower cost compared to that of a traditional data logger. However, sensors can be interfaced with different data acquisition devices, and their prices vary significantly among different models and accessories, so there is not a well-defined standard value for DAS cost.

In addition to sensor and DAS costs, the cost of an SHM system also includes labor costs. According to Titi et al. (2012), the typical labor cost of an instrumentation plan/design with construction drawings ranges from $5,000 to $10,000. Furthermore, the maintenance cost per trip

due to electrical storms or vandalism may be as much as $2,500 to $5,000, and the data processing cost depends on the frequency of data collection.

Requirements for Smart Pavement SHM

Sensor Selection

Selection of sensors can be crucial for pavement health monitoring. When assessing potential sensors, the following factors must be considered:

- Capability of measuring pavement response
- Reliability (i.e., accuracy, lifetime, survivability in pavement)
- Availability (i.e., shipping time)
- Cost
- Practicality for field instrumentation

Previous pavement instrumentation projects have revealed the limitations of traditional wired sensors, including high cost, low reliability, complexity of field instrumentation, etc. Furthermore, traditional sensors usually have a relatively large size and many external wires, so locating large numbers of sensors of different types to obtain continuous data may very likely cause logistical problems and potential damage to the structure. In addition, data acquisition systems must be placed in close proximity to the pavement, causing problems in, for example, power supply and data storage and transmission. However, an on-site data acquisition system for a test track may not experience such problems because on-site office structures are usually built alongside the test track in projects such as MnROAD and Virginia Smart Road; this situation is not realistic for an actual highway. All these drawbacks of traditional wired sensors combine to limit the use of SHM for pavement systems. Therefore, it is important that sensors used in pavement health monitoring should have a small size, be wireless, have a low cost, and include an onboard CPU. However, it should be noted that a strain gage must be sufficiently long to precisely capture the strain values in a concrete matrix. Based on Copley (1994), a gage length three to five times the maximum aggregate size should be sufficient.

It’s already universally accepted that MEMS sensor technology can provide improved system performance, reliability, longevity, and safety compared to existing traditional wired sensor systems. The onboard CPUs of MEMS technology support a more efficient type of data interrogation. Compared to a traditional sensor, a MEMS sensor has a lower unit cost and smaller size, making it possible to increase in-pavement array density to obtain more data. Furthermore, through the microfabrication of MEMS technologies, a highly integrated multifunction sensor capable of simultaneously measuring several parameters such as temperature, RH, and strain can be developed. This multifunctional MEMS sensor can also reduce the number of sensors needed, further reducing installation costs.

A wireless sensor system has many benefits, such as low installation costs and shorter installation times, elimination of wire damage, good flexibility, etc. The common wireless

technologies used in civil infrastructure include the described RFID and ZigBee, described above. However, the main challenge for a wireless sensor system is related to the battery issue. In general, pavement has a design life ranging from 20 to 50 years, and maintenance and rehabilitation can be scheduled every 5 to 15 years (Luhr et al. 2010). Therefore, the monitoring period should ideally extend over decades. However, current commercial battery life can only extend to as much as 10 years under ideal conditions, and common sensors equipped with internal batteries have only a 2 to 6 year continuous working time (Roberts 2006). For example, the iButton and the active RFID tag used in the US 30 project have maximum battery lifetimes of 2 and 6 years, respectively. The harsh climate in a real highway can greatly reduce battery life, and there is no feasible way to replace embedded sensor batteries in concrete. Accordingly, a passive wireless system needs to be more suitable for long-term pavement health monitoring.

The aforementioned passive RFID tag usually uses an antenna to convert the wireless signal from the RFID reader into operating power; the idea is to convert electromagnetic wave or RF radiation into DC electrical power. Other potential energy harvesting methods that might be used by self-sufficient systems include wind, solar, thermoelectricity, and physical vibration (Yildiz 2009). Among these options, physical vibration could be an ideal energy source for pavement health monitoring because it relies on strain changes caused by passing vehicles. Piezoelectric material can be used to make the accelerometer or transducer for harvesting energy from the physical vibration. In addition to using passive systems, the computational capabilities provided by logical blocks on a board-mounted CPU can be incorporated into the sensor by MEMS technologies to manage power. In this situation, energy might be conserved by putting the device into a sleep mode, as described above.

To summarize, a Smart Pavement SHM needs to have MEMS-based sensors, wireless capability, and multifunctionality and be self-powered. Therefore, a wireless MEMS multifunctional sensor containing a self-sufficient energy harvesting system represents a promising solution for a Smart Pavement SHM. Durable packaging is also required in this system to protect the sensor from the concrete. This kind of wireless multifunctional MEMS sensor is, however, not yet commercially available, because fully integrating all the sensing elements may result in relatively excessive device dimensions and high unit cost due to complex fabrication, assembly, and implementation. More importantly, energy consumption may be significant because of the need to simultaneously measure a number of parameters.

Sensor Installation

In planning an SHM system, questions emerge such as the number of sensors needed and where the sensors should be installed. Installing sensors throughout the entire structure can produce a superior data set but may not be realistic because of cost, logistics, and potential cracking issues. For that reason, the number and locations of sensors should be optimized at the planning stage.

Temperature, moisture, and strain sensors are the most common sensor types installed in pavement infrastructure. Vertical displacement gauges such as LVDTs placed at the pavement bottom are often used to measure the vertical movement of a concrete slab. Pavement sensors can be grouped into pavement response sensors, such as strain gages and LVDTs, and pavement

environmental condition monitoring sensors, such as temperature and moisture sensors. In optimizing the number of sensors and their locations, critical locations within the pavement should be determined.

A rigid pavement consists of a series of concrete slabs. The critical locations at which to monitor concrete slab response under load are at the middle of the longitudinal joint, the middle of the transverse joints, and the slab corners, which suffer more from load than other locations (Darestani 2007). The PCC pavement response sensors should be installed at these locations. Strain gages are usually installed at the top and bottom locations in the slab, while LVDTs are usually installed at the bottom, as shown in Figure 73.

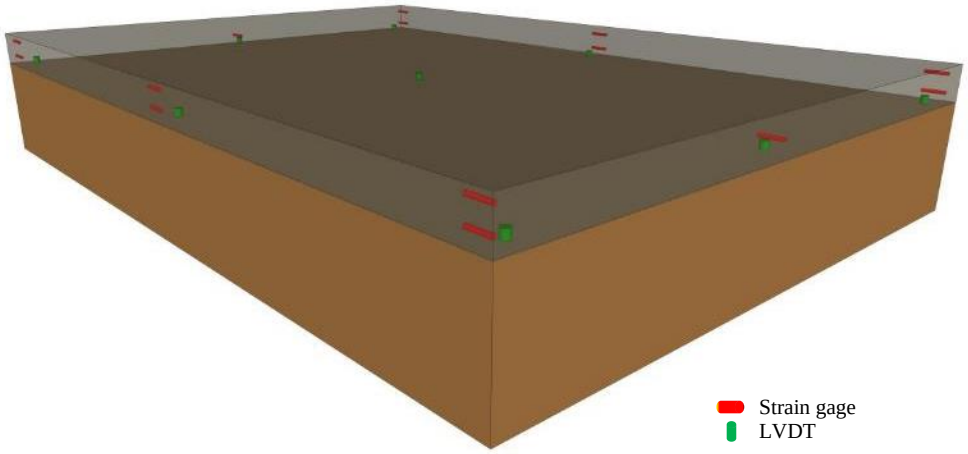

Figure 73. Typical installation layout of PCC pavement response sensors

For flexible pavement, critical locations include the pavement surface and bottom layers, the top of the intermediate layer, and the top of the subgrade (Timm et al. 2004). PCC pavement environmental condition monitoring sensors should be installed at the center but also at various depths to record temperature and moisture variations with depth, as shown in Figure 74.

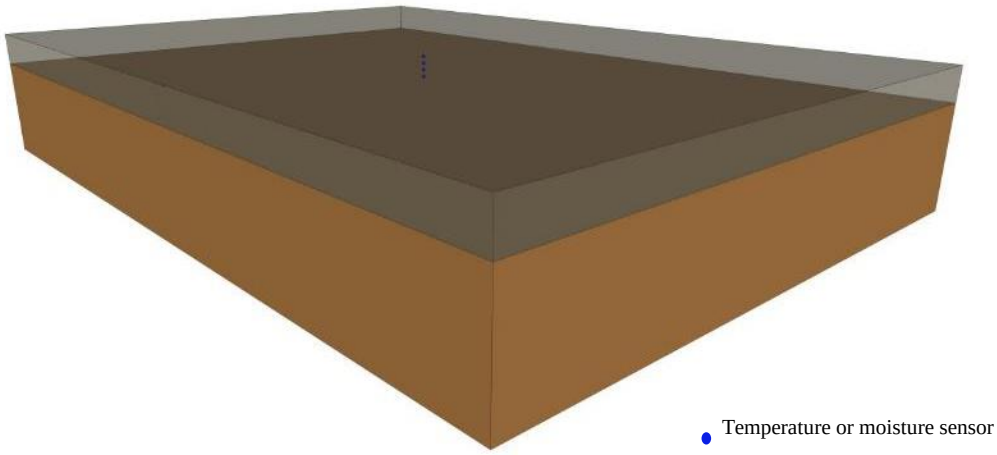

Figure 74. Typical installation layout of PCC pavement environmental condition monitoring sensors

It should be noted that the installation plan may require modification based on specific conditions, such as project purpose, sensor types, sensor size, budget, and other factors. However, it is recommended that temperature and moisture sensors always be installed every 2 in. along the depth from top to bottom. The highest sensor embedded in the concrete pavement should be only 1 to 2 in. away from the surface. If a sensor needs to be installed at lower depths, it is probably better to install it after concrete paving.

Pavement sensors are delicate, so they must be very well protected to increase their survivability. Previous projects using sensors anchored on wooden bars did not work well and led to a time-consuming installation process. Instead, a pre-manufactured cage may be useful in making the installation process both easier and faster. The sensor packaging and the wooden bar used to fix the location of sensors can be equipped with multiple screw holes to permit flexible mounting and to increase reliability. An oblong rather than a cylindrical bar shape might be more stable during concrete spreading. A sensor might be installed in an instrumented core or even inside a hollow wooden bar so that the core or wooden bar can act as a shell and protect the sensor. A sensor might also be installed in a specially designed gyroscopic frame so that its angle of orientation resulting from concrete paving can be measured. It is notable that the sheet metal boxes (see Figure 75) used in the pavement instrumentation research conducted by an Ohio University team had a 90% strain gage survival rate, so this approach might also be useful (Sargand and Khoury 1999).

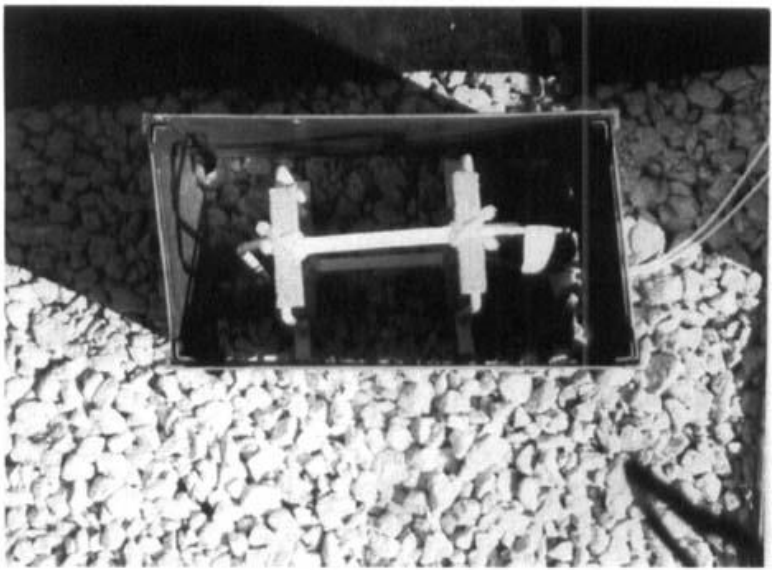

Figure 75. Sheet metal boxes

The quality of sensor installation directly affects sensor survivability in pavement, so training installers in advance increases the survivability rate and saves time. Furthermore, maintaining at least 1 in. of vertical distance from the top sensor to the paver and vibrator reduces the vibration effects from the construction equipment. Pouring some fresh concrete on the top of the sensor prior to paver operation can also mitigate the force from concrete spreading. The instrumented location should be remote from power lines to avoid electromagnetic noise, and the sensors and wires should be protected from shoulder paving and drainage system layout operations. It is essential to communicate with the construction crew in developing an optimal installation plan.

Sensor Packaging to Prevent Damage from Road Construction

As noted above, packaging is crucial in establishing a reliable sensor system, particularly a system with moisture sensors, to be used in pavement health monitoring. The cost of packaging can represent 75% to 95% of the overall product cost (Attoh-Okine and Mensah 2003). Sensor packaging involves more than just choosing standard chip packages; it includes packaging for the whole sensor system. Different system and assembly requirements must therefore be taken into account, especially when using multifunctional sensors (Wang et al. 2010, Frank 2013).

In general, packaging a system of MEMS sensors can be divided into three levels: die packaging, device packaging, and system packaging. The sensor die refers to the actual silicon chip containing the integrated circuit, whose packaging system includes wafer packaging, sometimes considered to be another level of packaging (Silicon Laboratories, Inc. 2014b). Device packaging provides protection for micromechanical components immediately after their manufacture, and system packaging protects the entire system, including the battery, antenna, and other components (Chiao and Lin 2006).

In the packaging process, the structure of a MEMS sensor is first encapsulated by bonding the device wafer to a second wafer to protect it from moisture contamination and particle impingement before assembling the sensor into a standard packaging module. During assembly of the die packaging, to reduce potential packaging material–induced stress on the sensor die, cavity packaging, a specially designed die coating, and a transfer molding process are used. Die bonding and wire bonding are used for device-level packaging, and system-level packaging is accomplished by inserting the device into a metal or plastic case. Figure 76 and Table 14 provide detailed descriptions for each level of packaging (Imego 2005, Amkor Technology 2014).

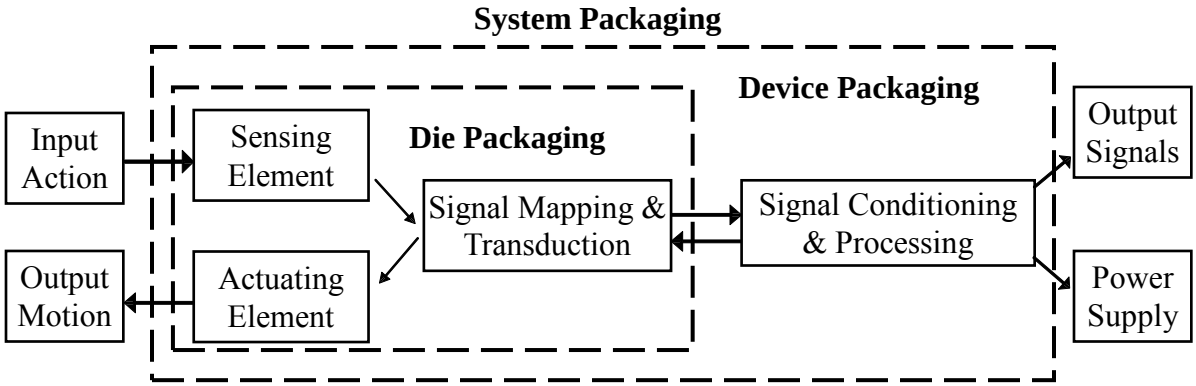

From Hsu 2008

Figure 76. MEMS sensor packaging system

Table 14. MEMS sensor packaging methods and materials

Levels	Packages
Die	Cavity packaging (CSP-cavity LGA package), CERDIP, Ceramic LCC, SOIC, and MLF derivatives
Device	Die bonding, wire bonding, interconnecting, etc.
System	Ceramic packages (basic dual in-line packages, chip carriers, flat packs, and multilayer packages), plastic packages (lead frame materials include copper alloy, nickel-iron, composite strips, etc.), metal packages (Kovar, cold-rolled steel, copper, molybdenum, silicon carbide–reinforced aluminum, etc.)

Sources: Adams and Layton 2009, Williams 2000, Zinck 2013

New packaging materials and methods emerge virtually every day, but MEMS sensors are application-specific, so it is difficult to develop one-size-fits-all packaging and sensor systems. Among the various sensors, the moisture sensor is most vulnerable to the environment because it must have access to its outside environment via an open pore to measure water vapor, which represents a severe challenge for MEMS sensor encapsulation (Wang et al. 2010). The most common packaging for moisture sensors is a pre-molded open-cavity package. In concrete, both the high pH environment and excessive water exposure can damage moisture sensors through their open pores. Therefore, a hand-made simple packaging approach is usually used for moisture sensors to improve their performance, as described by Ye et al. (2006), Choi and Won (2008), and Wells (2005). However, there are no 100% reliable moisture sensors with robust packaging yet available, and most moisture sensors tend to stop functioning in concrete

pavement a few weeks after road construction. As a result, engineers continue to pursue a reliable moisture sensor packaging method to be used in pavement applications. There are also companies specializing in sensor packaging design and manufacture. The following sections summarize packaging methods for moisture sensors used in pavement.

Simple Packaging Used in the Field

Ye et al. (2006) conducted a literature review on curing in PPC pavement, and a moisture sensor called Hygrochron was evaluated in that study. Choi and Won (2008) performed a similar study to identify compliance testing methods for curing, and a plastic pipe with Gore-Tex was used to protect the Hygrochron sensor in the concrete pavement, as shown in Figure 77.

Choi and Won 2008

Figure 77. Hygrochron sensor packaged in the field

However, the pore size or the configuration of this fabric may have influenced the RH measurements, and the readings in the concrete therefore may not have been consistent (Choi and Won 2008). Near the end of the study, an RH value over 100% was observed.

Figure 78 illustrates a packaging method developed by Wells (2005) used in a field pavement construction project, similar to that developed by Choi and Won (2008).

Wells 2005

Figure 78. Moisture sensor packaging

The University of Pittsburgh conducted a study in 2002 to investigate early-age concrete pavement behavior. In this study, a Sensirion SHT75 humidity sensor was used to monitor RH values; this was the same sensor used in the US 30 study described above. During road construction, the moisture sensor was inserted into a plastic cylindrical tube, and the enclosure was sealed with a circular Gore-Tex membrane vent using ordinary superglue. The idea behind this kind of packaging was to protect the sensors from direct contact with the concrete mixture, but the majority of the sensors later stopped functioning and unrealistic RH measurement values above 100% were observed. The reason for these failures was probably related to condensation along the sensor tips.

Quinn and Kelly (2010) performed a study to examine the feasibility of embedding wireless sensors into concrete for SHM. They used polyoxymethylene plastic to make a package for prevention of direct contact with liquid in fresh concrete.

A Gore-Tex screw-in vent was used to provide a protective seal over the sensor and allow diffusion of moisture vapor only. The final dimensions of this packaging were 65 mm in diameter and 45 mm in height.

Spherical Steel Platform

Lian (2010) developed the embedded wireless strain/stress/temperature sensor platform for highway applications shown in Figure 79.

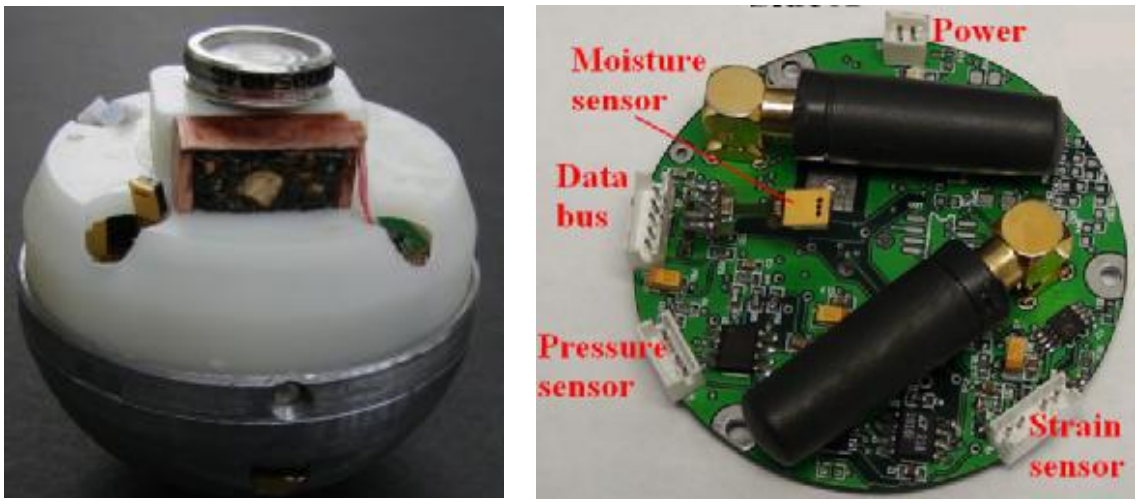

Lian 2010

Figure 79. Wireless strain/stress/temperature sensor platform

This steel platform developed by Lian (2010) was spherical in shape with a 3 in. diameter. The top half of this platform contained an RF data acquisition/control/communication board along with pressure, strain, moisture, temperature, and three-axial acceleration sensors, and the bottom half contained a rechargeable battery and Faraday energy-harvesting devices. The platform consumed a large amount of power and was still considered to be in the testing stage.

Porous Cement Paste

Bennett et al. (1999) installed temperature sensors in an instrumented core to measure the temperature of pavement, as described in the literature review in Chapter 2. Barroca et al. (2013) used a similar approach to embed a moisture sensor in a porous mortar cube. In the study by Barroca et al. (2013), the moisture sensor was fabricated by first welding a filter cap to a filter membrane, and it was then buried in a porous 2 in. mortar cube made with coarse sand using a low water-cement ratio of 1:3. In this packaging system, the mortar worked as a shell to protect the sensor wire connections during concrete casting, and the high porosity of this cube allowed the sensor to measure the RH level of the concrete through the pores.

Stainless Steel Jacket

Sarrfi and Romine (2005) conducted a study to develop a sensor capable of measuring both temperature and moisture. The sensor die was protected by a polymeric coating, and the whole chip was encapsulated in a stainless steel jacket equipped with a ceramic filter for RH measurement (Saafi and Romine 2005, Norris et al. 2008). The dimensions of the completed sensor were 3 mm in height and 5 mm in diameter.

Moisture Sensor with Detecting Probe

Several probe-based moisture sensors have been developed, including the MK33 Capacitive Humidity Sensor and the Hydro-Probe II Moisture Sensor, which the respective manufacturers claim are applicable to internal RH measurement in concrete. The MK 33, shown in Figure 80 (left), is a capacitive sensor that can be directly embedded in a concrete mixture because of its high solvent and hot water resistance. The Hydro-Probe II Moisture Sensor, shown in Figure 80 (right), is a sensor using digital microwave moisture measurement to measure RH in concrete. Similarly to the MK 33 Capacitive Humidity Sensor, the Hydro-Probe II Moisture Sensor can be directly placed in plastic concrete to provide reliable RH measurement. However, this sensor is very expensive, with a unit cost of more than $5,000 (Sebesta et al. 2013). In addition to the MK33 Capacitive Humidity Sensor and the Hydro-Probe II Moisture Sensor, other probe-based moisture sensors, such as TDRs and the Stevens Hydra Probe, are often used in soil moisture detection. These probe-based moisture sensors are, however, unable to provide an RH profile versus pavement depth.

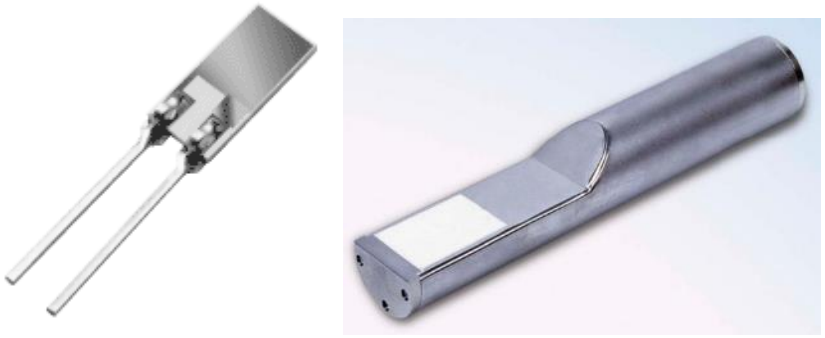

Every et al. 2009 (left) and Hydronix 2014 (right)

Figure 80. Moisture sensor with detecting probe: MK33 Capacitive Humidity Sensor (left) and Hydro-Probe II moisture sensor (right)

Monitoring

The monitoring period can be divided into either short-term or long-term intervals depending on project objectives, sensor survivability, and battery life. A short-term period might be just a few months, while a long-term period might be several years; a longer monitoring period is usually preferred, even if it is difficult to achieve. Data measuring intervals can vary from one minute up to one hour. Typically, half-hour intervals are sufficient for temperature and moisture measurements, while strain can be measured in one-minute intervals. Short intervals can provide more detailed data but consume more power, so a balance between the size of the data measuring interval and battery life should be established. One strategy is to adjust the interval depending on changes in situation. It is well known that the early-age behavior of concrete pavement may impact long-term performance, so at an early age a short measuring interval might be applied (Ruiz et al. 2005). Longer intervals can then be used for the remaining time to consume less energy; the intervals might then be shortened again when a critical situation is detected. Early age is defined by Federal Highway Administration (FHWA) guidelines as the first 72 hours after

pavement construction, although sometimes the term may refer to the time before opening to traffic (Ruiz et al. 2005).

Daily data collection and backup is preferred to guard against accidental data loss, but collection intervals may depend on specific situations affected by weather, distance, cost, and other factors. The on-site DAS and power sources should be protected from harsh climate and local animals. However, if wireless sensors are used, a moving truck mounted with a DAS could be used for data collection. To achieve this goal, reliable wireless transmission technology is required to provide a strong signal and eliminate electronic interference, as shown in Figure 81 (left) (Lajnef et al. 2013).

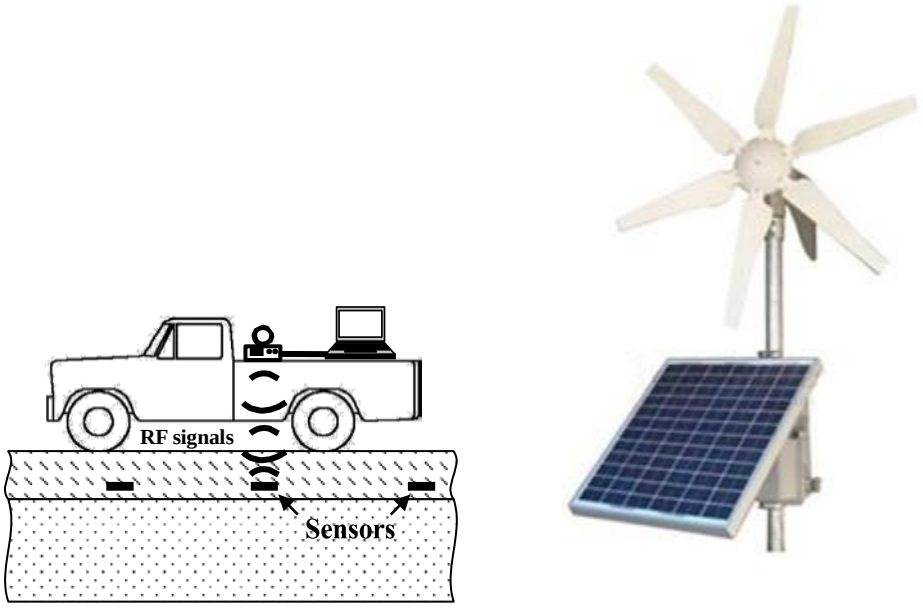

Lajnef et al. 2013 (left) and Wake, Inc. 2014 (right)

Figure 81. Advanced data acquisition system: RF reader mounted on a moving vehicle (left) and i-TOWER with turbine and solar panel (right)

In addition to a vehicle mounted with a DAS, a two-level wireless communication system for remote data collection might be employed. The first level would use a wireless communication device at the data collection site. This device would act as a transfer station to transmit data via the internet to the second level. Figure 81 (right) shows an example of this kind of wireless device, an i-TOWER used in the HardTrack Concrete Monitoring System. This device can transmit data via cellular internet with a built-in 3G/4G hotspot. Furthermore, it can be powered with either turbine or solar power (Wake, Inc. 2014).

Architecture of a Smart Pavement SHM System

Smart Pavement SHM is defined as a long-term, continuous, sustainable pavement system providing information about in situ pavement conditions to prevent multiple safety concerns, including pavement deterioration. The literature review in Chapter 2 described the need for

Smart Pavement SHM for both highway and airfield pavements. The basic concepts of Smart Pavement SHM are similar for both highway pavement and airfield pavement. For airfield pavement, an SHM system can be combined with a foreign object debris (FOD) detection system to provide timely warning of the appearance of FOD, which is any substance or debris that could cause aircraft damage (Ang 2013).

Figure 82 illustrates conceptual designs of highway and airport health monitoring systems, respectively.

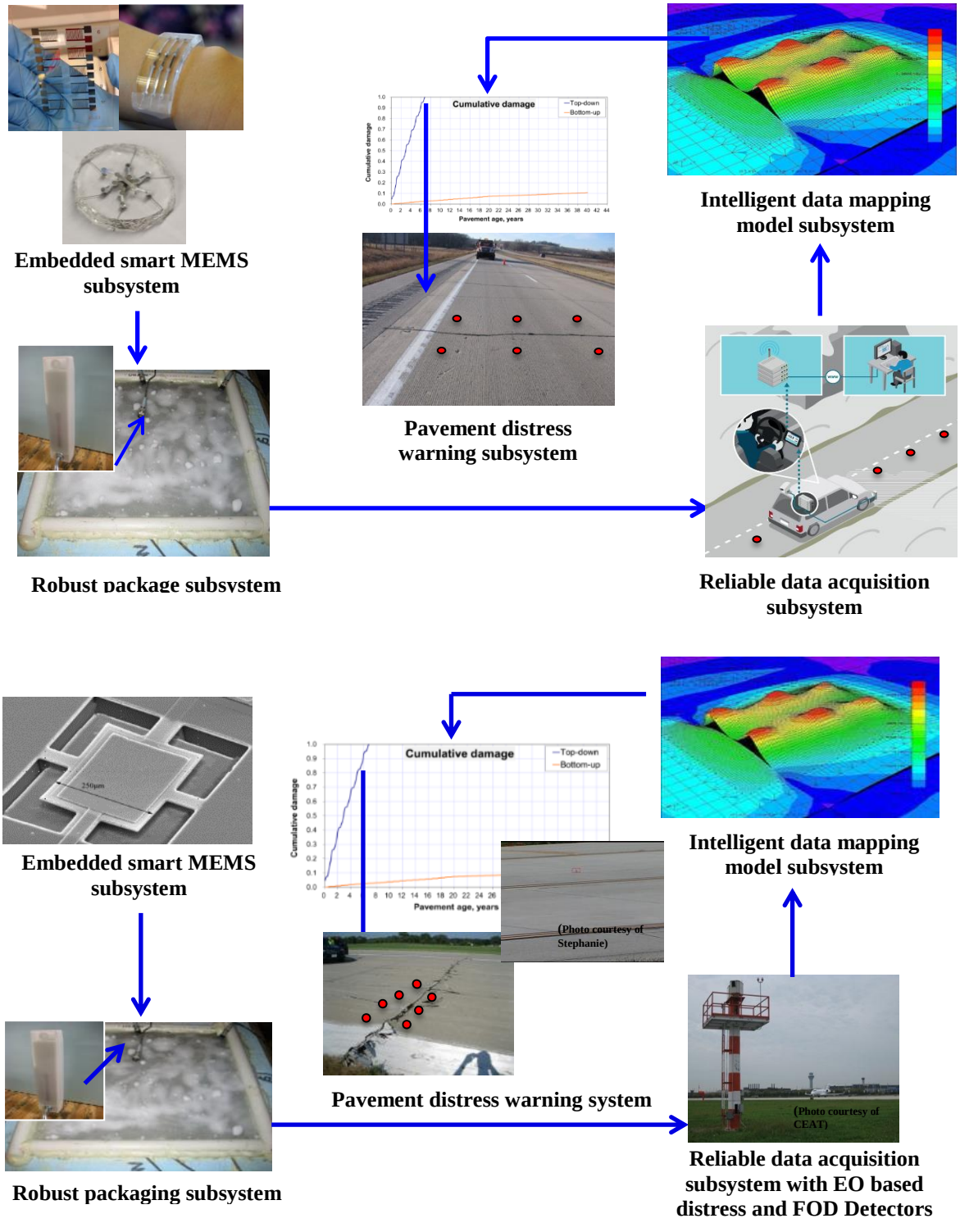

Figure 82. Smart pavement monitoring systems for highway pavement (top) and airfield pavement (bottom)

In Figure 82 (top and bottom), the embedded smart MEMS sensor subsystem is a wireless multifunction MEMS sensor able to simultaneously measure strain, temperature, and moisture. A

robust packaging subsystem should also be implemented to protect the embedded smart MEMS sensors from pavement construction, the high-alkali environment of concrete, and harsh climate and traffic conditions. A reliable DAS, mounted either on a moving vehicle for highway pavement or a control tower for airfield pavement, can be used for data collection, storage, and transfer from embedded MEMS sensors. An intelligent data mapping model subsystem employing sensor data fusion and a geo-spatial analysis approach can be utilized to map the data collected from the sensors installed at specific locations. Realistic characterization of pavement layer properties and responses through an intelligent data mapping model subsystem can be used to provide early warning about critical distress initiation, accurate airport pavement life predictions, and pavement management and planning activities, as well as calibration and validation of mechanistic-based pavement response prediction models. Unlike in highway pavement SHM, the smart MEMS sensor subsystem for airfield pavement SHM can be integrated with electro-optical (EO)–based distress and FOD detectors to monitor actual pavement surface conditions.

Other Potential Technologies for Development of Smart Sensing and Smart SHM for Pavement Infrastructure

Fiber Optic Sensor System

A fiber optic sensor is a type of sensor that can either monitor environmental conditions or transmit data using fiber optic communication, which modulates a light beam within a fiber. In general, fiber optic sensors have a small size and weight and can be used in explosive and corrosive environments. They can also be used to provide distributed sensing along the optical fiber. Theoretically, hundreds of locations along a fiber just 1 m long can be measured. Furthermore, fiber optic sensors can be used to measure strain, temperature, humidity, pH, and other properties (Balageas et al. 2006, Glisic and Inaudi 2007, Rice and Lloyd 2014).

Self-Sensing Concrete

Self-sensing concrete is a new alternative for Smart Pavement SHM that relies on making measurements based on electrical resistivity, impedance, capacitance, and so on (Han et al. 2014). This technology utilizes conductive materials such as nanotubes to configure an internal electric network inside the concrete, which allows properties such as stress and strain to be measured based on piezoresistivity effects; the data can be acquired using either wired or wireless methods (Li and Ou 2009, Sun et al. 2010, Han et al. 2014, Ubertini et al. 2014). Self-sensing concrete can also be used to monitor traffic or to melt snow (i.e., electrically conductive self-sensing concrete can be used for pavement heating) in transportation infrastructures. Figure 83 illustrates a self-sensing concrete system for strain measurement.

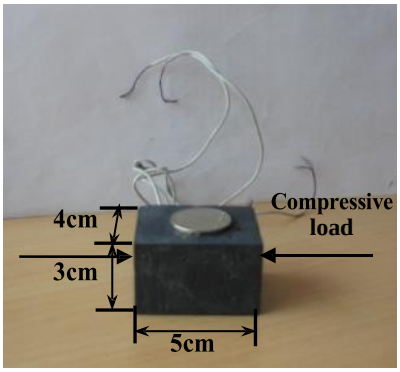

Li and Qu 2009

Figure 83. Self-sensing concrete system for strain measurement

Microbattery with Nuclear Power

Battery life is a key factor for active wireless sensors used in health monitoring, and traditional battery technology may extend the working life of sensors by as much as 10 years (Roberts 2006). Microbatteries using nuclear energy may provide a solution that can increase battery life up to several decades, with sizes at the micro or even nano scale. The main concept of this technology, which is still in the research stage, is to use radioisotopes rather than fossil or chemical fuels to generate electricity (Guo et al. 2008).

Vehicle Noise–Based Roadway Health Monitoring

Vehicle noise–based roadway health monitoring systems use a noise-based data collection system to evaluate infrastructure for proactive maintenance, operation, and safety. In such a system, a vehicle is used as a mobile sensor to measure noise, vibration, and harshness. Sensing devices such as accelerometers can be mounted on the vehicle for data measurement (Yousuf and Morton 2014). Figure 84 shows a versatile onboard traffic embedded roaming sensor (VOTERS) test van equipped with sensors, a camera, and a millimeter wave radar to measure pavement surface conditions.

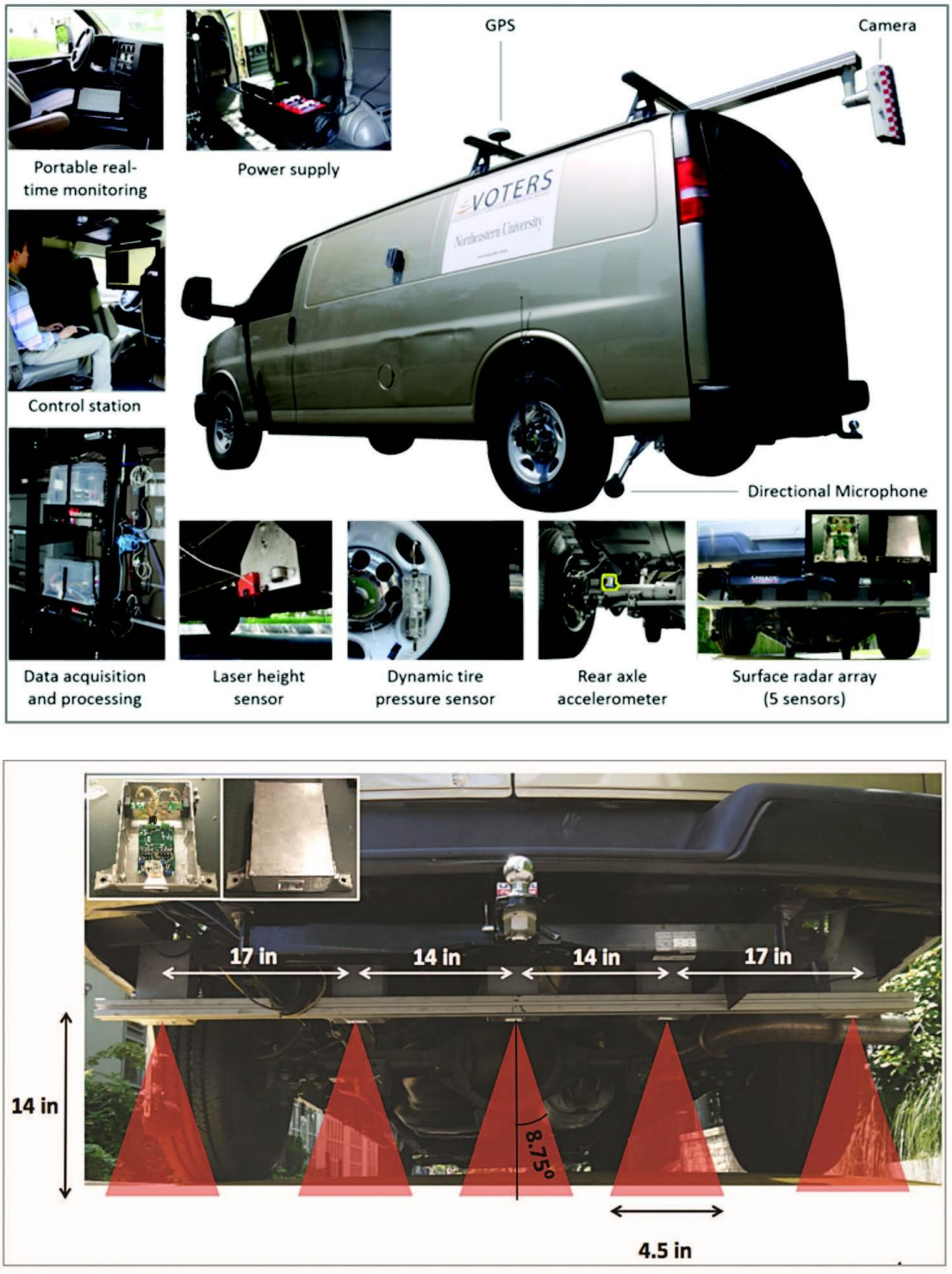

Yousuf and Morton 2014 © Boston University (top) and © Northeastern University (bottom)

Figure 84. Vehicle noise-based roadway health monitoring: VOTERS test van (top) and 24-GHz millimeter-wave radar array (bottom)

SUMMARY AND RECOMMENDATIONS

Key Findings

Early damage detection in transportation infrastructure systems can allow the development of better pavement maintenance and rehabilitation strategies to give pavement systems longer operational life. SHM was conceived to perform early damage detection in transportation infrastructure and has been implemented or is currently being implemented on pavement systems. Recent advancements in sensing technology have allowed SHM to evolve and have driven the development of Smart Pavement SHM. In the context of current changes in SHM due to new sensing technologies, this study (Volume I) discussed the use of MEMS-based smart wireless sensing technologies to monitor the health of concrete pavement. The results of a literature review pertaining to SHM applications for pavement infrastructure systems were discussed to evaluate the current pavement SHM practices and to identify the ways "smart sensors" and "smart SHM" have been defined in the literature and applied to transportation infrastructure systems.

MEMS and wireless sensing technologies and their applications to pavement SHM as reported in the literature were reviewed because these technologies have been considered promising for the development of smart sensor technology. MEMS represent an innovative solution in infrastructure condition monitoring that can be used to wirelessly detect and monitor the initiation and growth of structural and material durability related damage and distresses in concrete structures. A field demonstration of off-the-shelf MEMS and wireless sensor systems at an actual in-service concrete pavement site was conducted to evaluate their performance, identify their limitations, and demonstrate how the data they collect can be utilized to monitor concrete pavement behavior. The feasibility of implementing a wireless communication system using MEMS sensors was also investigated. Based on the literature review, the field demonstration, and the implementation of a wireless communication system, issues regarding concrete pavement SHM using currently available MEMS and wireless sensor technologies were summarized, and the requirements for achieving Smart Pavement SHM were explored to develop a conceptual design of smart health monitoring for both highway and airport pavement systems. The findings and recommendations drawn from this study can be summarized as follows:

Literature Review

- SHM can be useful for civil infrastructure to save both money and time by turning schedule-based maintenance into condition-based maintenance. However, the traditional sensor-based SHM approach has limitations, such as high installation costs and lengthy installation times, high array density, wire damage, and low survivability of sensors during long-term applications. Therefore, the traditional approach may provide neither continuous long-term monitoring of changes in pavement structural behavior nor real-time warnings of in-service pavement failures.

- A MEMS-based sensor system is a promising type of smart sensing technology that can be used to achieve Smart Pavement SHM. However, most MEMS-based sensors for SHM are still in the research stage and have not yet been commercialized.

- Wireless sensors can save both installation time and cost and do not present wire damage concerns. Although they represent a potentially significant benefit for SHM, they have not yet been widely applied to pavement health monitoring, and most research studies are still in the proof-of-concept stage.

Field Instrumentation and Evaluation

- Sensor survivability is critical for long-term SHM of pavement systems. In the field instrumentation study, about 78% of the embedded commercially available off-the-shelf MEMS sensors remained functional one month after the pavement was opened to traffic, but only 20% were still functional 10 months after opening to traffic.

- Temperature, moisture, and strain profiles were developed from the data collected during the monitoring period, and these profiles accurately reflected weather and seasonal changes, including thunderstorms, heat waves, and differing summer and winter temperatures. Furthermore, the curling and warping behavior of concrete that resulted from different temperatures at different concrete depths was observed and analyzed. According to the strain curve, the top of the concrete and the bottom of the concrete showed opposite patterns of curvature.

- The main reasons for the cessation of sensor functioning included concrete paver operation, the alkali-cement hydration reaction in concrete, corrosion of sensor wires, battery issues, harsh climate, and slab movement. The moisture sensor was quite sensitive to the chemical environment. Furthermore, the RFID tags had a low wireless communication range, probably due to battery issues, cold weather, and steel reinforcement in the concrete.

- Common concrete tests were conducted in the laboratory, and a concrete maturity curve was developed to estimate in-place concrete strength gain.

Implementation of a Wireless Communication System

- The ZigBee-based wireless network implemented for the MEMS sensors demonstrated reliable communication and achieved a high success rate over a 150 ft span.

- The power consumption of the wireless system was high, mainly due to the microcontrollers. Therefore, a power-saving mechanism, such as a power management circuit, could be added to extend the system's working life.

Requirements for a Smart Pavement Structural Health Monitoring System

- Procedures and strategies for pavement instrumentation must be considered well in advance of construction. Communication with the construction manager is important for increasing sensor survivability in the pavement.

- MEMS sensors usually have a lower per-unit sensor cost and a lower DAS cost.

- Robust packaging, especially for moisture sensors, is a key element for sensor survivability. However, no 100% reliable moisture sensor is yet available.

Recommendations

Based on the findings of this research, the following recommendations are proposed for the future development of smart sensors and smart SHM for pavement infrastructure systems:

- The future research topics for MEMS-based transportation infrastructure applications include the development of a chloride ion detection sensor for monitoring rust-inducing salts in concrete structures, detection of wrong-way of vehicle entry, overcoming the challenges of pavement health monitoring using smart sensing technologies, and evaluating the costs of smart pavement health monitoring systems.

- A wireless multifunctional MEMS sensor with an energy-harvesting system and durable packaging is recommended for Smart Pavement SHM. A power management circuit can also be used to reduce power consumption.

- An active RFID system has a long communication range but a limited lifetime and a relatively large size, while a passive RFID system has an unlimited lifetime but a short communication range. Therefore, a semi-passive RFID system that has an internal battery and that can also be self-powered may be a solution combining the advantages of both the active and passive RFID systems.

- The several types of wireless communication systems summarized in Chapter 5 are recommended for data collection. The first system would use a vehicle-mounted DAS to collect data using a passive wireless sensor system. Wireless communication range and onboard data storage capacity would be critical factors for this system. The second system would use a two-level wireless system with a local data transfer station powered by solar or wind energy. The data transfer station could both collect data from embedded sensors and transmit data to a remote office. For example, a small-scale structure near an office site could use an RFID system for first-level communication and a ZigBee network for second-level communication. Such a combined RFID- and ZigBee-based monitoring system could improve monitoring efficiency and promise low costs.

- For a large structure for which data must be transmitted to a remote office, the data can be transmitted via the internet (second level) to allow a technician to download the data either at home or at an office.

- RF communication usually has a limited range. The data can be lost if the transmission distance is too long, so a "hop" network can be used to resolve this problem and save power (Zhao and Guibas 2004).

- Sensor installation should use smart strategies to eliminate the effects of road construction activities, as described in Chapter 5. Communicating with the construction manager as soon as possible to optimize the installation method is critically important. An easy sensor installation method should also be investigated in the future. Specially designed tools or packaging for the sensors may be needed.

- Other sensing technologies such as fiber optic sensor systems, self-sensing concrete, microbatteries using nuclear power, and vehicle noise–based roadway health monitoring are recommended for future investigation.

The research team is tasked with expanding these project findings and accomplishments in infrastructure health monitoring during Phase I and Phase II studies into other areas of transportation infrastructure systems, such as the following in future research efforts:

- Flexible and composite pavement systems
- Geotechnical engineering and foundation systems
- Bridge structures and systems
- Mass concrete applications
- Construction quality control (QC) and quality assurance (QA)
- Construction management
- Critical infrastructure condition monitoring and pre-alert systems
- Monitoring of viaducts, drainage, and water channels
- Applications in unpaved and low-volume county and city roads (determination of freezing and thawing cycles and thawing periods using sensor systems, spring load restriction (SLR) guidance based on sensor data; etc.)
- Overweight-/heavy-vehicle loading pre-alert and detection systems
- Detection of pavement reflection cracking using radio-frequency identification-/RFID-based sensors
- Management of difficult-to-locate transportation assets using RFID-based sensors, etc.
- Use of smart sensors and systems in vehicle-to-vehicle and vehicle-to-infrastructure control

REFERENCES

Adams, T. M. and R. A. Layton. 2009. *Introductory MEMS: Fabrication and Applications. Concordia University*. University of California Press, Oakland, CA.

Al-Khatib, Z., J. Yu, H. G. Al-Khakani, and S. Kombarji. 2009. A *wireless multivariable control scheme for a quadrotor hovering robotic platform using IEEE® 802.15.4*. Concordia University, Canada.

AllAboutMEMS. 2002. What is MEMS? www.allaboutmems.com/whatismems.html. Last Accessed August 22, 2014.

Al-Qadi, I. L., A. Loulizi, M. Elseifi, and S. Lahouar. 2004. The Virginia SMART ROAD: the impact of pavement instrumentation on understanding pavement performance. *Journal of the Association of Asphalt Paving Technologists* 73.

Amkor Technology. 2014. MEMS & Sensors Packaging Technology Solutions. www.amkor.com/go/mems. Last Accessed August 26, 2014.

Andò, B., S. Baglio, N. Savalli, and C. Trigona. 2011. Cascaded "Triple-Bent-Beam" MEMS sensor for contactless temperature measurements in nonaccessible environments. *IEEE Transactions on Instrumentation and Measurement* 60(4): 1348-1357.

Ang, L. 2013. Research and design of an airfield runway FOD detection system based on WSN. *International Journal of Distributed Sensor Networks* 2013.

Arduino. 2014. Products. arduino.cc/en/Main/Products#.UxTTlfm9l8E. Last Accessed July 6, 2016.

Asbahan, R. E. 2009. Effects of the built-in construction gradient and environmental conditions on jointed plain concrete pavements. Ph.D. dissertation, University of Pittsburgh, PA.

American Society of Civil Engineers (ASCE). 2013. 2013 Report Card for America's Infrastructure. www.infrastructurereportcard.org/a/documents/2013-Report-Card.pdf. Last Accessed Oct 1, 2014.

AASHTO T336-11. 2011. Coefficient of Thermal Expansion of Hydraulic Cement Concrete. American Association of State Highway Transportation Officials, Washington, DC.

ASTM C39. 2005. Standard Test Method for Compressive Strength of Cylindrical Concrete Specimens. ASTM International, West Conshohocken, PA.

ASTM C403. 2008. Standard Test Method for Time of Setting of Concrete Mixtures by Penetration Resistance. ASTM International, West Conshohocken, PA.

ASTM C469. 2014. Standard Test Method for Static Modulus of Elasticity and Poisson's Ratio of Concrete in Compression. ASTM International, West Conshohocken, PA.

ASTM C496. 2011. Standard Test Method for Splitting Tensile Strength of Cylindrical Concrete Specimens. ASTM International, West Conshohocken, PA.

ASTM C1074. 2011. Standard Practice for Estimating Concrete Strength by the Maturity Method. ASTM International, West Conshohocken, PA.

Atmel Corporation. 2014. Atmel AVR 8-bit and 32-bit Microcontrollers. www.atmel.com/products/microcontrollers/avr/. Last Accessed August 4, 2014.

Attoh-Okine, N., and S. Mensah. 2003. MEMS application in pavement condition monitoring-challenges. *NIST SPECIAL PUBLICATION SP:* 387-392.

Aygun, B., and V. C. Gungor. 2011. Wireless sensor networks for structure health monitoring: Recent advances and future research directions. *Sensor Review* 31(3): 261-276.

Balageas, D., C. P. Fritzen, and A. Güemes. 2006. *Structural Health Monitoring*. ISTE Ltd., Newport Beach, CA.

Barroca, N., L. M. Borges, F. J. Velez, F. Monteriro, M. Gorski, and J. Castro-Gomes. 2013. Wireless sensor networks for temperature and humidity monitoring within concrete structures. *Construction and Building Materials* 40: 1156–1166.

Bennett, R., B. Hayes-Gill, J. A. Crowe, R. Armitage, D. Rodgers, and A. Hendroff. 1999. Wireless monitoring of highways. *SPIE Proceedings: Smart Systems for Bridges, Structures, and Highways* 3671: 173–182.

Bouhouche, T., M. A. El Khaddar, M. Boulmalf, M. Bouya, and M. Elkoutbi. 2014. A new middleware architecture for the integration of RFID technology into information systems. *Proceedings of the Multimedia Computing and Systems (ICMCS), International Conference, IEEE*: 1025-1030.

Brownjohn, J. M. W. 2007. Structural health monitoring of civil infrastructure. *Phil. Trans. R. Soc. A* 365(1851): 589-622.

Cao, H., S. K. Thakar, M. L. Oseng, C. M. Nguyen, C. Jebali, A. B. Kouki, and J. C. Chiao 2015. Development and characterization of a novel interdigitated capacitive strain sensor for structural health monitoring. *IEEE Sensors Journal* 15(11): 6542-6548.

Ceylan, H., K. Gopalakrishnan, P. C. Taylor, P. Shrotriya, S. Kim, M. Prokudin, S. Wang, A. F. Buss, and K. Zhang. 2011. *A Feasibility Study on Embedded Micro-Electromechanical Sensors and Systems (MEMS) for Monitoring Highway Structures*. Institute for Transportation, Iowa State University, Ames, IA.

Ceylan, H., K. Gopalakrishnan, S. Kim, P. C. Taylor, M. Prokudin, and A. F. Buss. 2013. Highway infrastructure health monitoring using Micro-Electromechanical Sensors and Systems (MEMS). *Journal of Civil Engineering and Management*, 19 (sup1): 188-201.

Chiao, M., and L. Lin. 2006. Device-level hermetic packaging of microresonators by RTP aluminum-to-nitride bonding. *Journal of Microelectromechanical Systems* 15(3): 515-522.

Cho, S., C. B. Yun, J. P. Lynch, A. T. Zimmerman, B. F. Spencer Jr, and T. Nagayama. 2008. Smart wireless sensor technology for structural health monitoring of civil structures. *International Journal of Steel Structures* 8(4): 267-275.

Choi, K. S., D. S. Kim, H. J. Yang, M. S. Ryu, and S. P. Chang. 2014. A highly sensitive humidity sensor with a novel hole array structure using a polyimide sensing layer. *RSC Advances* 4: 32075-32080.

Choi, S. and M. Won. 2008. *Identification of Compliance Testing Method for Curing Effectiveness*. FHWA Publication No. FHWA/TX-09/0-5106-2, Center for Transportation Research, the University of Texas, Austin, TX.

Copley, J. R. 1994. Route 2 rigid pavement instrumentation project: Installation and testing of selected instruments and data analysis for slabs 3, 4, 6, 7, & 9. Thesis, Ohio University, OH.

Daly, D., T. Melia, and G. Baldwin. 2010. Concrete embedded RFID for way-point positioning. Paper presented at the *2010 International Conference on Indoor Positioning and Indoor Navigation (IPIN)*, Zurich, Switzerland.

Darestani, M. Y. 2007. Response of concrete pavements under moving vehicular loads and environmental effects. Ph.D. dissertation, Queensland University of Technology, Australia.

Das, B. M. 2010. *Principles of Geotechnical Engineering*. 25th Edition. CENGAGE Learning, Stamford, CT.

Deng, F., Y. He, C. Zhang, and W. Feng. 2014. A CMOS humidity sensor for passive RFID sensing applications. *Sensors*, 14(5): 8728-8739.
Digi. 2014. ZigBee® Wireless Standard. www.digi.com/technology/rf-articles/wireless-zigbee. Last Accessed July 6, 2016.
Dong, M., and G. F. Hayhoe. 2000. *Denver International Airport Sensor Processing and Database*. Technical Report DOT/FAA/AR-00/17. U.S. Department of Transportation, Federal Aviation Administration, Office of Aviation Research, Washington, DC.
Every, E. V., F. Faridazar, and A. Deyhim. 2009. Embedded sensors for life-time monitoring of concrete. Paper presented at the 4th International Conference on Structural Health Monitoring on Intelligent Infrastructure (SHMII-4), Zurich, Switzerland.
Farrar, C. R. 2001. Historical Overview of Structural Health Monitoring. *Lecture Notes on Structural Health Monitoring Using Statistical Pattern Recognition*. Los Alamos Dynamics, Los Alamos, NM.
Farrar, C. R., and K. Worden. 2007. An introduction to structural health monitoring. *Phil. Trans. R. Soc. A*, 365(1851): 303-315.
Federal Aviation Administration (FAA). 2011. *Development of Standards for Nonprimary Airports*. Advisory Circular AC 150/5100-13B. U.S. Department of Transportation, Federal Aviation Administration, Washington, DC.
Federal Highway Administration (FHWA). 2012. *Pavement Assessment*. Federal Highway Administration Broad Agency Announcement No. DTFH61-12-R-00055. Federal Highway Administration, Washington, DC.
Frank, R. 2013. Smart Sensors: Packaging, Testing, and Reliability. www.memsjournal.com/2013/09/smart-sensors-packaging-testing-and reliability.html. Last Accessed August 17, 2014.
Geokon, Inc. 2014. Concrete Embedment. www.geokon.com/4200-Series. Last Accessed July 6, 2016.
Glisic, B., and D. Inaudi. 2007. *Fibre Optic Methods for Structural Health Monitoring*. John Wiley & Sons Ltd., Chichester, UK.
Guo, H., H. Li, A. Lal, and J. Blanchard. 2008. Nuclear microbatteries for micro and nano devices. *Proceeding of the Solid-State and Integrated-Circuit Technology (ICSICT), 9th International Conference, IEEE*: 2365-2370.
Han, J., P. Cheng, H. Wang, C. Zhang, J. Zhang, Y. Wang, L. Duan, and G. Ding. 2014. MEMS-based Pt film temperature sensor on an alumina substrate. *Materials Letters* 125: 224-226.
Haque, M. E., M. F. M. Zain, M. A. Hannan, M. Jamil, and H. Johari. 2012. Recent application of structural civil health monitoring using WSN and FBG. *World Applied Sciences Journal* 20(4): 585-590.
Hayhoe, G. F. 2004. Traffic testing results from the FAA's national airport pavement test facility. Paper presented at the 2nd International Conference on Accelerated Pavement Testing, Minneapolis, MN.
Hsu, T. R. 2008. *MEMS & Microsystems: Design, Manufacture, and Nanoscale Engineering*. John Wiley & Sons, Inc., NJ.
Hugo, F., and A. L. Epps Martin. 2004. *NCHRP Synthesis 325: Significant Findings from Full-Scale Accelerated Pavement Testing*. National Cooperative Highway Research Program, Washington, DC.

Hydronix. 2014. Hydro-Probe II Moisture Sensor for Bins, Chutes and Conveyor Belts. www.hydronix.com/products/hydroprobe.php. Last Accessed May 22, 2014.
Identec Solutions. 2008. Technology Rises with New York Skyline. www.wakeinc.com/PDF/FreedomTowerRelease.pdf. Last Accessed May 22, 2014.
Imego. 2005. Sensor-System Packaging. www.imego.com/Expertise/electronic-packaging/sensor-system-packaging.aspx. Last Accessed May 1, 2014.
Islam, T., A. Khan, J. Akhtar, and M. Rahman. 2014. A digital hygrometer for trace moisture measurement. *IEEE Transactions on Industrial Electronics* 61(10): 5599-5605.
Kang, I., M. J. Schulz, J. H. Kim, V. Shanov, and D. Shi. 2006. A carbon nanotube strain sensor for structural health monitoring. *Smart Materials and Structures* 15(3): 737-748.
Krüger, M., C. U. Große, and P. J. Marrón. 2005. Wireless structural health monitoring using MEMS. *Key Engineering Materials* 293: 625-634.
Kuang, K. S. C. 2014. Development of a wireless, self-sustaining damage detection sensor system based on chemiluminescence for structural health monitoring. *SPIE Proceedings: Smart Sensor Phenomena, Technology, Networks, and Systems Integration* 9062.
Lajnef, N., K. Chatti, S. Chakrabartty, M. Rhimi, and P. Sarkar. 2013. *Smart Pavement Monitoring System*. Federal Highway Administration, Turner-Fairbank Highway Research Center, McLean, VA.
Lajnef, N., M. Rhimi, K. Chatti, L. Mhamdi, and F. Faridazar. 2011. Toward an integrated smart sensing system and data interpretation techniques for pavement fatigue monitoring. *Computer-Aided Civil and Infrastructure Engineering* 26(7): 513-523.
Lee, J. 2004. *Use of MEMS Sensors in Structural Engineering*. Final Project of CEE 619. Advanced Structural Dynamics and Smart Structures, University of Michigan, MI.
Lee, J. S., Y. W. Su, and C. C. Shen. 2007. A Comparative study of wireless protocols: Bluetooth, UWB, Zigbee, and Wi-Fi. Industrial Electronics Society (IECON). Paper presented at the 33rd Annual Conference of the IEEE, Taipei, Taiwan.
Lee, X. G., M. Hovan, R. King, M. Y. Dong, and G. F. Hayhoe. 1997. Runway instrumentation at Denver International Airport development of database. *Aircraft/pavement technology: in the midst of change*: 348-362.
Lewis, F. L. 2004. Wireless sensor networks. *Smart Environments: Technologies, Protocols, and Applications*: 11-46.
Li, H., and J. P. Ou. 2009. Smart concrete, sensors and self-sensing concrete structures. *Key Engineering Materials* 400: 69-80.
Lian, K. 2010. *Developing Embedded Wireless Strain/Stress/Temperature Sensor Platform for Highway Applications*. Report No. NCHRP IDEA Project 129. National Cooperative Highway Research Program, Washington, DC.
Lin, C. H., L. M. Fu, and C. Y. Lee. 2014. MEMS-based humidity sensor based on thiol-coated gold nanoparticles. Paper presented at the 9th IEEE International Conference on Nano/Micro Engineered and Molecular Systems, Waikiki Beach, HI.
Liu, C. R., L. Guo, J. Li, and X. Chen. 2007. Weigh-in-motion (WIM) sensor based on EM resonant measurements. *Antennas and Propagation Society International Symposium*, IEEE: 561-564.
Liu, T., J. Yin, J. Jiang, S. Wang, and S. Zou. 2015. Differential-pressure-based fiber-optic temperature sensor using Fabry-Perot interferometry. *Optics Letters* 40(6): 1049-1052.
Lloret, J. 2009. Introduction to network protocols and algorithms. *Network Protocols and Algorithms* 1: 1-6.

Lu, Y. F., W. Z. Lou, and M. R. Guo. 2014. Rapid temperature measurement of meteorological detection system based on MEMS. *Key Engineering Materials* 609: 1185-1188.

Luhr, D., C. Kinne, J. S. Uhlmeyer, and J. P. Mahoney. 2010. Chapter 8. What we don't know about pavement preservation. *Proceedings of the 1st International Conference on Pavement Preservation*. Newport Beach, CA.

Lynch, J. P. 2002. *Decentralization of Wireless Monitoring and Control Technologies for Smart Civil Structures*. Technical Report No.140. John A. Blume Earthquake Engineering Center, Stanford, CA.

Lynch, J. P., and K. J. Loh. 2006. A summary review of wireless sensors and sensor networks for structural health monitoring. *The Shock and Vibration Digest* 38(2): 91-128.

Lynch, J. P., A. Sundararajan, K. H. Law, A. S. Kiremidjian, and E. Carryer. 2003. Power-efficient wireless structural monitoring with local data processing. *Proceedings of the International Conference on Structural Health Monitoring and Intelligent Infrastructure* 1: 331–338.

Maluf, N. 2000. *An Introduction to Microelectromechanical Systems Engineering*. Artech House, Boston, MA.

Maser, K., R. Egri, A. Lichtenstein, and S. Chase. 1996. Field evaluation of a wireless global bridge evaluation and monitoring system. *Proceedings of the 11th Conference on Engineering Mechanics* 2: 955-958.

Maxim Integrated. 2014. Overview of IButton Sensors and Temperature/Humidity Data Loggers. www.maximintegrated.com/en/products/ibutton/ibuttons/thermochron.cfm. Last Accessed June 2, 2014.

MEMSnet. 2014. What is MEMS Technology? www.memsnet.org/about/what-is.html. Last Accessed July 6, 2014.

Minnesota Department of Transportation (MnDOT). 2016. MnROAD Development. www.dot.state.mn.us/mnroad/history.html. Last Accessed July 15, 2016.

MnROAD. 2014. MnROAD: Safer, Smarter, Sustainable Pavement through Innovative Research. www.dot.state.mn.us/mnroad/pdfs/2014MnROADBrochure.pdf. Last Accessed July 5, 2016.

Modares, M. and N. Waksmanski. 2012. Overview of structural health monitoring for steel bridges. *Practice Periodical on Structural Design and Construction* 18(3): 187-191.

Mohammed, A. A., W. A. Moussa, and E. Lou. 2011. High-performance piezoresistive MEMS strain sensor with low thermal sensitivity. *Sensors* 11(2): 1819-1846.

Moradi, M., and S. Sivoththaman. 2013. Strain transfer analysis of surface-bonded MEMS strain sensors. *Sensors Journal* 13(2): 637-643.

Mullen, M. 2011. *Special inspections of paved areas during excessive heat periods*. Central Region Airport Certification Bulletin. Federal Aviation Administration, Central Region, Airports Division, Kansas City, MO.

Nagayama, T., and B. F. Spencer Jr. 2007. *Structural Health Monitoring Using Smart Sensors*. Technical Report No. NSEL-001. Newmark Structural Engineering Laboratory. University of Illinois at Urbana-Champaign, IL.

Nassiri, S. 2011. Establishing permanent curl/warp temperature gradient in jointed plain concrete pavements. Ph.D. dissertation, University of Pittsburgh, PA.

Norris, A., M. Saafi, and P. Romine. 2008. Temperature and moisture monitoring in concrete structures using embedded Nanotechnology/Microelectromechanical Systems (MEMS) sensors. *Construction and Building Materials* 22(2): 111-120.

O'Connor, M. C. 2006. RFID cures concrete. *RFID Journal* (October 2006). www.wakeinc.com/PDF/rfidcures.pdf. Last Accessed March 3, 2014.

Ong, J. B., Z. You, J. Mills-Beale, E. L. Tan, B. D. Pereles, and K. G. Ong. 2008. A wireless, passive embedded sensor for real-time monitoring of water content in civil engineering materials. *Sensors Journal* 8(12): 2053-2058.

Ooe, H., T. Eimori, M. Nomura, H. Nishikawa, K. Fujimoto, and T. Hasegawa. 2015. Low drift mems humidity sensor by intermittent heating. Paper presented at the 2015 IEEE International Meeting for the Future of Electronic Devices, Kyoto, Japan.

Phares, B. M., T. J. Wipf, L. F. Greimann, and Y. S. Lee. 2005. *Health Monitoring of Bridge Structures and Components Using Smart-Structure Technology, Volume I*. Bridge Engineering Center, Iowa State University, Ames IA.

Pei, J. S., C. Kapoor, T. L. Graves-Abe, Y. Sugeng, and J. P. Lynch. 2005. Critical design parameters and operating conditions of wireless sensor units for structural health monitoring. Paper presented at the 23rd International Modal Analysis Conference (IMAC XXIII), Orlando, FL.

Pei, J. S., R. A. Ivey, H. Lin, A. R. Landrum, C. J. Sandburg, T. King, M. M. Zaman, H. H. Refal, E. C. Mal, O. Oshlake, A. Heriba, and E. Hurt. 2007. Monitoring pavement condition using "smart dust" under surge time synchronization. *SPIE Proceedings: Sensors and Smart Structures Technologies for Civil, Mechanical, and Aerospace Systems* 6529: 173–182.

Pei, J. S., R. A. Ivey, H. Lin, A. R. Landrum, C. J. Sandburg, N. Ferzli, and E. C. Mai. 2009. An experimental investigation of applying Mica2 Motes in pavement condition monitoring. *Journal of Intelligent Material Systems and Structures* 20: 63-85.

Plankis, A., and P. Heyliger. 2013. *Off-Grid MEMS Sensors Configurations for Transportation Applications*. Technical Report No. MPC-13-257. North Dakota State University, Fargo, ND.

Potter, J. F., H. C. Mayhew, and A. P. Mayo. 1969. *Instrumentation of the full scale experiment on A1 trunk road at Conington, Huntingdonshire*. RRL Report. Transport Research Laboratory (Road Research Laboratory), Wokingham, Berkshire, UK.

Qi, G. Z., G. Xun, X. Z. Qi, W. Dong, and P. Chang. 2005. Local measurement for structural health monitoring. *Earthquake Engineering and Engineering Vibration* 4(1): 165-172.

Qin, Y. 2011. Numerical study on the curling and warping of hardened rigid pavement slabs. Ph.D. dissertation, Michigan Technological University, MI.

Quinn, B., and G. Kelly. 2010. Feasibility of embedded wireless sensors for monitoring of concrete curing and structural health. *SPIE Proceedings: Sensors and Smart Structures Technologies for Civil, Mechanical, and Aerospace Systems* 7647.

CoolTerm. 2014. Free Download and Software Reviews. download.cnet.com/CoolTerm/3000-2383_4-10915882.html#ixzz2ueTEGqCd. Last Accessed April 2, 2014.

Rice, J. A., and J. Lloyd. 2014. *Optimization of A Pavement Instrumentation Plan for A Full-Scale Test Road: Evaluation*. Florida Department of Transportation, FL.

Roberts, C. M. 2006. Radio frequency identification (RFID*). Computers & Security* 25(1): 18-26.

Rollings, R. S., and D. W. Pittman. 1992. Field instrumentation and performance monitoring of rigid pavements. *J. Transp. Eng.* 118(3): 361-370.

Ruan, Q., W. Xu, and G. Wang. 2011. RFID and ZigBee-based manufacturing monitoring system. *Proceedings of the 2011 IEEE International Conference on Electric Information and Control Engineering (ICEICE)*: 1672-1675.

Rufino, D., J. Roesler, and E. Barenberg. 2004. *Mechanistic Analysis of Pavement Responses from Denver International Airport*. FAA Center of Excellence (COE) for Airport Technology Report No.26. Department of Civil and Environmental Engineering, University of Illinois at Urbana-Champaign, IL.

Ruiz, J. M., R. O. Rasmussen, G. K. Chang, J. C. Dick, and P. K. Nelson. 2005. *Computer-Based Guidelines for Concrete Pavements, Volume II--Design and Construction Guidelines and HIPERPAV II User's Manual*. Technical Report No. FHWA-HRT-04-122. The Transtec Group, Inc., Austin, TX.

Saafi, M., and P. Romine. 2005. Preliminary evaluation of MEMS devices for early age concrete property monitoring. *Cement and Concrete Research* 35(11): 2158-2164.

Saboonchi, H. and D. Ozevin. 2012. Numerical simulation of novel MEMS strain sensor for structural health monitoring. *Proceedings of the 20th Analysis and Computation Specialty Conference*: 139-150.

Sackin, D., J. Garret, K. Gabriel, and M. Patton. 2000. MEMS for civil infrastructure: smart aggregate for concrete. *Advanced Technology in Structural Engineering*: 1-8.

Salman, N., I. Rasool, and A. H. Kemp. 2010. Overview of the IEEE 802.15. 4 standards family for low rate wireless personal area networks. *Wireless Communication Systems (ISWCS), 7th International Symposium, IEEE*: 701-705.

Sargand, S. M., and I. S. Khoury. 1999. Sensor installation in rigid pavement. *Experimental Techniques* 23(3): 25-27.

Scott, S., A. Kovacs, L. Gupta, J. Katz, F. Sadeghi, and D. Peroulis. 2011. Wireless temperature microsensors integrated on bearings for health monitoring applications. *Proceedings of the Micro Electro Mechanical Systems (MEMS), 2011 IEEE 24th International Conference*: 660-663.

Scott, S., F. Sadeghi, and D. Peroulis. 2012. Highly reliable MEMS temperature sensors for 275°C applications, Part 1: Design and technology. *Journal of Microelectromechanical Systems* 22(1): 225-235.

Sebaaly, P. E., N. Tabatabaee, B. Kulakowski, and T. Scullion. 1991. *Instrumentation for Flexible Pavements-Field Performance of Selected Sensors*. Technical Report No. FHWA-RD-91-094. Federal Highway Administration, Washington, DC.

Sebesta, S., J. Oh, S. I. Lee, M. Sanchez, and R. Taylor. 2013. *Initial Review of Rapid Moisture Measurement for Roadway Base and Subgrade*. Technical Report No. FHWA/TX-13/0-6676-1. Texas A&M Transportation Institute, College Station, TX.

Sensirion, Inc. 2014. Datasheet SHT7X Humidity and Temperature Sensor. www.sensirion.com/en/products/humidity-sensors/pintype-digital-humidity-sensors/. Last Accessed July 13, 2016.

Silicon Laboratories, Inc. 2014a. The Evolution of Wireless Sensor Networks. www.silabs.com/Support%20Documents/TechnicalDocs/evolution-of-wireless-sensor-networks.pdf. Last Accessed June 16, 2014.

Silicon Laboratories, Inc. 2014b. Integrating Raw Die Can Enable Innovative Packaging Solutions for Embedded Systems. www.silabs.com/support%20documents/technicaldocs/mcu-die-sales-enables-innovation.pdf. Last Accessed June 16, 2014.

Smith, D. 2012. Multisensor MEMS for temperature, relative humidity, and high-g shock monitoring. Thesis, Rochester Institute of Technology, NY.

Southwest Center for Microsystems Education (SCME). 2013. History of MEMS. scmenm.org/index.php?option=com_docman&task=cat_view&gid=63&Itemid=162. Last Accessed September 24, 2014.

Sparkfun Electronics. *CoolTerm (Windows, Mac, Linux)*. learn.sparkfun.com/tutorials/terminal-basics/coolterm-windows-mac-linux. Last Accessed August 16, 2014

Spencer, B. F., M. E. Ruiz-Sandoval, and N. Kurata. 2004. Smart sensing technology: opportunities and challenges. *Structural Control and Health Monitoring* 11(4): 349-368.

Sun, M., W. J. Staszewski, and R. N. Swamy. 2010. Smart sensing technologies for structural health monitoring of civil engineering structures. *Advances in Civil Engineering* 2010.

Texas Instruments. 2013. ZigBee Wireless Networking Overview. www.ti.com/lit/sg/slyb134d/slyb134d.pdf. Last Accessed April 16, 2014.

Texas Instruments. 2014. TPL5000 Datasheet. pdf1.alldatasheet.com/datasheet-pdf/view/530828/TI/TPL5000.html. Last Accessed April 16, 2014.

Timm, D. H., A. L. Priest, and T. V. McEwen. 2004. *Design and Instrumentation of the Structural Pavement Experiment at the NCAT Test Track*. NCAT Report 04-01. National Center for Asphalt Technology, Auburn University, Auburn, AL.

Titi, H., H. Tabatabai, K. Sobolev, J. Crovetti, and C. Foley. 2012. *Feasibility Study for a Freeway Corridor Infrastructure Health Monitoring Instrumentation Testbed*. Technical Report No. CFIRE 04-08. National Center for Freight and Infrastructure Research and Education (CFIRE), University of Wisconsin-Madison, Madison, WI.

Tompkins, D., and L. Khazanovich. 2007. *MnROAD Lessons Learned*. Technical Report No. MN/RC-2007-06. Minnesota Department of Transportation, University of Minnesota, Minneapolis, MN.

Tully, R. 2007. *The use of low cost "iButton" Temperature Logger Arrays to Generate High Spatial Resolution Tidal Inundation Regime Data*. Marine Resource Management, Oregon State University, Corvallis, OR.

Ubertini, F., A. L. Materazzi, A. D'Alessandro, and S. Laflamme. 2014. Natural frequencies identification of a reinforced concrete beam using carbon nanotube cement-based sensors. *Engineering Structures* 60: 265-275.

Varadan, V. K., and V. V. Varadan. 2000. Microsensors, Microelectromechanical Systems (MEMS), and electronics for Smart Structures and systems. *Smart Materials and Structures* 9(6): 953-972.

Wake, Inc. 2014. The HardTrack System. www.wakeinc.com/hardtrack.html. Last Accessed July 5, 2016.

Wang, L., A. Bos, T. Van Weelden, and F. Boschman. 2010. The next generation advanced M & sensor packaging. *Proceeding of the Electronic Packaging Technology & High Density Packaging (ICEPT-HDP), 2010 11th International Conference, IEEE*: 55-60.

Wang, X., M. L. Wang., Y. Zhao, H. Chen, and L. L. Zhou. 2004. Smart health monitoring system for a prestressed concrete bridge. *SPIE Proceedings: Smart Structures and Materials: Sensors and Smart Structures Technologies for Civil, Mechanical, and Aerospace System* 5391.

Wang, X. T. 2013. Study of sensor network applications in building construction. Thesis, Kungliga Tekniska Högskolan (Royal Institute of Technology), Sweden.

Wang, Y., J. P. Lynch, and K. H. Law. 2007. A wireless structural health monitoring system with multithreaded sensing devices: Design and validation. *Structure & Infrastructure Engineering: Maintenance, Management, Life-Cycle Design and Performance* 3(2):103-20.

Watters, D. G., P. Jayaweera, A. J. Bahr, D. L. Huestis, N. Priyantha, R. Meline, and D. Parks. 2003. Smart pebble: Wireless sensors for structural health monitoring of bridge decks. *SPIE Proceedings: Smart Systems and Nondestructive Evaluation for Civil Infrastructures* 5057.

Wells, S. A. 2005. Early age response of jointed plain concrete pavements to environmental loads. Thesis, University of Pittsburgh, PA.

Williams, K. R. 2000. Packaging for MEMS. robotics.eecs.berkeley.edu/~pister/245/2005S/Lectures/packagingKirtWilliams.pdf. Last Accessed July 14, 2016.

Wong, K. 2004. Instrumentation and health monitoring of cable-supported bridges. *Struct. Control Health Monit* 11(2): 91-124.

Xue, W., L. Wang, D. Wang, and C. Druta. 2014. Pavement health monitoring system based on an embedded sensing network. *Journal of Materials in Civil Engineering* 26(10): 1-8.

Ye, D., D. Zollinger, S. Choi, and M. Won. 2006. *Literature Review of Curing in Portland Cement Concrete Pavement*. FHWA Publication No. FHWA/TX06/0-5106-1. Center for Transportation Research, University of Texas, Austin, TX.

Yildiz, F. 2009. Potential Ambient Energy-Harvesting Sources and Techniques. *Journal of Technology Studies* 35(1).

Yousuf, M and T. Morton. 2014. *Use of Vehicle Noise for Roadways, Bridge, and Infrastructure Health Monitoring: Workshop Summary Report, August 20-21, 2013.* Technical Report No. FHWA-HRT-14-059. Federal Highway Administration, Office of Corporate Research, Innovation Management, and Technology, McLean, VA.

Zhao, F., and L. J. Guibas. 2004. *Wireless Sensor Networks: An Information Processing Approach*. Morgan Kaufmann Publishers Inc., San Francisco, CA.

Zinck, C. 2013. MEMS & Sensors Packaging Evolution. www.semi.org/eu/sites/semi.org/files/docs/ASE%20MEMS%20packaging%20-%20SEMI%202013%20C%20Zinck%20final%20new2.pdf. Last Accessed June 16, 2014.

APPENDIX A. TEMPERATURE, MOISTURE, AND STRAIN PROFILES FROM US 30

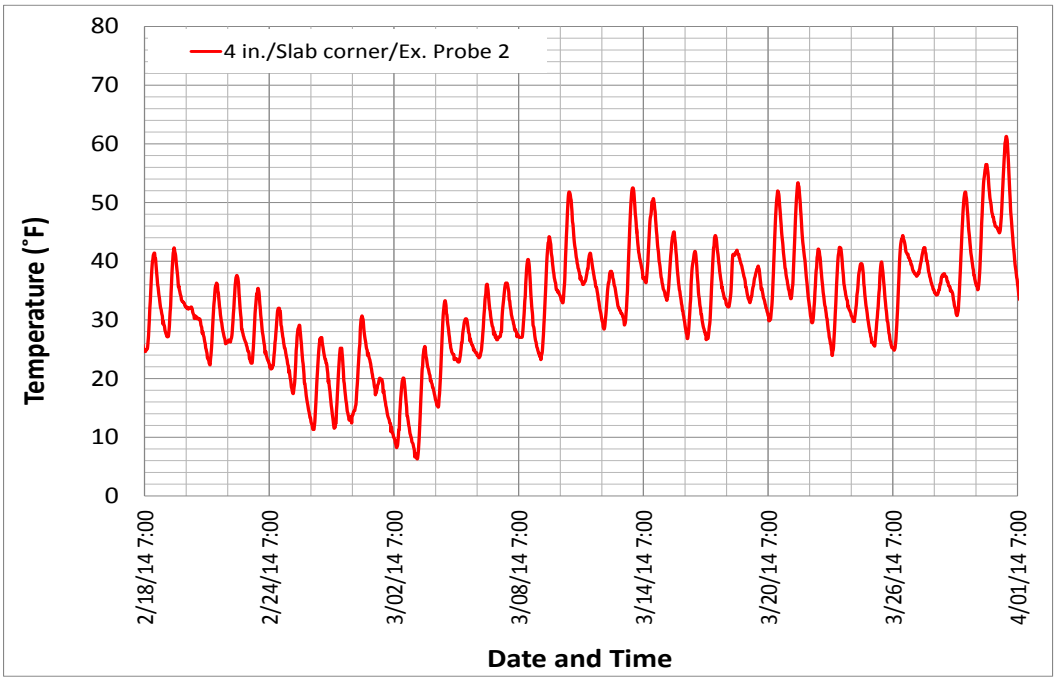

Figure A.1. RFID extended probe measurement in spring 2014

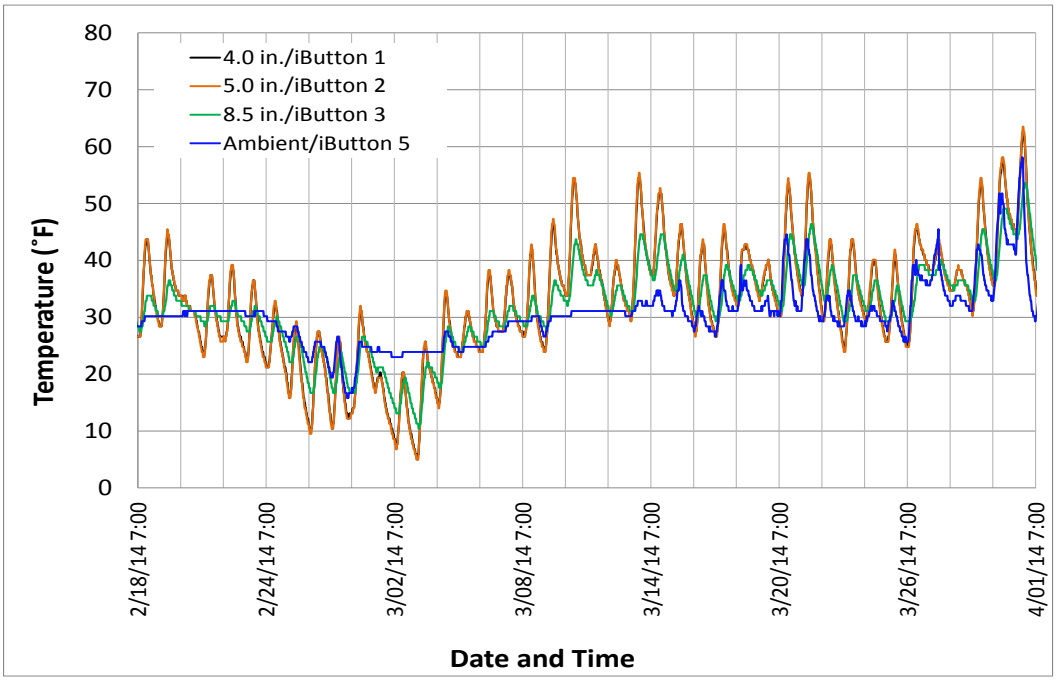

Figure A.2. iButton measurement in spring 2014

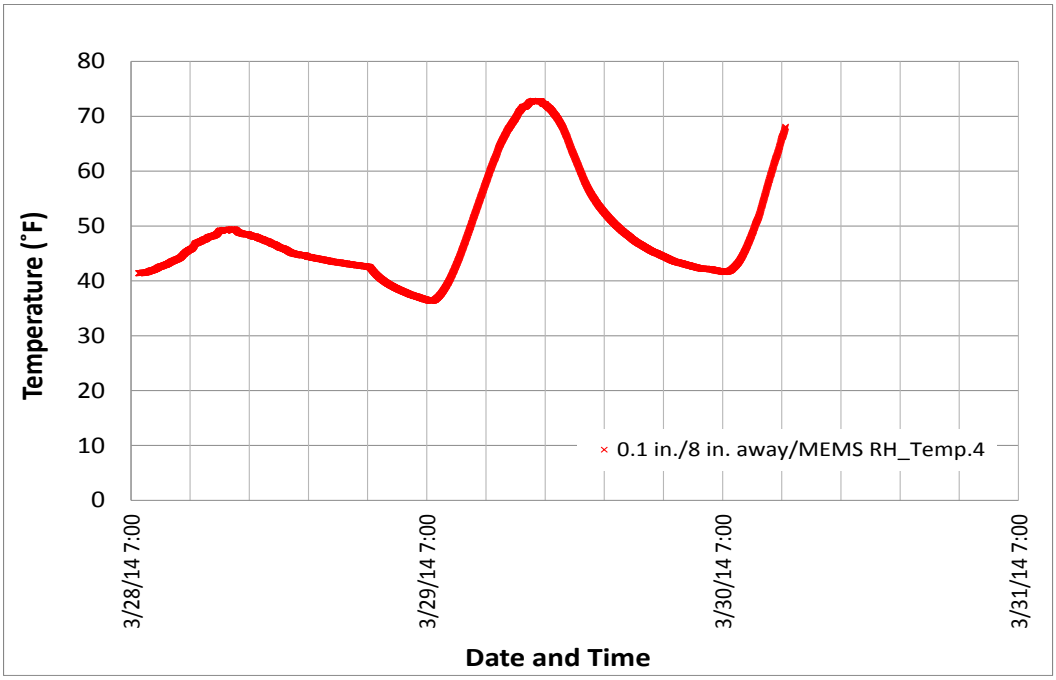

Figure A.3. MEMS digital humidity sensor temperature measurement in spring 2014

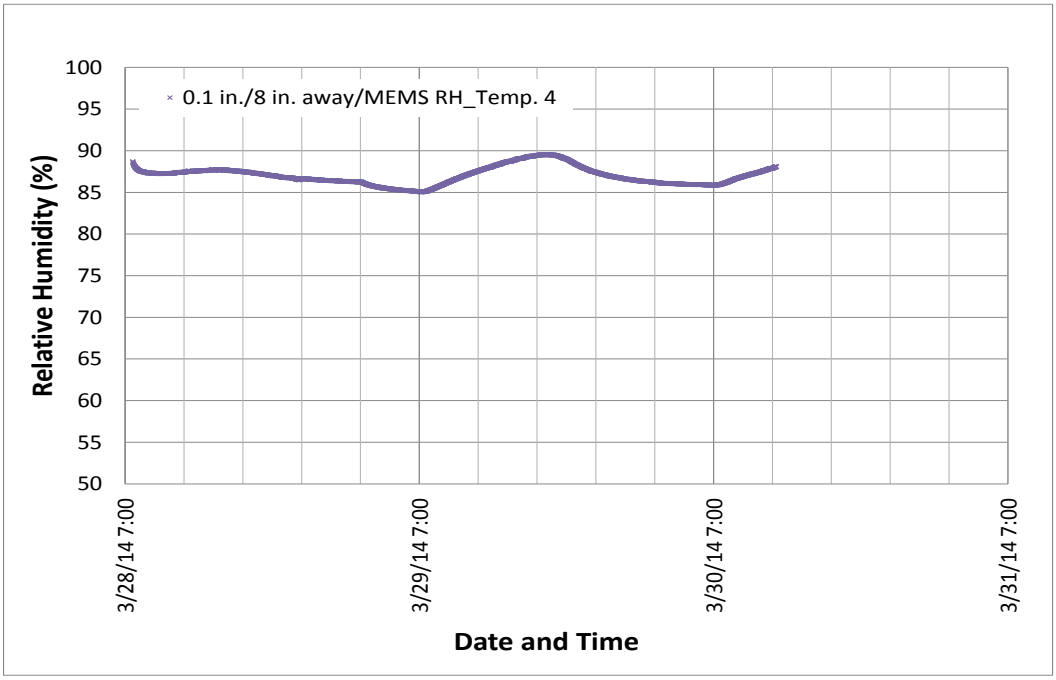

Figure A.4. MEMS digital humidity sensor RH measurement in spring 2014

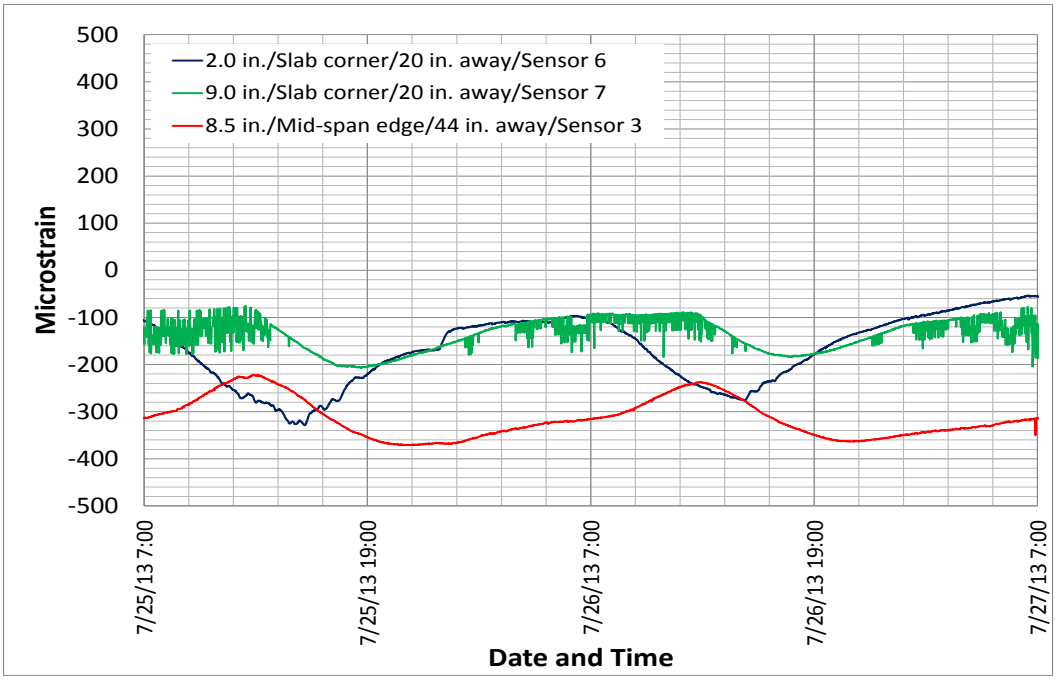

Figure A.5. Strain measurement in summer 2013

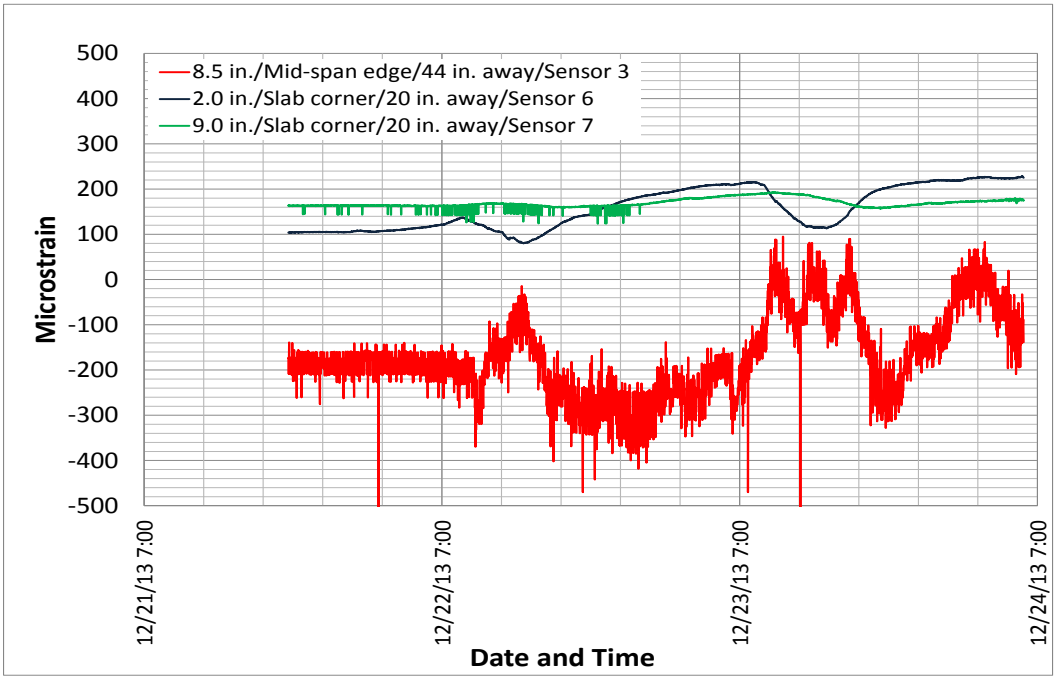

Figure A.6. Strain measurement in winter 2013

APPENDIX B. SET TIME TESTING (ASTM C403)

This appendix displays the set time test in accordance with ASTM C403.

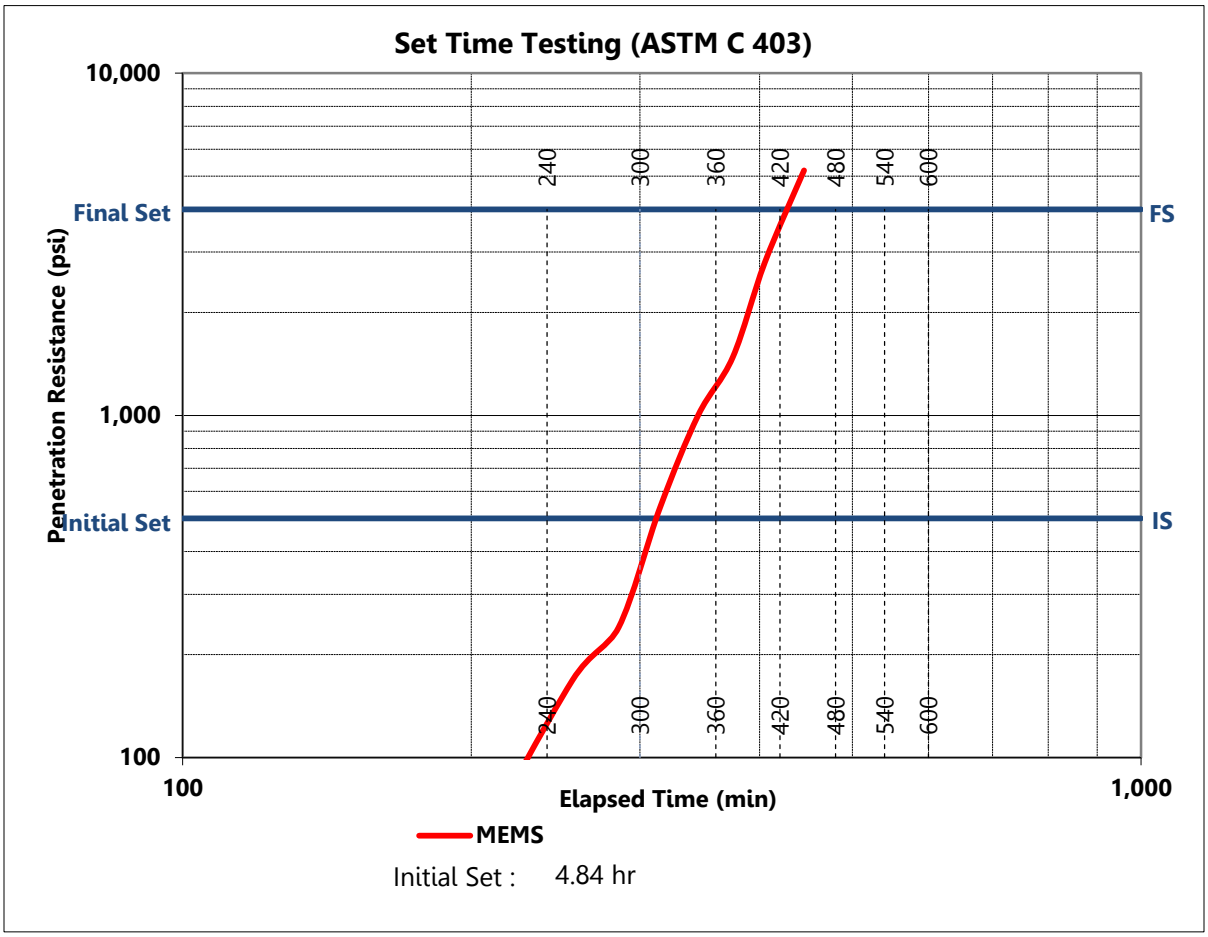

Figure B.1. Set time test (ASTM C403)

APPENDIX C. WIRELESS MEMS SYSTEM – SUCCESS RATE TEST RESULTS

This appendix displays the results from the wireless MEMS success rate tests, as well as the temperature and moisture data obtained from the test.

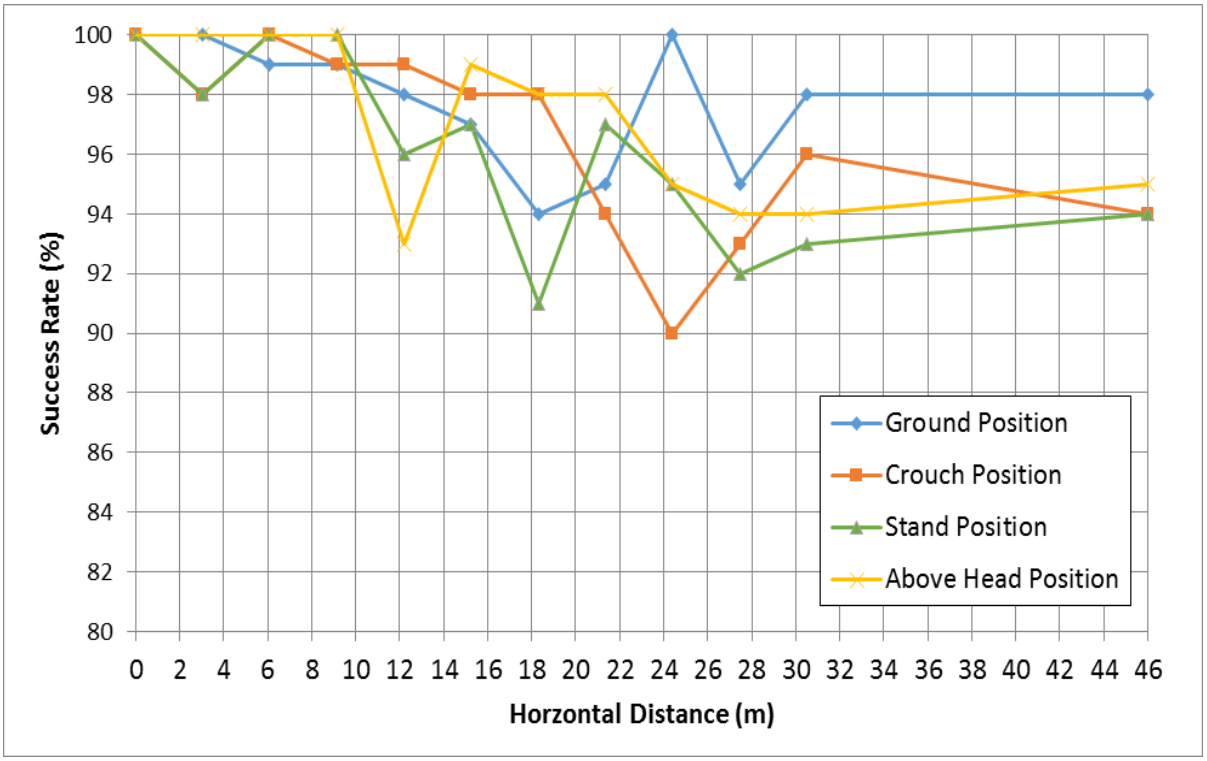

Figure C.1. Success rate test results

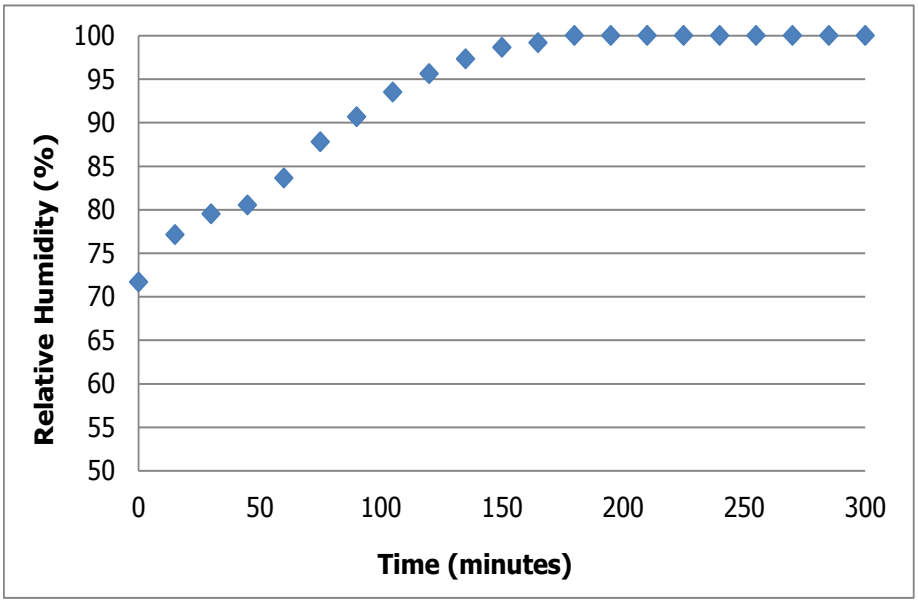

Figure C.2. RH measurement from success rate test

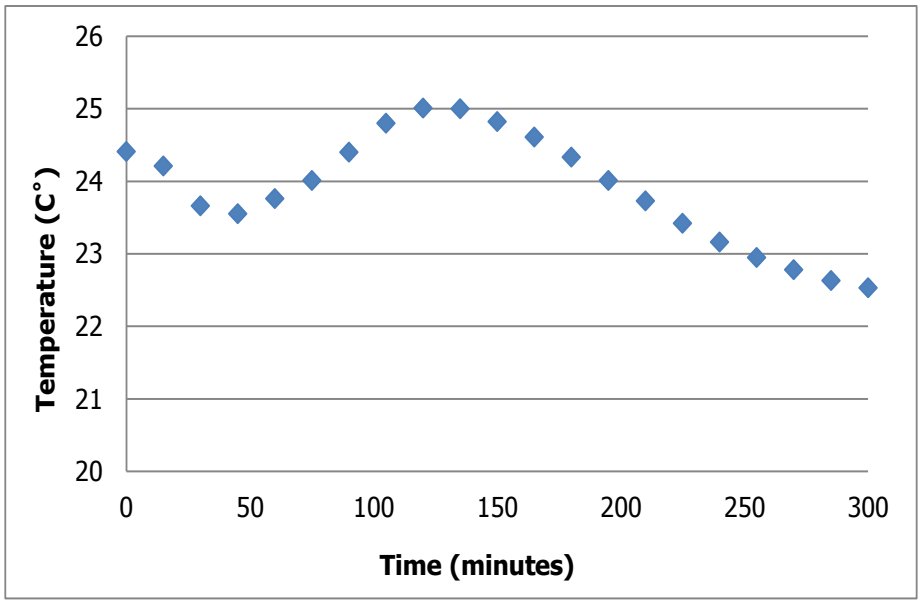

Figure C.3. Temperature measurement from success rate test